Hannu Leppinen

Integration of a GPS subsystem into the Aalto-1 nanosatellite

School of Electrical Engineering

Thesis submitted for examination for the degree of Master of Science in Technology.

Espoo 12.4.2013

Thesis supervisor:

Prof. Kai Zenger

Thesis instructors:

Prof. Martin Vermeer

D.Sc. (Tech.) Jaan Praks

Aalto University
School of Electrical
Engineering

AALTO UNIVERSITY
SCHOOL OF ELECTRICAL ENGINEERING

ABSTRACT OF THE
MASTER'S THESIS

Author: Hannu Leppinen

Title: Integration of a GPS subsystem into the Aalto-1 nanosatellite

Date: 12.4.2013 Language: English Number of pages:10+91

Department of Automation and Systems Technology

Professorship: Control Engineering Code: AS-74

Supervisor: Prof. Kai Zenger

Instructors: Prof. Martin Vermeer, D.Sc. (Tech.) Jaan Praks

GPS is increasingly used for spacecraft navigation in low Earth orbit. Equipping a satellite with a GPS receiver enables it to determine position, velocity and time autonomously, without the need for ground-based tracking stations. Using commercial off-the-shelf GPS components enables autonomous positioning even for low-cost nanosatellites. However, the components need to be selected and qualified carefully. This thesis presents the design of a GPS subsystem and a plan for its integration into the Aalto-1 nanosatellite. Although the flight model of the satellite won't be ready by the completion of the thesis, the plan can be used in the integration of the final satellite system. The thesis also evaluates the feasibility of using this kind of commercial components in a satellite application.

The thesis begins by introducing the Aalto-1 satellite project, basics of the Global Positioning System, and satellite tracking with GPS. After this necessary background information, the design for the GPS subsystem is presented, as are its mechanical, electrical and software interfaces. A verification plan is outlined that aims to ensure that the subsystem will operate correctly in space. Some initial steps of the verification plan are done as a part of the thesis and are also described, most importantly GPS signal simulations, PCB prototype tests and antenna performance tests. Finally, conclusions about the spaceworthiness of the GPS subsystem are given, as are suggestions for the final integration of the subsystem into the satellite.

Keywords: GPS, Aalto-1, CubeSat, nanosatellite, satellite tracking

AALTO-YLIOPISTO
SÄHKÖTEKNIIKAN KORKEAKOULU

DIPLOMITYÖN
TIIVISTELMÄ

Tekijä: Hannu Leppinen

Työn nimi: GPS-alijärjestelmän integraatio Aalto-1-nanosatelliittiin

Päivämäärä: 12.4.2013 Kieli: Englanti Sivumäärä:10+91

Automaatio- ja systeemitekniikan laitos

Professuuri: Systeemitekniikka Koodi: AS-74

Valvoja: Prof. Kai Zenger

Ohjaajat: Prof. Martin Vermeer, TkT Jaan Praks

GPS:ää käytetään lisääntyvässä määrin matalan kiertoradan avaruusalusten navigoinnissa. Satelliitin varustaminen GPS-vastaanottimella mahdollistaa paikan, nopeuden ja ajan tarkan määrittämisen autonomisesti ilman tarvetta usealle maanpäälliselle seuranta-asemalle. Yleisten kaupallisten GPS-komponenttien käyttö mahdollistaa autonomisen paikannuksen jopa edullisille nanosatelliiteille. GPS-komponentit on kuitenkin valittava ja niiden toimivuus varmistettava huolellisesti.
Diplomityön tavoite on tuottaa tarkka suunnitelma GPS-alijärjestelmästä, joka tullaan integroimaan Aalto-1-nanosatelliittiin. Vaikka satelliitin avaruuteen menevä malli ei ole diplomityön lopussa valmis, diplomityön sisältämää suunnitelmaa voidaan suoraan käyttää lopulliseen järjestelmäintegraatioon. Työssä myös arvioidaan tämänkaltaisten GPS-laitteiden soveltuvuutta avaruussovelluksiin.
Diplomityössä esitellään aluksi taustatietona Aalto-1-satelliittiprojekti, GPS-paikannusjärjestelmän toiminta yleisesti sekä satelliittien seuranta GPS:llä. Perustietojen esittelyn jälkeen kuvataan Aalto-1-satelliittiin suunniteltu GPS-alijärjestelmä sekä sen mekaaniset, sähköiset ja ohjelmistorajapinnat. Suunnitellulle alijärjestelmälle hahmotellaan verifiointisuunnitelmaa, jolla pyritään varmistamaan alijärjestelmän toimivuus avaruudessa halutulla tavalla. Myös joitakin verifiointisuunnitelman alkuvaiheen testejä esitellään, tärkeimpinä GPS-signaalisimulaatiot, PCB-prototyyppitestit ja antennin suorituskykytestit. Lopuksi esitetään loppupäätelmät järjestelmän toimivuudesta sekä ehdotuksia järjestelmän lopulliseen integrointiin satelliittiin.

Avainsanat: GPS, Aalto-1, CubeSat, nanosatelliitti, satelliittien seuranta

Preface

It was almost exactly one year from the first idea of this thesis to submitting it in hard covers. A job interview at Space Systems Finland Oy in March 2012 first introduced me to an idea of working with an Aalto-1-related thesis about Aalto-1 on-board computer software. This original idea did not materialize, but I ended up with a research assistant position at the Department of Radio Science and Engineering at Aalto University. My job: integrate a GPS subsystem into Aalto-1, and make a thesis out of it. The work got underway during summer 2012, with the subject being approved in early Autumn 2012 with a deadline of March 2013.

I thank Kai Zenger for supervising the work, and Martin Vermeer and Jaan Praks for instructing and for expert advice. I owe a lot of thanks also to the whole Aalto-1 team, of which I could mention Antti Kestilä for providing me the starting points for the project and advice in system engineering related issues, Jaakko Jussila and Mikko Lankinen for help in RF design, Konsta Hölttä for help in software design issues, Maria Komu for help in verification issues and Kalle Nordling for help in mechanical design. I would also like to thank Stefan Söderholm of Fastrax Oy for providing the GPS receivers and for insightful discussions, and Mårten Ström and Heikki Laitinen of Space Systems Finland Oy for allowing the use of their equipment for the GPS signal simulations and for expert advice about using GPS in space. I also thank Ari-Matti Harri of the Finnish Meteorological Institute for allowing the use of their thermal chamber for thermal qualification tests.

Thanks go also to my family for supporting me in my studies at the university.

Finally, I wish the greatest success for the Aalto-1 project. I am glad to have been a part of it.

Otaniemi, 8.4.2013

Hannu T. Leppinen

Contents

Symbols and abbreviations

Symbols

$\mathbf{r}$	vector from receiver to GPS satellite
$\mathbf{s}$	GPS satellite position vector in ECEF frame
$\mathbf{u}$	receiver position vector in ECEF frame
p	pseudorange
c	speed of light in vacuum (299792458 m/s)
t	time
t_u	offset between receiver clock and GPS system time
$x_\mathrm{u}, y_\mathrm{u}, z_\mathrm{u}$	receiver coordinates
x_i, y_i, z_i	i:th GPS satellite coordinates
f_R	received frequency
f_T	transmitted frequency
$\mathbf{v}_\mathrm{r}$	receiver velocity
$\mathbf{a}$	unit vector pointing from receiver toward GPS satellite
$\mathbf{H}$	design matrix
$\mathbf{Q}$	normal matrix
σ_p	position error estimate
σ_UERE	UERE error estimate
$\mathbf{r}_\mathrm{ITRS}$	position vector in ITRS frame
$\mathbf{r}_\mathrm{GCRS}$	position vector in GCRS frame
$\Pi(t)$	polar motion
$\Theta(t)$	rotation of the Earth around its axis
$\mathbf{N}(t)$	nutation of the Earth's axis
$\mathbf{P}(t)$	precession of the Earth's rotation axis from epoch J2000
t_GPS	GPS system time
t_rcv	receiver time
t_UTC	UTC time
Δt_LS	integer number of leap seconds
δt_A	fractional part of GPS clock correction
$\mathbf{F}$	force
m	mass of small body
G	gravitational constant (6.67384*10^{-11} $m^3 kg^{-1} s^{-2}$)
M	mass of large body
e	orbital eccentricity
r_a	apoapsis radius
r_p	periapsis radius
a	semi-major axis
b	semi-minor axis

i	orbital inclination
Ω	longitude of the ascending node
ω	argument of periapsis
ν	true anomaly
$(C_S)_{dB}$	recovered signal power from satellite SVi (dBW)
$(N_0)_{dB}$	thermal noise power component in a 1-Hz bandwidth (dBW)
$(C_{Ri})_{dB}$	received signal power from SVi at antenna input (dBW)
$(G_{SVi})_{dB}$	antenna gain toward SVi (dBic)
L_{dB}	receiver implementation loss (dB)
k	Boltzmann's constant ($1.38 * 10^{-23}$ J/K)
T_{ant}	antenna noise temperature
T_{amp}	amplifier noise temperature
$(N_F)_{dB}$	amplifier noise figure at 290K (dB)
Z_0	impedance of free space ($\approx 376.73031\ \Omega$)
ϵ_r	relative permittivity of the substrate
w	width of the conductor
h	height of the substrate
t_c	thickness of the conductor

Abbreviations

1U, 2U, 3U	CubeSat sizes: (Approx.) 10, 20 or 30 cm x 10cm x 10cm
ADCS	Attitude Determination and Control System
C/A	Coarse/Acquisition
CDR	Critical Design Review
CEP95	Circular Error Probable 95 %
CN	Criticality Number
CNR	Carrier to Noise Ratio
COTS	Commercial off-the-shelf
DOP	Dilution of Precision
ECEF	Earth-centered Earth-fixed
ECI	Earth-centered inertial
ECSS	European Cooperation on Space Standardization
EM, EMC	Electromagnetic (Compatibility)
EPS	Electrical Power System
ESA	European Space Agency
FAA	Federal Aviation Administration (United States)
FM	Flight Model
FMECA	Failure Modes, Effects and Criticality Analysis
FMI	Finnish Meteorological Institute
GCRF	Geocentric Celestial Reference Frame
GCRS	Geocentric Celestial Reference System
GDOP	Geometric Dilution of Precision
GPIO	General Purpose Input/Output

GPS	Global Positioning System
ICRF	International Celestial Reference Frame
ICRS	International Celestial Reference System
IERS	International Earth Rotation and Reference Systems Service
ITRF	International Terrestrial Reference Frame
ITRS	International Terrestrial Reference System
LEO	Low Earth Orbit
LLA	Latitude-Longitude-Altitude
NASA	National Aeronautics and Space Administration (United States)
NIMA	National Imagery and Mapping Agency (United States)
NMEA	National Marine Electronics Assocation (United States)
NORAD	North American Aerospace Defense Command
OBC	On-board Computer
PC	Personal Computer
PCB	Printed circuit board
PDOP	Position Dilution of Precision
PDR	Preliminary Design Review
PFM	Protoflight Model
PN	Probability Number
POSIX	Portable Operating System Interface
PPS	Pulse Per Second
PRN	Pseudo-Random Noise
QM	Qualification Model
RADMON	Radiation Monitor
RF	Radio Frequency
RMS	Root Mean Square
SIS	Signal-In-Space
SN	Severity Number
SPS	Standard Positioning Service
TAI	International Atomic Time
TBD	To be determined
TLE	Two-Line Element Set
TDOP	Time Dilution of Precision
TOA	Time of arrival
TT	Terrestrial Time
TTFF	Time to First Fix
TTL	Transistor-to-Transistor Logic
UART	Universal Asynchronous Receiver/Transmitter
UERE	User Equivalent Range Error
USB	Universal Serial Bus
UT1	Universal Time
UTC	Coordinated Universal Time
VHF/UHF	Very High Frequency/Ultra High Frequency
VSWR	Voltage Standing Wave Ratio
VTT	Technical Research Centre of Finland
WGS84	World Geodetic System 1984

1 Introduction

On a dark clear night, faint dots of light can sometimes be observed moving across the sky, slowly brightening and then dimming again. Many of these dots are some of the thousands of man-made satellites orbiting the Earth, on their missions of communication, navigation, science and so on.

Small satellites are a class of satellites that are smaller and can perform less functions than the so-called conventional satellites. The small satellite design philosophy minimizes cost and development time by using commercial off-the-shelf (COTS) components as much as possible. As small satellites are easier and faster to design, they have been embraced by the amateur and the academic community. The first artificial satellite of the Earth, Sputnik 1, was launched in 1957; OSCAR 1, the first amateur small satellite, was launched only four years later in 1961. OSCAR 1 weighed only 4.5 kg, was powered by a battery and transmitted a radio signal based on a temperature sensor. (Fortescue, Stark, and Swinerd 2003, p. 581-611)

Owing to the rapid development of microelectronic technology during the latter part of the 20th century, it has become possible to fit more sophisticated functions into smaller spaces. Small satellites continue to be used for communication, remote sensing and space science. They also offer an opportunity to train young space scientists and engineers with hands-on projects. (Fortescue, Stark, and Swinerd 2003, p. 581-611)

Nanosatellites are a class of small satellites with a mass between 1 kg and 10 kg. Although OSCAR 1 could be categorized as one, the first modern nanosatellites were launched in the late 1990s. A popular standard for nanosatellites, CubeSat, was introduced in 1999. The first batch of CubeSats was launched in 2003. As of today, more than 40 CubeSats have been launched, with many more in development. (Bouwmeester and Guo 2010)

Following the example of several universities around the world, Aalto University has also begun its own Aalto-1 nanosatellite project. In addition to the on-orbit mission of the satellite, its aim is to inspire Finnish space engineering. (Näsilä et al. 2012)

The mission and payloads of Aalto-1 require accurate position information during the mission, and this information can be provided with a Global Positioning System (GPS) receiver. The purpose of this master's thesis is to present the integration of a GPS subsystem into Aalto-1. In this case, the GPS subsystem refers to the GPS receiver, GPS antenna, antenna cable, GPS circuit board and their various mechanical, electrical and software interfaces.

According to Fortescue, Stark, and Swinerd (2003, p. 615-617), a space engineering project can be divided into the following phases:

1. **Phase A: feasibility study.** A feasible design approach is selected during this

phase.

2. **Phase B: detailed definition.** The system is defined in more detail, subsystem requirements and design specifications are identified.

3. **Phase C/D: development, manufacture, integration and test.** During this phase, the subsystems are developed and manufactured. Later in this phase the subsystems are integrated into a larger system, which is then tested.

4. **Phase E: mission operations and data analysis.** The space mission is operated and the received data is analysed.

As of this thesis, Aalto-1 is in the phase C/D. A preliminary design review (PDR) was conducted in late 2011, during which the system design was evaluated against the requirements. The project is currently heading toward a critical design review (CDR), which will largely freeze the system design. Flight model assembly will begin after CDR.

1.1 Aim of the thesis

The research problem is to integrate a GPS subsystem into the Aalto-1 nanosatellite; that is, to create a solution that makes it possible to use GPS for the positioning of Aalto-1 in space.

The research question could be phrased as:

> "What kind of GPS receiver and antenna are required for Aalto-1, and how should they be integrated into the satellite in order to use GPS for navigation of the satellite?"

System integration means putting together various subsystem components and ensuring that the assembled whole works as a system. Particularly in a space engineering project, interdependence of systems is a major challenge: changing the aspects of one system could force design changes in other systems as well. This problem can be mitigated by specifying interfaces between systems as early as possible. Interface requirements were a major design driver for the GPS subsystem from the start.

This thesis presents the design of a GPS subsystem, a plan for its integration into the Aalto-1 nanosatellite, and a plan for its verification. Although the flight model of the satellite won't be ready by the completion of the thesis, the plan can be used in the integration and verification of the final satellite system. The primary intended audience of the thesis are the students and researchers working in the Aalto-1 project, and the approach to the subject has been chosen accordingly.

1.2 Organization of the thesis

The work is divided into five chapters, the first of which is this introductory chapter. Chapter 2 contains necessary background information for understanding the thesis: the Aalto-1 project is described in Section 2.1, Section 2.2 gives a brief overview of the Global Positioning System, and satellite tracking with GPS is discussed in Section 2.3. The design and integration of the GPS subsystem is presented in Chapter 3. Verification of the subsystem is discussed in Chapter 4. Finally, conclusions are given in Chapter 5.

2 Background

This chapter provides the background for understanding the thesis. The Aalto-1 project is briefly introduced in the first section of this chapter to give the reader an overview of the satellite and its purpose. A more detailed description of Aalto-1 can be found in Kestilä et al. (2013). The second section is an overview of the Global Positioning System and its capabilities. The third section considers using GPS in satellite tracking.

2.1 The Aalto-1 nanosatellite

Aalto-1, shown in fig. 1, is a nanosatellite designed, built and operated by students and researchers at Aalto University. The mission of the satellite is to operate its payloads in Earth orbit. The work on the satellite began in 2010. (Praks et al. 2011)

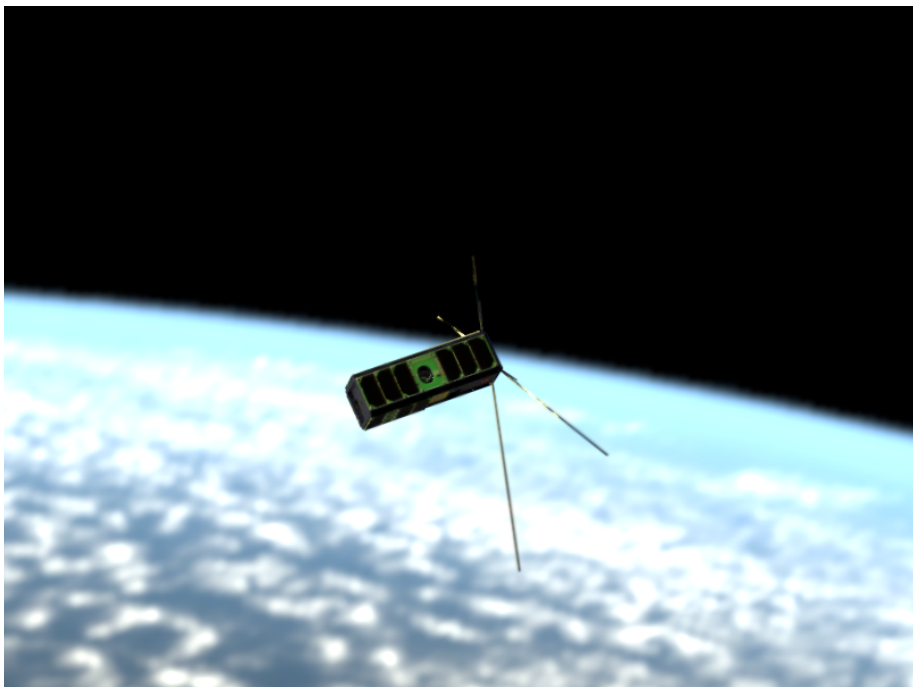

Figure 1: An artist's vision of Aalto-1 in orbit. 3D render by Pekka Laurila.

The main payload of Aalto-1 is a Fabry-Pérot spectral imager, which will be used for remote sensing of the Earth. It is being built at the Technical Research Centre of Finland (VTT). The spectral imager will produce images of the Earth in several narrow visual and near-infrared wavelength bands.

The second payload is a radiation detector built at University of Turku and University of Helsinki. It will be used to gather data on the radiation environment around the Earth.

The third payload is an electrostatic plasma brake built by a consortium led by the

Finnish Meteorological Institute (FMI). After remote sensing and radiation measurements, the satellite will be deorbited using the plasma brake. (Praks et al. 2011)

As of this writing, Aalto-1 is planned to be launched in 2014. The satellite is planned to be launched to a polar sun-synchronous orbit, which is suitable for the remote sensing and plasma brake experiments. If successful, Aalto-1 will be the first Finnish satellite. The main parameters of Aalto-1 are listed in table 1. (Kestilä et al. 2013)

Table 1: Main parameters of the Aalto-1 mission. (Näsilä et al. 2012, p. 10-22) (Kestilä et al. 2013)

The Aalto-1 mission	
Operator	Aalto University
Mission type	Earth observation Technology demonstration
Payloads	Fabry-Pérot spectral imager Radiation monitor Electrostatic plasma brake
Launch date	TBD, target 2014
Orbit	TBD, ideally 500 to 900 km midday-midnight sun-synchronous
Launch vehicle	TBD
Mission duration	Approx. 2 years
Mass	4 kg (max)
Dimensions	340.5 mm x 100.0 mm x 100.0 mm
Attitude	3-axis stabilized
Power supply	4.5 W (average, solar panels)

The mission phases of Aalto-1 will include:

1. **Launch.** The satellite is launched with a suitable launch vehicle to a polar orbit.
2. **Separation.** The satellite is deployed from the launch vehicle. The satellite starts to power up and detumble. Antennas are deployed.
3. **Commissioning.** All the payloads are tested to see if they are operable, and if data from the payloads can be transmitted to the ground station.
4. **Science.** The longest phase of the mission with a duration of 1 to 3 years. In the first part, the spectral imager and radiation monitor are used in their respective scientific missions for 6 to 12 months. In the second part, the plasma brake is deployed by spinning the satellite. The spin renders the spectral imager unusable. The braking force produced by the plasma brake is measured for 6 to 18 months. The brake will deorbit the satellite at the end of the mission.
5. **Burn.** The satellite re-enters the atmosphere at the end of the mission.

2.1.1 Structure

Aalto-1 is based on the 3U CubeSat standard, which sets the satellite size at 340.5 mm x 100.0 mm x 100.0 mm and maximum mass at 4 kg. Using the CubeSat standard allows co-operation with and learning from other academic CubeSat projects, which makes satellite development faster. The stack structure of the satellite is depicted in fig. 2. (Näsilä et al. 2012, p. 16)

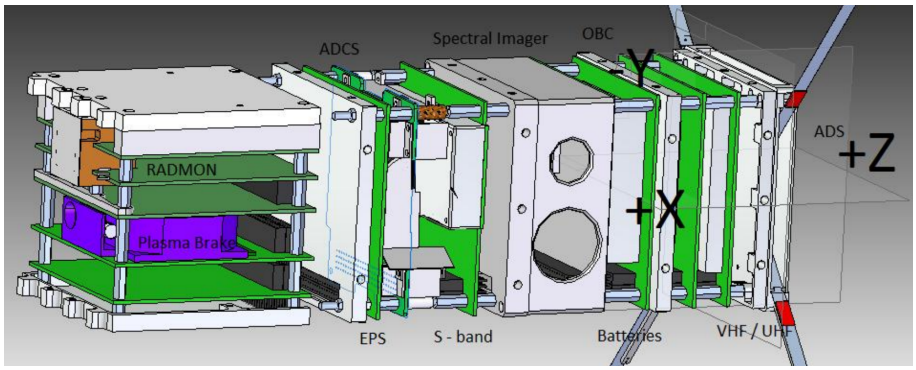

Figure 2: The Aalto-1 stack structure. On the left is the short stack, which contains the electrostatic plasma brake and the radiation monitor (RADMON). On the right is the long stack, which contains the electrical power system (EPS), the attitude determination and control system (ADCS), the S-band radio and GPS, the spectral imager, batteries, the onboard computer (OBC), VHF/UHF radios and the antenna deployment system. (Kestilä et al. 2013)

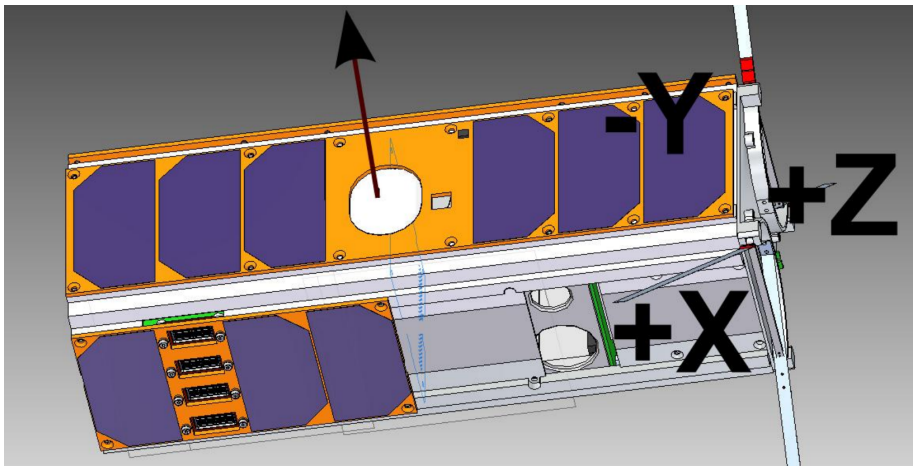

Figure 3: The Aalto-1 outer frame. On the -Y side, a large round hole for the star tracker of the ADCS and a smaller rectangular hole for the GPS antenna are visible. (Kestilä et al. 2013)

The spacecraft electronics are placed on PCBs that are based on the CubeSat Kit standard. The PCBs are placed on two stacks: the long stack and the short stack. The PCBs on the long stack are stacked along the long axis of the satellite, making the long stack

approximately 2U (20 cm) long. The short stack is 1U (10 cm) long and is rotated 90 degrees with respect to the long stack. The short stack is rotated in order to allow the electrostatic plasma brake tether deployment mechanism to extend the tether along the long axis of the satellite. The PCB stacks are contained in the satellite's 1.5 mm aluminium frame. The frame is covered with solar panels providing electrical power. The frame has holes for instruments, and the S-band and GPS patch antennas are situated on the surface of the frame. The outer frame is depicted in fig. 3. (Kestilä et al. 2013)

2.2 The Global Positioning System

This section gives a brief description of how the Global Positioning System works. Due to the type of the receiver considered later in the work, the section concentrates on the C/A code Standard Positioning Service (SPS) GPS on L1 frequency. Other, more accurate forms of GPS are mentioned briefly, as are other satellite navigation systems. Relevant coordinate and time systems are described, and navigation performance of SPS GPS is also discussed.

2.2.1 History

GPS has its origins in land-based radio navigation systems and some predecessors in satellite navigation.

Several radio navigation systems using land-based beacons had already been operational, but spaceflight made it possible to put radio navigation beacons to Earth orbit, achieving global coverage easily. The first space-based navigation system, TRANSIT, was developed in the 1960s and was used by U.S. Navy. The Soviet Union later developed a similar Tsikada system. They were able to provide accurate and global two-dimensional positioning. The U.S. and Soviet navies needed such a system for their ballistic missile submarines.

TRANSIT satellites broadcast time information and orbit information for the satellites, which allowed the receiver to calculate the satellite's position. The Doppler shift of the satellite signal was measured for several minutes. A trial position and the known satellite motion was used to generate a trial Doppler curve. The two curves were compared with the least-squares method and the trial position was moved until the measured and trial Doppler curves agreed.

TRANSIT only allowed one fix per 110 minutes at the equator and one fix per 30 minutes at 80° latitude on average. Obtaining a position fix also required 10 to 15 minutes of processing. TRANSIT was therefore suitable only for slow-moving users, such as ships, but not for aircraft and high-dynamic users. A better navigation system, which would provide continuous, accurate and global three-dimensional positioning, was desired. GPS was designed to fill this role. (Kaplan and Hegarty 2006, p. 1-3)

2.2.2 Overview

GPS is a U.S.-built satellite navigation system that provides continuous and accurate three-dimensional position, velocity and time information worldwide. It was originally designed for military applications, but after 1990 it has been widely adopted for civilian use as well. Today, GPS is used in military, commercial and recreational applications. Majority of users are land-based, but uses in aviation and shipping are also important. GPS has also increasingly been used aboard spacecraft. (Kaplan and Hegarty 2006, p. 3-4, 10-14)

The GPS space segment nominally consists of 24 satellites in six orbital planes, but usually additional satellites are in orbit to serve as spares and to augment the system; the number of operational satellites is currently around 30. The number of satellites means that at least 6 satellites should be visible at any time from almost anywhere on Earth. The satellites orbit at an altitude of approximately 20200 km with a 55° inclination. As only four satellites are needed for a navigation fix, GPS is able to provide global and continuous positioning. The GPS control segment is a world-wide network of ground stations that monitor the health of the satellites and upload required navigational information. User segment refers to the GPS receivers that use the satellite-transmitted signals for navigation. The segments are depicted in fig. 4. (Kaplan and Hegarty 2006, p. 3-4)

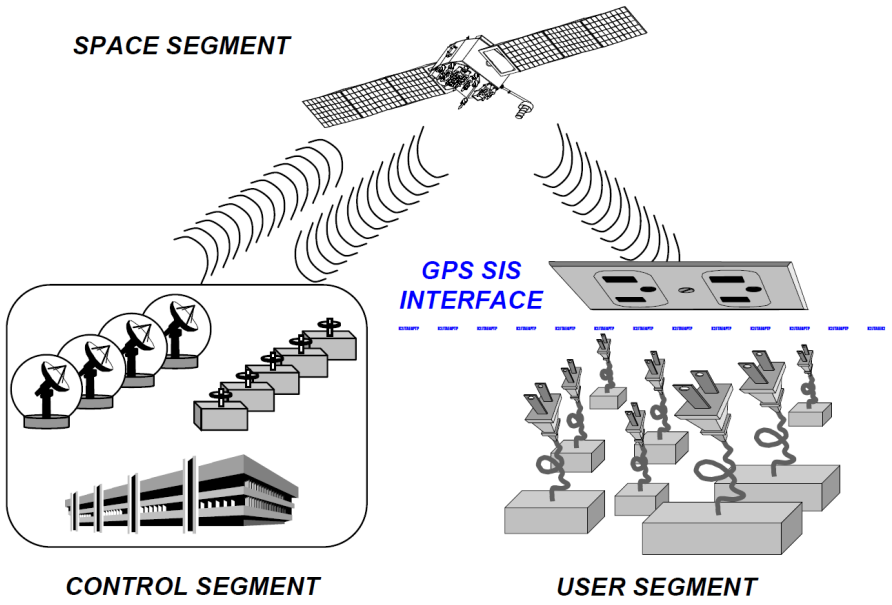

Figure 4: GPS consists of three segments: the control segment, the space segment and the user segment. The control segment maintains the operation of the space segment. The satellites of the space segment provide the GPS signal-in-space (SIS) interface, which can be used by the user segment (GPS receivers) for navigation. (USDOD 2008)

2.2.3 Positioning

GPS uses time of arrival (TOA) ranging. The atomic clocks aboard all GPS satellites are synchronized to a time referred to as the GPS system time. GPS satellites continuously transmit signals that can be picked up by a GPS receiver. If a receiver's clock is also perfectly synchronized with the GPS system time, the distance between the receiver and a satellite can be calculated from the signal travel time. In an ideal case, 3 satellites would be enough for a three-dimensional position fix, but in practice a fourth satellite is needed to correct the receiver's clock. (Kaplan and Hegarty 2006, p. 21-26, 50-63)

GPS satellites transmit on several frequencies, which have various civilian and military applications. The most common frequency in civilian navigation applications is the L1 frequency at 1575.42 MHz. L1 band is modulated by the coarse-acquisition code (C/A). (Kaplan and Hegarty 2006, p. 3)

The C/A signal consists of repeating time-based sequences of pseudorandom noise (PRN code). Each satellite has its own unique sequence. The satellites also broadcast GPS navigation messages on the L1 frequency which include Kepler orbit parameters and correction terms for the GPS satellites (see 2.3.1), time and other information required for navigation.

A receiver picks up the PRN code generated by a certain satellite, and uses its own clock to generate a similar time-based sequence. As the satellite-generated sequence has taken some time to arrive, there is an offset between the satellite-generated sequence and the receiver-generated sequence. The receiver-generated sequence is time-shifted until it correlates with the satellite-generated sequence. If the receiver clock is in perfect synchronization with the GPS system time, the amount of time shift Δt gives the true signal propagation time. This is depicted in fig. 5. Multiplying the time shift with the speed of light gives the pseudorange p. (Kaplan and Hegarty 2006, p. 21-26, 50-58)

However, the receiver clock is not usually synchronized with the system time, which means that a fourth satellite is needed to correct the clock. There can also be an offset between the GPS system time and an individual GPS satellite's clock, but corrections to this offset are included in the GPS navigation messages. (Kaplan and Hegarty 2006, p. 53-54)

The vector $\mathbf{r}$ from the receiver to a GPS satellite can be expressed as

$$\mathbf{r} = \mathbf{s} - \mathbf{u} \tag{1}$$

where $\mathbf{s}$ is the GPS satellite position vector and $\mathbf{u}$ is the receiver position vector. Let r be the true distance.

$$r = ||\mathbf{s} - \mathbf{u}|| \tag{2}$$

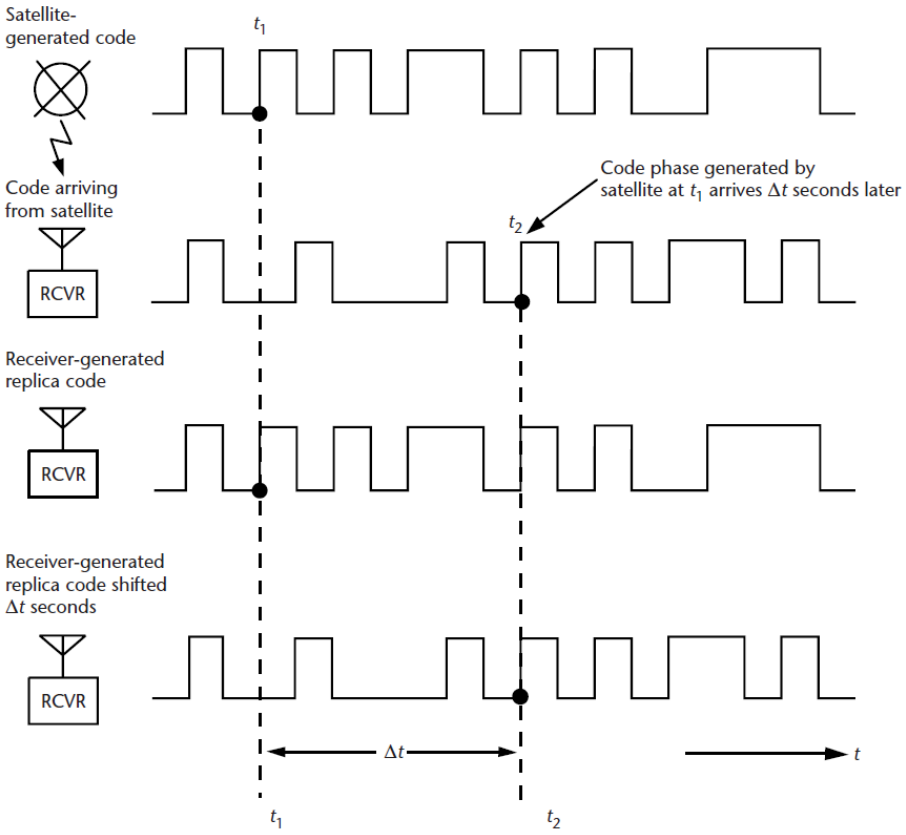

Figure 5: The receiver picks up the PRN code transmitted by a GPS satellite and creates an identical sequence with its own clock. The receiver-generated sequence is offset until it correlates with the satellite-generated sequence. This offset, Δt, is the amount of time it took for the signal to travel from the GPS satellite to the receiver, and the pseudorange can be obtained by multiplying the offset with the speed of light. (Kaplan and Hegarty 2006, p. 52)

The previously obtained pseudorange p can be expressed as

$$p = r + c\,t_{\mathrm{u}} \tag{3}$$

where c is the speed of light and t_u is the offset between the receiver clock and the GPS system time. Now eq. (2) and eq. (3) can be combined:

$$p - c\,t_{\mathrm{u}} = ||\mathbf{s} - \mathbf{u}|| \tag{4}$$

This is actually an equation for a sphere centered on the GPS satellite. We have a set of four unknowns $(x_{\mathrm{u}}, y_{\mathrm{u}}, z_{\mathrm{u}}, t_{\mathrm{u}})$: the receiver position and the time offset. With four

satellites available, eq. (4) can be expanded to a system of four equations:

$$\begin{aligned} p_1 &= \sqrt{(x_1 - x_\mathrm{u})^2 + (y_1 - y_\mathrm{u})^2 + (z_1 - z_\mathrm{u})^2} + c\,t_\mathrm{u} \\ p_2 &= \sqrt{(x_2 - x_\mathrm{u})^2 + (y_2 - y_\mathrm{u})^2 + (z_2 - z_\mathrm{u})^2} + c\,t_\mathrm{u} \\ p_3 &= \sqrt{(x_3 - x_\mathrm{u})^2 + (y_3 - y_\mathrm{u})^2 + (z_3 - z_\mathrm{u})^2} + c\,t_\mathrm{u} \\ p_4 &= \sqrt{(x_4 - x_\mathrm{u})^2 + (y_4 - y_\mathrm{u})^2 + (z_4 - z_\mathrm{u})^2} + c\,t_\mathrm{u} \end{aligned} \tag{5}$$

where (x_i, y_i, z_i) are the individual GPS satellite positions, which are known because the GPS satellites transmit them. The receiver can determine its position and the time offset by solving this system of equations, which means finding the intersection of the spheres centered on the GPS satellites. It can be seen from eq. (5) that if t_u is 0, three satellite positions suffice. In the general case, four are required. If more than four GPS satellites are available, the system is overdetermined and can be solved for example with a least squares method. (Kaplan and Hegarty 2006, p. 21-26, 50-58)

The receiver velocity can be obtained by either forming an approximate derivative of the position or by studying the Doppler shift of the signal from individual satellites. (Kaplan and Hegarty 2006, p. 21-26, 50-58)

The GPS satellite motion relative to the user produces Doppler shift in the GPS signal. The received frequency f_R can be expressed as

$$f_\mathrm{R} = f_\mathrm{T} \left(1 - \frac{\mathbf{v}_\mathrm{r} \cdot \mathbf{a}}{c}\right) \tag{6}$$

where f_T is the satellite transmitted frequency, $\mathbf{v}_r$ is the satellite velocity vector relative to the user, $\mathbf{a}$ is a unit vector pointing from the user to the satellite and c is the speed of light. The dot product produces the radial component of the relative velocity of the GPS satellite, as seen by the user. The actual velocity of the GPS satellite in an Earth-fixed coordinate frame can be calculated from the navigation information transmitted by the satellite. The actual transmitted frequency f_T of a satellite can slightly differ from the nominal value, but corrections to this are included in the navigation messages. Combining Doppler measurements from several satellites yields a three-dimensional velocity vector. (Kaplan and Hegarty 2006, p. 58-61)

More advanced techniques include using the carrier phase of the incoming signal to smooth the pseudorange obtained from the code phase. This is based on the carrier wave having a higher frequency and therefore much shorter wavelength than the code signal. Geodetic-grade receivers use the carrier waves of two different frequencies transmitted by the GPS satellite to completely eliminate ionospheric error (see 2.2.4), which dramatically increases accuracy.

2.2.4 Error sources

While the previous section considered the basics of obtaining a GPS navigation solution, this section gives an overview of the performance and error sources of SPS GPS. (Kaplan and Hegarty 2006, p. 243, 292-295, 305-320)

GPS satellites carry atomic clocks that are synchronized to the GPS time. However, this synchronization is not perfect, and clock corrections are broadcast in the GPS navigation data message to be used by the receiver. The clock corrections are not perfect either, and a residual error remains.

Group delay error is introduced by the imperfect synchronization of different signal paths inside the GPS satellite relative to the satellite clock.

The GPS control segment determines the GPS satellite orbits. The orbital positions are broadcast in the navigation data message as the satellite ephemerides. This position determination will have an error which then affects the navigation solution as well.

RF effects that can degrade GPS performance include radio frequency interference, multipath effects and atmospheric scintillation. Radio frequency interference is caused by any unwanted signals received by the GPS receiver. Interference can be intentional jamming, or unintentional out-of-band signals from other radio sources.

Ionospheric scintillation refers to the effect the Earth's ionosphere can have on the GPS signal levels. The ionosphere is an area around the Earth beginning from above an altitude of c. 50 km, that contains free positive ions and free electrons. The main effect of the ionosphere on GPS is signal delay, which can degrade position accuracy, but variations in electron densities can cause drops in signal levels as well.

Tropospheric delay refers to signal refraction in the electrically neutral, lowest part of the Earth's atmosphere. The delay is dependent on viewing angle toward the satellite and the local temperature, pressure and relative humidity.

Multipath effects result from GPS signal being reflected from surfaces between the GPS satellites and the receiver, which will result in the GPS signal arriving to the receiver through one direct path and through some indirect paths. The arriving signals need to be processed to recover the direct-path signal, because the indirect path signals could cause error in the pseudorange as they have traveled a longer distance.

Additionally, the imperfection of GPS receivers introduces a noise and resolution-related error component.

The effects of the error sources on the pseudorange measurements are listed in table 2.

Table 2: User equivalent range error budgets as defined by the GPS SPS Performance Standard (2008). The total UERE values can be used to estimate pseudorange error, which then can be used to estimate the error in the final navigation solution. Zero AOD refers to the instant when the ephemerides are updated to the GPS satellites. It is the instant when all the parameters are the most accurate. The user segment values depend on the receiver model. (USDOD 2008)

Segment	**Error source**	**Effect (m) (Zero AOD)**
Space	Clock stability	0.0
	Group delay stability	3.1
	Other space segment errors	1.0
Control	Clock/ephemeris estimation	2.0
	Clock/ephemeris curve fit	0.8
	Ionospheric delay model terms	9.8-19.6
	Group delay time correction	4.5
	Other control segment errors	1.0
User	Ionospheric delay compensation	N/A
	Tropospheric delay compensation	3.9
	Receiver noise and resolution	2.9
	Multipath	2.4
	Other user segment errors	1.0
Total	95% UERE (Zero AOD)	12.7-21.2
	Max 95% UERE (Max AOD)	24.1

2.2.5 Performance of SPS GPS

Dilution of Precision (DOP) values can be used to describe how much the user-satellite geometry affects positioning accuracy through propagation of pseudorange error to position and time error. As a rule of thumb, a small number of satellites concentrated on a small part of the sky produces worse (higher) DOP than a large number of satellites spread evenly around the sky. Only the computation of DOPs is considered here, and a more rigorous derivation can be found in Kaplan and Hegarty (2006, p. 322-326).

The design matrix **H** can be defined as

$$\mathbf{H} = \begin{bmatrix} a_{x1} & a_{y1} & a_{z1} & 1 \\ a_{x2} & a_{y2} & a_{z2} & 1 \\ \vdots & \vdots & \vdots & \vdots \\ a_{xn} & a_{yn} & a_{zn} & 1 \end{bmatrix}, \tag{7}$$

where $a_{xi,yi,zi}$ are unit vectors from the (approximate) receiver position toward the n GPS satellites. They are the directions of the pseudorange errors.

A normal matrix is then formed to describe how the error from the pseudorange measurements is propagated to position and time errors. The normal matrix **Q** is computed as

$$\mathbf{Q} = (\mathbf{H}^T\mathbf{H})^{-1}, \tag{8}$$

and it can be expanded to

$$\mathbf{Q} = \begin{bmatrix} d_x^2 & d_{xy}^2 & d_{xz}^2 & d_{xct}^2 \\ d_{xy}^2 & d_y^2 & d_{yz}^2 & d_{yct}^2 \\ d_{xz}^2 & d_{yz}^2 & d_z^2 & d_{zct}^2 \\ d_{xt}^2 & d_{yt}^2 & d_{zt}^2 & d_{ct}^2 \end{bmatrix}. \tag{9}$$

The DOP values are calculated using the diagonal terms of the **Q** matrix. Geometric Dilution of Precision (GDOP) is the most general of the DOP values, and it is defined as

$$GDOP = \sqrt{d_x^2 + d_y^2 + d_z^2 + d_{ct}^2}. \tag{10}$$

Position Dilution of Precision (PDOP) is defined as

$$PDOP = \sqrt{d_x^2 + d_y^2 + d_z^2}, \tag{11}$$

and Time Dilution of Precision (TDOP) is defined as

$$TDOP = \sqrt{d_{ct}^2}. \tag{12}$$

PDOP can be used to estimate the position error σ_p of SPS GPS with the equation

$$\sigma_\mathrm{p} = PDOP * \sigma_\mathrm{UERE}, \tag{13}$$

where the value for σ_UERE can be found in table 2. Some position error values obtained with this equation are presented in table 3.

With a fully functioning GPS constellation and an open view of the sky, PDOP should almost always be less than 6. (USDOD 2008) In addition, the current number of operational satellites, around 30, is likely to improve GPS performance. A global GPS performance report in summer 2012 indicated that PDOP around the world was 2.755 or less for 99.9% of the time. (FAA 2012)

More sophisticated GPS receivers can achieve better UERE performance. In addition, more accurate GPS satellite ephemerides can be obtained from the National Geodetic Survey, and they can be used in the post-processing stage.

Table 3: 95% spherical position error based on 12.7 m and 24.1 m 95% UEREs. Measurements with over 10 or 20 PDOP are usually discarded. For example, a navigation fix with 8 PDOP is accurate to within 101.6 meters with 95% certainty with 12.7 m UERE. DOP values are dependent on the user-satellite geometry and the number of visible satellites.

PDOP	**95% position error (m)** 95% UERE 12.7 m	**95% position error (m)** 95% UERE 24.1 m
1	12.7	24.1
2	25.4	48.2
3	38.1	72.3
4	50.8	96.4
5	63.5	120.5
6	76.2	144.6
8	101.6	192.8
10	127.0	241.0
20	254.0	482.0

2.2.6 Coordinate systems

Two types of coordinate systems are important for GPS: Earth-centered Earth-fixed (ECEF) frames for relating the GPS position fixes to geographic locations, and Earth-centered inertial (ECI) frames for orbit determination. Receivers do their calculations in an ECEF frame and also provide their navigation fixes in this frame. On the other hand, determining the satellite orbit from these observations requires transforming them to an ECI frame. (Kaplan and Hegarty 2006, p. 26-28)

The main reference frames used are the International Terrestrial Reference Frame (ITRF) and the Geocentric Celestial Reference Frame (GCRF). (Petit and Luzum 2010) Both are described in this section.

Earth-fixed coordinate systems

GPS receivers calculate the user's position in an Earth-centered, Earth-fixed coordinate frame known as WGS84. WGS84 is a standard controlled by the United States Department of Defense which provides an earth-fixed reference frame, a model of the gravitational field of the Earth and an ellipsoidal model of the Earth's shape. (Kaplan and Hegarty 2006, p. 29)

The origin of the WGS84 frame is located at the Earth's center of mass, and the axes are fixed with respect to the Earth's surface. The z-axis points toward the direction of the North Pole (IERS Reference Pole). The equator is defined as the plane normal to the z-axis and intersecting the origin. The x-axis intersects the IERS Reference Meridian (Greenwich meridian) at equator and the y-axis completes the right-handed set, also

intersecting the equator. This kind of coordinate system is suited for most navigation applications, as the WGS84 ECEF coordinates can be easily transformed to latitude, longitude and altitude. (NIMA 2000, p. 2-1 - 2-2) (Kaplan and Hegarty 2006, p. 28)

The International Terrestrial Reference Frame (ITRF) is an ECEF frame maintained by the International Earth Rotation and Reference Systems Service (IERS). A new ITRF frame is produced every few years with new measurements by using the International Terrestrial Reference System (ITRS), which describes the procedures for producing such frames. ITRS is defined very similarly to WGS84. (Petit and Luzum 2010, p. 31-42)

WGS84 differs slightly from the International Terrestrial Reference Frame. However, as the error is in the centimeter range worldwide, the two frames can be considered equivalent. (NIMA 2000, p. 2-5, 7-1)

Celestial coordinate systems

Orbit determination is easier in an Earth-centered inertial (ECI) coordinate frame, because in an inertial frame Newton's equations of motion apply in their simplest form. The origin of an ECI frame is also at the center of mass of the Earth, but its coordinate axes are fixed with respect to distant astronomical objects. The orbits of GPS satellites are determined and expressed in an ECI frame, as will be done with Aalto-1. (Kaplan and Hegarty 2006, p. 27-28)

The International Celestial Reference Frame (ICRF) is an inertial frame maintained by the IERS. As with the ITRF, new ICRF frames are produced every few years with new measurements by using the International Celestial Reference System (ICRS). (Montenbruck and Gill 2003, p. 169-172)

ICRF is currently the standard astronomical reference frame used to define the positions of the Earth, other planets and other astronomical objects. ICRF is fixed with respect to extragalactic radio sources, providing a nearly perfect inertial frame. The origin of ICRF is at the barycenter of the Solar System. A system called FK5 J2000 was previously used as the standard astronomical reference frame, and the FK5 J2000 axes directions were carried to ICRF to within the accuracy of the former. The x-axis points toward the vernal equinox at the epoch J2000 and the z-axis is parallel with the Earth's rotation axis toward the north at the same epoch. The y-axis completes the right-handed set. Epoch J2000 refers to 12:00 TT (Terrestrial Time) on January 1, 2000. (Montenbruck and Gill 2003, p. 169-172)

An inertial coordinate system centered on the Earth is useful for calculating orbits around the Earth. The Geocentric Celestial Reference Frame (GCRF) has its coordinate axes defined as in ICRF, but the origin is at the Earth's center of mass. (Montenbruck and Gill 2003, p. 169-172)

ECEF and ECI frames are depicted in fig. 6.

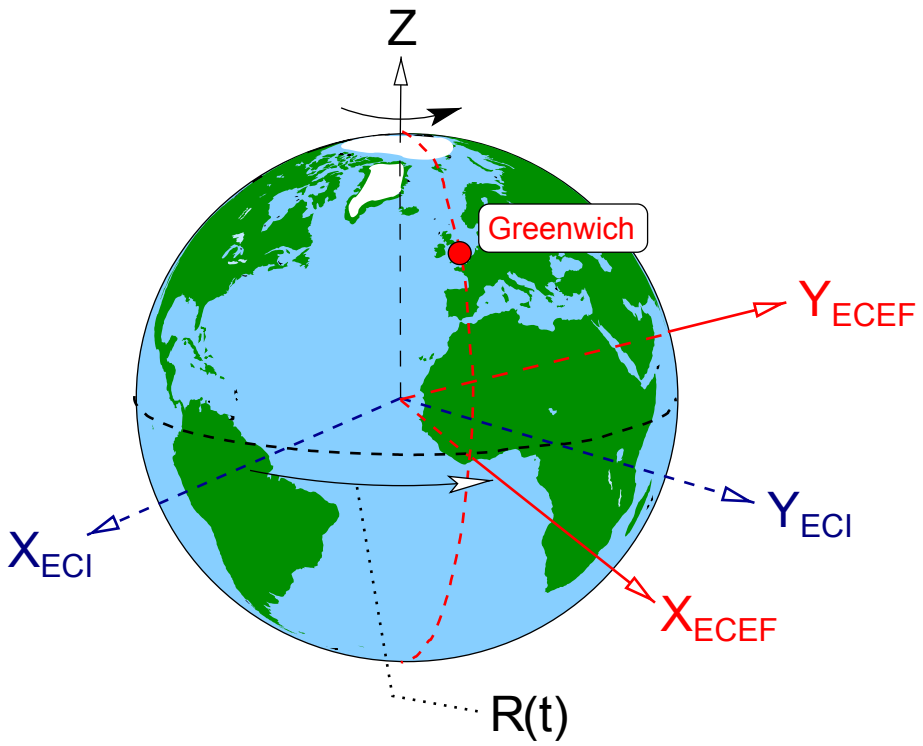

Figure 6: ECEF and ECI frames and the rotation R(t) between them. Earth's rotation around its axis is by far the dominant factor in the rotation in short timescales. X_{ECI} points toward the J2000 vernal equinox. Adapted from an original by Martin Vermeer.

Transformations between GCRS and ITRS

IERS provides transformations between the ITRS and GCRS. The transformation is a function of time, and consists of four rotation matrices:

- $\mathbf{P}(t)$: precession of the Earth's rotation axis (from epoch J2000).
- $\mathbf{N}(t)$: nutation of the Earth's rotation axis.
- $\Theta(t)$: rotation of the Earth about its axis.
- $\Pi(t)$: difference between the Earth's true rotation axis and the IERS Reference Pole. Also known as polar motion.

The transformation from GCRS to ITRS can be expressed as

$$\mathbf{r}_{\mathrm{ITRS}} = \Pi(t)\ \Theta(t)\ \mathbf{N}(t)\ \mathbf{P}(t)\ \mathbf{r}_{\mathrm{GCRS}}, \tag{14}$$

where $\mathbf{r}_{\mathrm{ITRS}}$ and $\mathbf{r}_{\mathrm{GCRS}}$ are the ITRS and GCRS position vectors, respectively. Equivalently, the transformation from ITRS to GCRS can be expressed as

$$\mathbf{r}_{\mathrm{GCRS}} = \mathbf{P}^T(t)\,\mathbf{N}^T(t)\,\Theta^T(t)\,\Pi^T(t)\,\mathbf{r}_{\mathrm{ITRS}}. \tag{15}$$

Formulas for the rotation matrices can be found in Petit and Luzum (2010, p. 43-78) or in Montenbruck and Gill (2003, p. 172-185).

2.2.7 Time systems

In terms of this thesis, two time systems - UTC and GPS time - are relevant for general time-keeping and for GPS. UTC can be used for time tagging of Aalto-1 mission events, while GPS time is used by the receiver in its navigation solution.

UTC

Coordinated Universal Time (UTC) is the primary time standard in the world, used to coordinate clocks worldwide. UTC is a composite of atomic clock time (International Atomic Time, TAI) and a measure of the Earth's rotation angle with respect to the Sun (Universal Time, UT1).

TAI is a combined measurement made by more than 200 atomic clocks in laboratories around the world. These clocks measure the passing of SI seconds. SI second is defined as

> "the duration of 9,192,631,770 periods of the radiation corresponding to the transition between the two hyperfine levels of the ground state of the caesium 133 atom." (BIPM 2006)

TAI is a uniform time standard as no leap seconds are added and seconds are always of the same length. Terrestrial Time (TT) mentioned in Section 2.2.6 is an ideal time standard related to TAI that cannot be exactly reproduced by clocks, but a realization of it can be stated within millisecond accuracy as

$$TT = TAI + 32.184\ \mathrm{s} \pm 0.001\ \mathrm{s}. \tag{16}$$

UT1 is one of the components in the Earth's ECEF orientation parameters with respect to an ECI frame. Variations in the Earth's rotation rate mean that UT1 is a non-uniform time standard.

The passing of UTC is measured by TAI, but leap seconds are added to UTC so that it agrees with UT1 to within 0.9 seconds. UTC was defined to be TAI - 10 s on epoch 00:00:00 January 1, 1972. Since then, leap seconds have been added to UTC. As of early 2013, UTC is TAI - 35 s. (Kaplan and Hegarty 2006, p. 61-62)

GPS time

GPS time is derived from UTC. Similarly to TAI, it is measured by atomic clocks, which are located in the GPS satellites and at control segment components. No leap seconds are added to GPS time. GPS and UTC times were coincident on 00:00:00, January 6, 1980. The GPS control segment is required by the GPS standard to steer GPS time to within 1 μs of UTC (not counting leap seconds), but the difference is typically within 50 ns. A GPS day is exactly 86400 seconds. GPS time is also measured by GPS weeks that are numbered sequentially beginning on Saturday-Sunday midnight 00:00:00, January 6, 1980.

GPS receivers solve the exact GPS time as a part of solving the navigation equations. UTC time can be obtained from this time to within 1 μs by subtracting the integer number of leap seconds from GPS time, and more accurately by also adding the fractional difference between UTC and GPS time which is provided as a part of the GPS navigation messages.

The exact GPS time t_{GPS} can be solved by the receiver as

$$t_{\mathrm{GPS}} = t_{\mathrm{rcv}} - t_{\mathrm{u}} \tag{17}$$

where t_{rcv} is the receiver clock time and t_{u} is the receiver clock correction solved as a part of eq. (5).

When the receiver has solved the GPS time, UTC time t_{UTC} can be solved as

$$t_{\mathrm{UTC}} = t_{\mathrm{GPS}} - \Delta t_{\mathrm{LS}} + \delta t_{\mathrm{A}} \tag{18}$$

where Δt_{LS} is the integer number of leap seconds and δt_{A} is the fractional part of the clock correction obtained from the GPS navigation message. (Kaplan and Hegarty 2006, p. 62-63)

2.2.8 Related global navigation systems

In addition to GPS, the Russian GLONASS navigation system is also operational and the Chinese Compass and European Galileo systems are in development.

GLONASS is a Russian satellite navigation system, and paralleled GPS in development until the late 1990s when the system deteriorated due to lack of funding. GLONASS was

designed for military and civilian use and is remarkably similar to GPS. After restarting funding, the system became fully operational again in late 2011. Like GPS, GLONASS also has a constellation of 24 satellites. However, the satellites are located on three orbital planes with a slightly higher inclination than GPS, which allows for better operation near the polar regions. As of this writing, GPS and GLONASS are the only fully operational global navigation satellite systems. (Kaplan and Hegarty 2006, p. 595-615)

Compass will be the second stage of the Chinese BeiDou navigation system, which is currently operational in areas in or near China. Compass will consist of 35 satellites, of which 5 will be on geostationary orbits and the rest 30 on medium Earth orbits somewhat similar to GPS. (Kaplan and Hegarty 2006, p. 615-625)

Galileo is a navigation system being developed by the European Union. Galileo will consist of 30 satellites of which 27 are active and 3 serve as spares. The satellites will orbit on three evenly spaced orbital planes with a 56° inclination. It differs from the other navigation systems discussed that it is designed primarily for civilian use. Higher-precision navigation is reserved for paying customers and for the military. (Kaplan and Hegarty 2006, p. 559-594)

Both Compass and Galileo aim to provide global navigation services by 2020.

2.3 Satellite tracking with GPS

This section discusses satellite tracking with GPS. A brief introduction to satellite orbits is given first to enable the reader to understand the movement of satellites in space.

2.3.1 Satellite orbits

Traditionally Newtonian mechanics has been used in orbit analysis, and it is also suitable for the purposes of this thesis. In orbit analysis, a rigid spacecraft can be approximated as a point mass at the center of mass of the spacecraft. For this analysis, Newton's second law can be expressed as

$$\ddot{\mathbf{r}} = \frac{\sum \mathbf{F}(t, \mathbf{r}, \dot{\mathbf{r}})}{m}, \tag{19}$$

where $\mathbf{r}$ is the position, $\dot{\mathbf{r}}$ is the velocity, $\ddot{\mathbf{r}}$ is the acceleration, t is time, $\sum F$ is the sum of the forces acting on the satellite and m is the mass of the satellite. An Earth-centered inertial reference frame is used for the vector quantities. (Fortescue, Stark, and Swinerd 2003, p. 49-58)

As can be seen from eq. (19), the forces affecting the motion of the satellite depend on time, position and velocity. The near-Earth space environment includes forces such as

Earth's gravity and the gravity of other celestial bodies (most importantly the Sun and the Moon), solar radiation pressure and atmospheric drag. Propulsion systems can be used to produce desired forces. In Earth orbit, Earth's gravity is by far the most dominant force affecting the motion of a satellite. Using an ECI frame, an approximation of the acceleration caused by the Earth's gravity (Newton's law of gravitation) can be written as:

$$\ddot{\mathbf{r}} = -\frac{GM}{|\mathbf{r}|^2}\hat{\mathbf{r}}, \tag{20}$$

where G is the gravitational constant, M is Earth's mass and $\hat{\mathbf{r}}$ is a unit vector toward the satellite.

While the position and velocity of a satellite at time instant t can be numerically integrated from eq. (19), this description of the satellite's current state is not very intuitive for predicting its future or past state. Kepler orbit parameters provide a more intuitive description of a satellite's orbit.

According to Johannes Kepler (1571-1630), a satellite in orbit around a much more massive body travels along an ellipse on a two-dimensional plane, of which a circular orbit is a special case. The other focus of the ellipse is at the center of mass of the massive body. This approximation only takes into account the gravity of the central body, but is sufficient for crude orbit analysis.

Six parameters are named after Kepler that unambiguously specify the satellite position around a massive central body. The first two, semi-major axis a and eccentricity e, specify the shape of the ellipse. Eccentricity for elliptical orbits is defined as

$$e = \frac{r_\mathrm{a} - r_\mathrm{p}}{r_\mathrm{a} + r_\mathrm{p}} = \sqrt{1 - \frac{b^2}{a^2}}, \tag{21}$$

where e is the eccentricity, r_a is the apoapsis distance, r_p is the periapsis distance, a is the semi-major axis and b is the semi-minor axis. These are depicted in fig. 7.

Inclination i, longitude of the ascending node Ω and argument of periapsis ω specify the orientation of the ellipse in three-dimensional space. Finally, true anomaly ν specifies the angular position of the satellite along the ellipse. The latter four parameters are depicted in fig. 8.

2.3.2 Orbit perturbations

If satellites followed Kepler orbits precisely, their positions would be easy to determine and satellite tracking would be almost unnecessary after determining the initial orbit parameters. However, Earth's gravity field is not symmetrical due to uneven mass

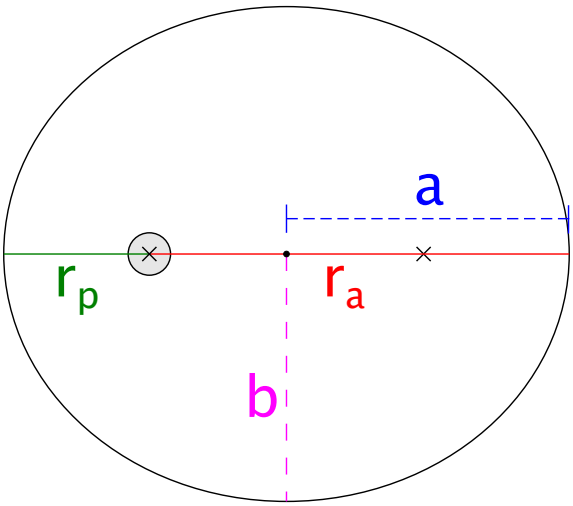

Figure 7: The orbit of a satellite around the Earth is (approximately) an ellipse with one focus at the center of mass of Earth. In a circular orbit, both focii coincide. Periapsis distance r_p is the closest approach to the planet, while the apoapsis distance r_a is the greatest distance. Measured from the center of the ellipse, semi-major axis a is the longest and semi-minor axis b is the shortest distance to the perimeter of the ellipse. In elliptical orbits, eccentricity e is a measure of how much the orbit deviates from a circle.

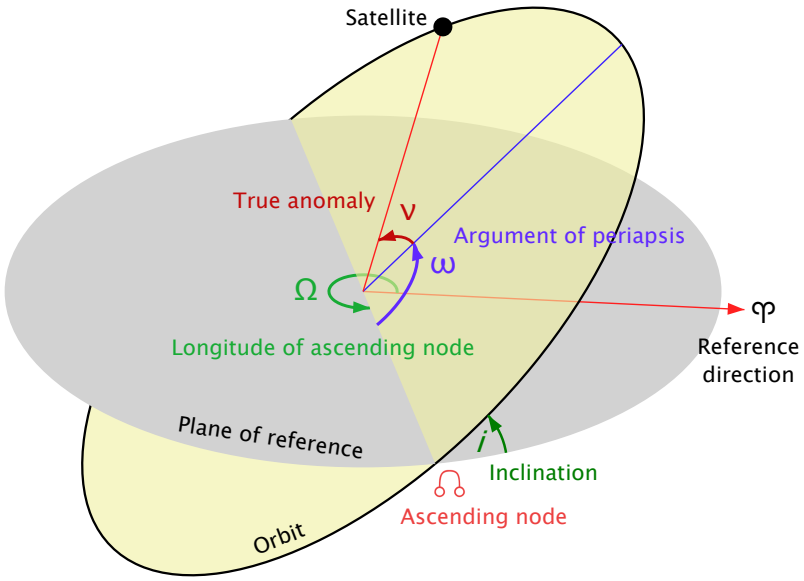

Figure 8: Three of the Kepler parameters - inclination, longitude of the ascending node and argument of periapsis - specify the orientation of the orbital ellipse in three-dimensional space. The reference direction is specified in the used ECI frame (see Section 2.2.6.) Periapsis refers to the lowest point of the orbit and the ascending node refers to the position where the satellite ascends over the equator from south to north. The last parameter, true anomaly, specifies the angular position of the satellite. Adapted from an original by Lucas Snyder.

distribution. Because gravity is the dominant force affecting orbital motion, this asymmetry necessitates the use of more complex models of the Earth's gravity field in orbit propagation.

Atmospheric drag, solar radiation pressure and gravity of other celestial bodies also perturb satellite orbits. Table 4 lists the approximate magnitudes of accelerations caused by different sources on a 500 km Earth orbit. Models describing these forces are not discussed here, but can be found in literature, for example in Montenbruck and Gill (2003).

Table 4: Approximate magnitude of different sources of acceleration on a free-flying 500 km Earth orbit. A/M is the ratio of projected area toward the source of acceleration (A) and the mass of the spacecraft (M). (Fortescue, Stark, and Swinerd 2003, p. 93)

Force	**Magnitude** (m/s^2)
Earth's gravity	8.4
Air drag	$6 \cdot 10^{-5} \cdot A/M$
Radiation pressure	$4.7 \cdot 10^{-6} \cdot A/M$
Sun's gravity (mean)	$5.6 \cdot 10^{-7}$
Moon's gravity (mean)	$1.2 \cdot 10^{-6}$
Jupiter's gravity (max)	$8.5 \cdot 10^{-12}$

The perturbing forces cause the orbit parameters of a satellite change in a way that cannot be modeled exactly. This necessitates regular tracking of satellites. For the same reason, the GPS satellite navigation messages include orbit correction terms in addition to the Kepler orbit parameters, because the GPS navigation messages transmitted by the GPS satellites usually change only once every two hours.

2.3.3 Satellite tracking

Although modern satellites are very autonomous in functionality, commands and data need to be transmitted to and from satellites to make them useful. The satellite position needs to be known in order to know when communication is possible via radio, and where to point the ground station antennas. Many missions also require more accurate position information for their payloads. (Montenbruck and Gill 2003, p. 8)

Traditionally, the orbit of a satellite has been determined by tracking the satellite with a radio link or a radar. Radiometric tracking determines the direction of the satellite's radio signal. Distance can be measured from the signal travel time to the satellite and back, if the satellite carries a transponder. Doppler shift of the signal can be used to determine the velocity of the satellite. Optical and laser tracking of satellites is also used. Laser ranging can be used to determine the direction and distance to a retroreflector-equipped satellite very accurately. (Montenbruck and Gill 2003, p. 8)

Radiometric, optical or laser tracking requires ground stations to be available during the satellite lifetime, which increases the cost of the mission. (Rush 2000)

North American Aerospace Defense Command (NORAD) tracks all sizeable objects in Earth orbit and regularly publishes their orbit parameters at their website in two-line element sets (TLE). This data has a position accuracy of around 1 kilometer when published. TLEs are often used with an orbit propagator known as Simplified General Perturbations 4 (SGP4), with which the position error grows at a rate of 1 to 3 kilometers per day. Because of this, NORAD regularly updates the TLEs. Satellite missions with loose position accuracy requirements can use the TLEs to locate the satellite for communication. (Greene and Zee 2009)

In addition to these techniques, GPS can be used to provide autonomous navigation for satellites in low Earth orbit.

2.3.4 GPS in space applications

NASA's LANDSAT-4 imaging satellite in 1982 was the first satellite with a GPS receiver. (Kaplan and Hegarty 2006, p. 657) In the early 1990s, only a few satellites with GPS receivers were launched; in 1998, more than 30. GPS has also been used in manned spacecraft, such as the Space Shuttle. GPS allows for accurate orbit determination and time synchronization, and for coarse attitude determination. GPS satellite visibility remains similar from sea level to an altitude of about 3000 km. (Rush 2000)

Traditionally, the orbit of a satellite has been determined by tracking the satellite with a radio link or a radar. Radiometric tracking requires tracking stations to be available during the satellite lifetime, which increases the cost of the mission. GPS enables a satellite to independently determine its position and orbit. (Rush 2000)

If the positioning accuracy requirements are moderate, the smoothed navigation solutions produced by the GPS receiver in the WGS84 ECEF frame can be directly used for navigation in real-time. If more accuracy is desired, raw GPS measurements can be downloaded from the satellite to be be post-processed to produce a more accurate navigation solution. (Montenbruck and Gill 2003, p. 206)

GPS receivers also need to solve the current time very accurately to enable accurate positioning. As a byproduct, this time can be output from the receiver to synchronize a satellite's clock with high accuracy. A GPS receiver can be used to steer a low-cost oscillator to a correct time, rather than to use a high precision oscillator with a higher cost. A GPS receiver can be a cheaper option than other means of accurate onboard timing. (Rush 2000)

GPS can also be used for coarse attitude determination. If the direction of the GPS satellite signals can be found, the orientation of the antennas can be found by comparing with the known GPS satellite positions. (Rush 2000)

Because GPS enables a satellite to determine its time and position independently, GPS can be used for satellite automation, such as executing functions at certain positions or maneuvering the satellite for formation flight. (Rush 2000)

2.3.5 GPS in nanosatellites

During the recent years, use of GPS on small satellites has also increased. (Montenbruck et al. 2007) The availability of small, low-power receivers has meant that GPS navigation is increasingly used in nanosatellites as well: Bouwmeester and Guo (2010) found that 16 % of 94 studied pico- and nanosatellites carried a GPS receiver. Some recent examples are presented in table 5. Not all these missions were successful, and some had problems with their GPS subsystems.

Table 5: Some recent nanosatellite missions with an onboard GPS receiver.

Name	Launch	Operator	Mass	GPS receiver
CanX-2[a]	2008	Univ. of Toronto, Canada	3.5 kg	OEM4-G2L
Compass-1[b]	2008	FH Aachen, Germany	1 kg	Phoenix
AggieSat-2[c]	2009	Texas A&M Univ., USA	3.5 kg	DRAGON
Bevo-1[d]	2009	Univ. of Texas at Austin, USA	5 kg	DRAGON
UWE-2[e]	2009	Univ. of Würzburg, Germany	1 kg	Phoenix
AISSat- 1[f]	2010	Norwegian Space Centre, Norway	6 kg	OEM4-G2L
RAX-1[g]	2010	Univ. of Michigan, USA	3 kg	OEMV-1-L1
EDUSAT[h]	2011	Sapienza Univ. of Rome, Italy	10 kg	?
Jugnu[i]	2011	IIT Kanpur, India	3 kg	?
RAX-2[g]	2011	Univ. of Michigan, USA	3 kg	OEMV-1-L1
Goliat[j]	2012	Univ. of Bucharest, Romania	1 kg	?
STRaND 1[k]	2013	SSTL, UK	4.3 kg	SGR-05

[a] Kahr et al. (2011) [b] Scholz et al. (2010) [c] Cluster (2007) [d] Cote et al. (2011)
[e] Schmidt et al. (2008) [f] Dwyer (2009) [g] Arlas and Spangelo (2012)
[h] Paolillo (2008) [i] IIT Kanpur (2011) [j] Balan et al. (2008)
[k] Bridges et al. (2011)

The main benefits of a GPS subsystem for a small satellite are global coverage and high accuracy at a low cost along with the real-time onboard availability of navigation data. The power consumption of GPS receivers vary depending on their type but are usually in the range from 100 mW to a few watts. Usually single-frequency receivers are chosen for general navigation applications while dual-frequency receivers are chosen for GPS-related scientific purposes.

Single-frequency receivers produce real-time navigation solutions with an accuracy of around 10 meters. Dual-frequency receivers can achieve real-time accuracy of around 1 meter by eliminating most of the ionospheric error, but consume more power. Post-

processing can improve the accuracy of both types of receivers. Some GPS receivers used in nanosatellites are listed in table 6. (Montenbruck et al. 2007)

GPS subsystems in nanosatellites need to operate with low power. For example, the average power available for a 3U CubeSat such as Aalto-1 could be around 5 W. (Clark and Logan 2011)

Table 6: Some single- and dual-frequency GPS receivers adapted or designed for space applications that could be suitable for nanosatellites based on their weight and power consumption. Especially the Phoenix and NovAtel receivers have been popular in recent nanosatellites.

Name	**Channels**	**Power**	**Weight**
SSTL SGR-05	12 C/A	800 mW	20 g
DLR Phoenix	12 C/A	850 mW	20 g
NovAtel OEM4-G2L	12x2 C/A, P2	1500 mW	50 g
NovAtel OEMV-1-L1	14 C/A	1100 mW	22 g

2.3.6 The space environment for GPS components

It cannot be immediately assumed that a component designed for terrestrial applications will work in space. The space environment is very different from the one on Earth, and potentially very hostile to electronics and materials. Components in space will be subjected to a near-total vacuum, extreme cold and hot temperatures and higher levels of radiation than on Earth. Additionally, during the launch various mechanical stresses are placed on the components. (Fortescue, Stark, and Swinerd 2003, p. 589-592)

The vacuum of space can cause outgassing in some materials, especially in some plastics. Outgassing refers to the evaporation of surface atoms of a material when the surrounding pressure drops down to the level of the vapour pressure of the material. Increase in temperature will increase outgassing. This problem can be mitigated by selecting components that include materials which experience little outgassing. (Fortescue, Stark, and Swinerd 2003, p. 39-40, 589)

Thermal environment in space is also extreme, as temperature variations on the outer surface of a spacecraft can be more than 100°C. The variations are caused by part of the spacecraft sometimes being in direct sunlight, while part of it is in the shadow. For a part of the orbit, the whole spacecraft can be shadowed by the Earth. This extreme temperature range requires passive or active thermal control, and selecting components that can endure the temperature variations. Thermal control is also complicated by the fact that in vacuum, heat is transferred away from spacecraft only by thermal radiation. (Fortescue, Stark, and Swinerd 2003, p. 355-391, 589)

Ionizing radiation is an issue for electronic components in space, as a spacecraft in orbit is not protected by the Earth's magnetic field and atmosphere. Effects caused

by radiation can be divided into total dose effects and single-event effects. Total dose effects refer to degradation of electronic components due to accumulated radiation dose. The degradation causes the components to deviate from their specified operating parameters, and possibly to break down. Single-event effects occur when ionizing particles pass through the component, and may cause single-event upsets ("bit flips") or single-event latch-ups, possibly destructive short circuits, that can be fatal. Single-event upsets may either corrupt run-time data or data stored in on-board memory for long periods. Run-time errors can be corrected by restarting the software. The effects of radiation can be mitigated by selecting components that degrade little due to radiation, designing software in a way that it can recover from single-event upsets, limiting possible currents to safe levels and by implementing error correction. (Fortescue, Stark, and Swinerd 2003, p. 474-476, 589-592)

GPS receivers designed for terrestrial applications can have software-related problems in orbital conditions. Due to U.S. export restrictions, most civilian GPS receivers are firmware-limited not to produce navigation fixes above c. 18 km altitude or above c. 500 m/s velocity. In orbit, GPS signal dynamics are increased as in LEO the orbital velocity of the satellite will be around 7 km/s, which produces much larger Doppler shifts - around 40 kHz - than are encountered on Earth. Line-of-sight acceleration between the receiver and the GPS satellites can also be higher and cause problems due to the larger rate of change of the Doppler shift. It is possible to resolve or mitigate these problems by tuning the firmware parameters. (Langley et al. 2004)

The main difference between space-grade components and COTS components is that while space-grade components are much more expensive, they have already been designed and qualified to work in space. Selecting a COTS component for a spacecraft means that the component needs to be verified by the spacecraft designer. This can be done by using environmental and functional testing to check the compliance of the component to the mission requirements. (Fortescue, Stark, and Swinerd 2003, p. 589-592)

2.3.7 Example of GPS receiver qualification

An example of qualifying a commercial GPS receiver for space applications is provided here to give an idea how the issues mentioned in the previous section can be tested.

NovAtel's OEM4-G2L dual-frequency COTS GPS receiver was qualified by Langley et al. (2004) for the Canadian Space Agency's CASSIOPE satellite. The velocity and altitude restrictions in the firmware were removed, but otherwise the receivers were not modified for the qualification. Using COTS GPS receivers rather than space qualified ones was a cost-driven decision.

The issues considered critical for the receiver were its ability to navigate in orbit and to survive the radiation, thermal and vacuum environment. Several tests were performed on the receiver to ensure that it will work in space. These included GPS signal simula-

tor tests, radiation tests and thermal vacuum tests. GPS signal simulations were used to test GPS signal acquisition and tracking performance in orbit while radiation and thermal vacuum tests were used to ensure that the receiver will function in the space environment. Another space-qualified GPS receiver, DLR's Phoenix, was developed from commercial components using similar methods. (Montenbruck and Renaudie 2007)

GPS signal environment in orbit was simulated with a Spirent STR4760 GPS signal simulator. The signal simulator was connected to the antenna input of the GPS receiver, and produced the kind of GPS signals the receiver would receive from its antenna in orbit. The navigation accuracy of the receiver was determined by comparing the receiver navigation solutions to reference values from the orbit scenario in the simulator. The test indicated that the receiver could navigate in orbit without modifications to the firmware settings.

Radiation testing was done by radiating a few receivers during two sessions with doses between 6 to 10 krad. Radiation caused the failure of at least a voltage monitor chip, which was then changed to a later test. After the switch, no breakups occurred. As the dose accumulated, a small increase in receiver power consumption was noted.

Thermal vacuum testing from -35°C to +50°C in a 10^{-5} torr vacuum was performed on the receiver to determine the thermal and vacuum effects on the system. No change in the receiver performance was noted.

The qualified receiver, NovAtel OEM4-G2L, was successfully used in 2008 aboard another Canadian satellite, CanX-2. (Kahr et al. 2011)

2.3.8 Antenna considerations

GPS antenna radiation patterns are often hemispherical, as GPS antennas need to be able to receive signals from several satellites which can be almost anywhere in the sky. Hemispherical pattern also decreases interactions with the satellite frame, when the hemisphere is directed away from the satellite. In general, antennas in space need to be very reliable, because in-orbit replacement is nearly impossible. Antennas must also have high performance while at the same time being small and light. Additionally, active antennas - which are often used with GPS - should not consume excessive amounts of power. (Gao et al. 2009)

The space environment also affects antenna design, as antennas too need to survive the radiation, vacuum and thermal environment as well as the mechanical loads during the launch. It must be possible to physically place the antenna into the satellite without disturbing other systems. Electromagnetic compatibility with other satellite electronics needs to be taken into account, as well as radio frequency compatibility issues with the satellite frame and other radios in the satellite. The satellite frame will affect the antenna radiation pattern. (Gao et al. 2009) A poor antenna will cause loss of

GPS fix, fewer satellites to be available and poor accuracy. (Saarnimo 2010)

A combination of simulations and measurements can be used to detect EMC and RF issues. (Gao et al. 2009) As the RF effects of the satellite are dominated by the structures close to the antenna, antenna candidates can be tested by attaching them to crude mockups of the satellite. This will give results about the effect of the frame on the antenna pattern. (Ingvarson et al. 2007) Testing the GPS subsystem performance during the development and as a part of the final, complete system is recommended. (Saarnimo 2010)

Carrier-to-noise ratio can be used to assess the quality of the signal from a GPS satellite to the GPS receiver. Carrier-to-noise ratio (CNR) $(C_S/N_0)_{dB}$ is the ratio between the received carrier signal power C_S and the received noise power N_0. It is expressed in dB-Hz and can be calculated as

$$(C_S/N_0)_{dB} = (C_S)_{dB} - (N_0)_{dB} \tag{22}$$

$$(C_S)_{dB} = (C_{Ri})_{dB} + (G_{SVi})_{dB} - L_{dB} \tag{23}$$

$$(N_0)_{dB} = 10\log_{10}[k(T_{ant} + T_{amp})] \tag{24}$$

$$T_{amp} = 290(10^{\frac{(N_F)_{dB}}{10}} - 1), \tag{25}$$

where $(C_S)_{dB}$ is the recovered signal power from satellite SVi (dBW), $(N_0)_{dB}$ is the thermal noise power component in a 1-Hz bandwidth (dBW), $(C_{Ri})_{dB}$ is the received signal power from SVi at antenna input (dBW), $(G_{SVi})_{dB}$ is the antenna gain toward SVi (dBic), L_{dB} is the receiver implementation loss (dB), k is Boltzmann's constant $1.38 * 10^{-23} J/K$, T_{ant} is the antenna noise temperature (K), T_{amp} is the amplifier noise temperature (K) and $(N_F)_{dB}$ is the amplifier noise figure at 290K (dB). (Kaplan and Hegarty 2006, p. 262-263). According to Saarnimo (2010), the minimum usable CNR for signal acquisition is around 27 to 33 dB-Hz.

2.3.9 Orbit determination from GPS measurements

GPS receivers can usually output fixes in the WGS84 ECEF frame, as position determination is done in this frame. On the other hand, satellite orbits are usually calculated in an ECI frame as the equations of motion are simpler in an inertial frame. GPS receivers produce noisy measurements of the position-velocity state vector of the satellite at certain instants of time. This measured state vector can be transformed into a measured ECI position-velocity state vector as discussed in 2.2.6. The measurements can also be weighted based on the presumed fix quality, which can be evaluated based on signal-to-noise ratios, DOPs and number of satellites. Raw pseudorange data can sometimes be obtained from a receiver for post-processing.

As position-velocity-time data points are obtained, they can be used to determine the orbit of the satellite. This can be done either by post-processing the measurements or in real-time. Numerous methods for fitting an orbit to this kind of set of points in the post-processing stage exist, but the classical method is least squares analysis. Kalman filters are often used in real-time onboard navigation. (Montenbruck and Gill 2003, p. 257-289)

When the satellite orbit has been determined for an epoch, its position and velocity can be solved for any instant of time near that epoch. This means that GPS needs to be on only as long as it takes to reliably produce the number of fixes that determine the orbit at the desired epoch with the required accuracy. Power can therefore be saved by using GPS only when necessary.

2.3.10 Examples of GPS performance in nanosatellites

The performance of two example receivers is described here. The first one is the DLR Phoenix single-frequency receiver and the second one is the NovAtel OEM4-G2L geodetic-grade dual-frequency receiver. Notably, the single-frequency receiver outperformed the dual-frequency receiver.

Phoenix is COTS component-based single-frequency GPS receiver designed for space applications by the German Aerospace Center (DLR). The receiver has 12 C/A channels like the Fastrax IT03 considered in the practical part of the thesis. However, its custom software is designed for space applications which is evident in its performance. The performance example is from Proba-2, which was not a nanosatellite mission, but the receiver has been used in nanosatellites as well. (Markgraf et al. 2010)

During the Proba-2 mission, the receiver was often subjected to radiation induced latch-ups, which did not cause permanent damage due to utilization of overcurrent protection. The latchups led to the decision to use the receiver for usually only one orbit per day, which allowed an orbit propagation accuracy of around 100 m in the post-processing phase. The receiver was used always in cold start mode (discarding any existing navigation information) and time to first fix (TTFF) was usually around 5 to 15 minutes. The receiver tracked around 10 satellites on average. At a PDOP value of 1.5, 2 m RMS error was achieved in real-time positioning, and post-processing was able to improve this to around 0.5 m. The navigation fixes were compared to a precise orbit determination solution. (Markgraf et al. 2010)

The geodetic-grade dual-frequency OEM4-G2L receiver by NovAtel was used aboard the Canadian CanX-2 nanosatellite. The receiver has 12 channels for two L1 and L2 frequencies to compensate for ionospheric error. The receiver has originally been designed for terrestrial applications but had been space-qualified by DLR as outlined in 2.3.7. The receiver had shown sub-meter positioning accuracy in GPS signal simulations. (Kahr et al. 2011)

The receiver used aiding scripts to improve startup performance, and TTFF values of 2 to 5 minutes were achieved. However, the carrier-to-noise ratio of the signal provided by the antenna was unexpectedly poor, which affected the navigation performance. Additionally there were problems with the startup aiding scripts, which caused poorer GPS satellite tracking performance than with the receiver's automatic search algorithm. This resulted to around 6 to 7 satellites being tracked when the scripts were used to 9 to 10 when the automatic search algorithm was used. The position solution had RMS error ranging from 16.1 m to 55.5 m, with peak errors of almost 200 m. The signal and antenna problems in CanX-2 didn't allow the use of OEM4-G2L with its full potential. (Kahr et al. 2011)

3 Design and integration

This chapter presents both the design and integration of a GPS subsystem into Aalto-1. While the design presented in this chapter should be almost final, it should be noted that because the flight model of the satellite won't be ready by the completion of the thesis, only a plan for the final integration can be given.

3.1 Rationale for a GPS subsystem in Aalto-1

Options for performing orbit determination for a nanosatellite mission such as Aalto-1 include ground-based tracking, relying on NORAD-provided orbit parameters, or using GPS. Aalto-1 may have only one ground station available and the satellite will only be visible to this ground station for a limited time per day. Some tracking can be performed, but the achievable accuracy is uncertain. NORAD-provided TLEs can be used for coarse positioning, but the position error can be several kilometers. While this is good enough for most nanosatellite missions, Aalto-1 needs more accurate positioning.

Aalto-1's spectral imager will be used to image various land areas on Earth. The position of Aalto-1 must be known very accurately when taking a picture, as the position information is required in image processing. Error in position knowledge contributes to error in positioning the obtained image geographically. (Kestilä et al. 2013) GPS can provide exact position and time fixes to correct the position estimate obtained from an orbit model.

When deployed, the plasma brake will gradually decelerate Aalto-1. This will decrease the orbital altitude. GPS measurements are needed to determine accurately the changes to the orbit caused by the plasma brake. The radiation monitor also measures the radiation environment as a function of position.

Based on these considerations, it was decided that integrating a GPS receiver into the satellite is the best option for providing accurate positioning. As a side product, the satellite clock can be synchronized very accurately. If the GPS subsystem fails, NORAD-provided TLEs can be used as a backup for positioning. Radio positioning with one ground station may also be attempted. (Kestilä et al. 2013)

3.2 Requirements for the GPS subsystem

When the need for a GPS subsystem in Aalto-1 was recognized, a list of requirements for the subsystem was defined. As the subsystem development progressed, additions and modifications were made to this list.

1. **Operational requirements**

   (a) The GPS subsystem must produce navigation information that allows positioning the satellite within 100 meters of its true position near the measurement epoch. The related velocity information must be accurate to within 20 m/s.

   (b) The GPS subsystem must be able to communicate this navigation information to the on-board computer of the satellite.

   (c) The on-board computer must be able to start and stop the subsystem when needed.

2. **Mechanical requirements**

   (a) The GPS receiver, the required electrical circuit and the antenna connector must fit in the same PCB with the S-band radio, with approximately 3 cm × 10 cm of allocated space.

   (b) The GPS antenna must fit in a space 17.0 mm × 58.0 mm wide and 8.0 mm thick on the flight direction (-Y) side of the satellite.

   (c) The antenna cable from the GPS antenna to the GPS PCB must be of suitable length and thickness, and it must be fastenable along its length to the satellite frame in a way that its vibration or movement cannot damage itself or other systems.

3. **Electrical requirements**

   (a) The GPS subsystem must work with a total power budget of 160 mW.

   (b) The GPS subsystem must work with the voltage levels provided by the electrical power system: 3.3 V, 5 V or 12 V.

   (c) The GPS subsystem must have a shutdown mode consuming a minimal amount of power (< 1 mW).

   (d) The GPS subsystem must work within the electromagnetic environment created by the rest of the satellite system, and should not cause EM interference to other subsystems.

4. **Software requirements**

   (a) The GPS software running on the on-board computer must receive navigation data from the GPS receiver and make selected, relevant parts of it available to other software in the OBC.

   (b) The GPS software running on the on-board computer must be able to send required commands to the GPS receiver, such as configuring parameters, starting, restarting and stopping the receiver.

   (c) The GPS software running on the on-board computer must be able to reprogram the firmware of the GPS receiver in case this firmware becomes corrupted.

5. **Environmental requirements**

   (a) The GPS subsystem must work in a temperature range of -65 °C to +90 °C.

   (b) The GPS subsystem must not contain materials susceptible to outgassing. The subsystem must survive the vacuum of space.

   (c) The GPS subsystem must mitigate and survive radiation damage, including total dose and single-event effects.

   (d) The GPS subsystem must survive the vibration, acceleration and mechanical stresses placed on it by the launch.

3.3 Receiver and antenna selection

3.3.1 Selection criteria

The selection was done based primarily on the requirements outlined in the previous section, but also based on the off-the-shelf availability of the components. Fastrax Oy agreed to provide Aalto-1 project with IT03 receivers and with required support. Selecting the GPS antenna was a longer process, and required several development tests. Based on development tests with the IT03, it was decided that the GPS antenna should provide a carrier-to-noise ratio (CNR) of around 45 dB-Hz or more. Combining the 45 dB-Hz CNR requirement with a strict size budget was found to be hard, but finally the ADA-15S antenna by Adactus AB was selected for further development due to it conforming to the initial requirements and due to it being available with custom-length cables and custom antenna connectors.

3.3.2 The receiver

Figure 9: A Fastrax IT03 GPS receiver module.

The Fastrax IT03 GPS receiver module, shown in fig. 9, was selected for Aalto-1 due to its small size, low power consumption and support offered by Fastrax Oy. The receiver was considered promising, and conformance to the remaining requirements would be tested. The main specifications of the module are listed in table 7.

Table 7: Fastrax IT03 main specifications. (Fastrax Oy 2007) (Fastrax Oy 2010, p. 9)

Receiver	GPS L1 C/A code, SPS
Channels	12
Update rate	< 5 Hz (1 Hz default)
Sensitivity, acquisition	-141 dBm (-171 dBW)
Sensitivity, navigation	-155 dBm (-185 dBW)
Dimensions	22 mm x 23 mm x 2.9 mm
Mass	3 g
Supply voltage, RF	2.7 V ... 3.3 V, max 2 mV (RMS) ripple
Supply voltage, digital	2.7 V ... 3.3 V
Power consumption	100 mW typical (not including antenna)
Operating and storage temperature	-40°C ... +85°C
Serial protocols	NMEA 0183, iTalk

For navigation, Fastrax IT03 uses the Atheros uN8130 processor and the Atheros uN8021 RF down-converter. It also has amplifiers and a band-pass filter for the radio signal, flash memory and IO pads. The receiver has a 12-channel tracking unit, which allows the receiver to track 12 GPS satellites simultaneously. A block diagram of the receiver is presented in fig. 10. (Fastrax Oy 2010, p. 7)

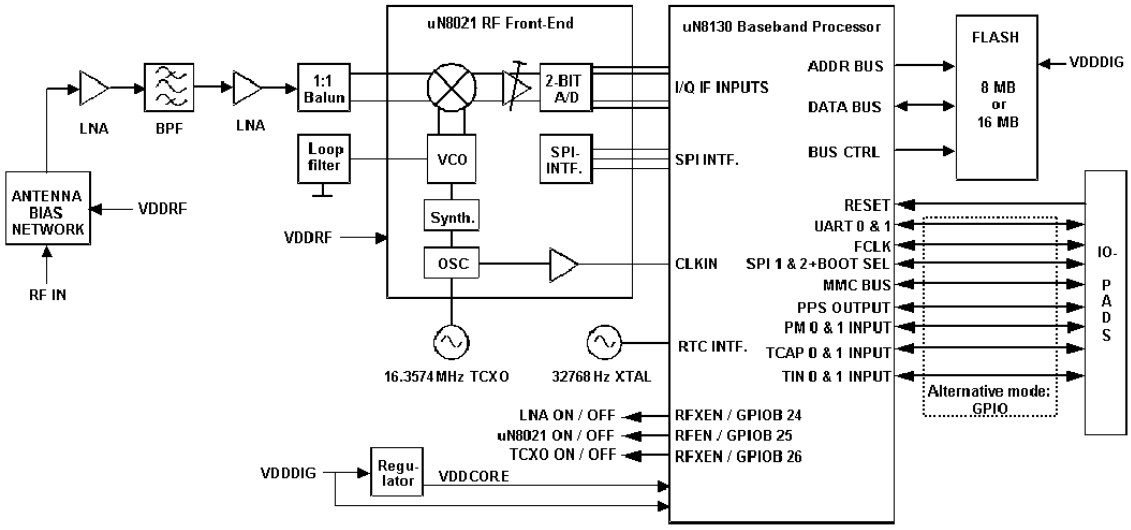

Figure 10: Fastrax IT03 internal block diagram.

By default, the receiver automatically starts to navigate when powered on. The receiver can be commanded to an idle mode, during which the processor remains active, but does not navigate. The receiver can also be commanded to a sleep mode, in which it

consumes very little power but nonetheless maintains clock information, which makes restarting navigation faster. The receiver also has a programming mode, which allows the firmware to be updated. (Fastrax Oy 2010, p. 11-12)

IT03 can be configured to provide a PPS timing pulse at the beginning of each GPS second. The rising edge of this pulse can be used to synchronize the OBC clock with microsecond accuracy.

The receiver supports UART communication. The data format can be selected between the NMEA 0183 standard and Fastrax's own iTalk protocol. The receiver uses transistor-transistor level (TTL) logic at its I/O pins, which means that it can be directly connected to the Aalto-1 OBC. (Fastrax Oy 2010, p. 9)

3.3.3 The antenna

Selection of a suitable antenna and proper integration is critical for the operation of the GPS subsystem. (Scholz et al. 2010) (Kahr et al. 2011)

It was decided during the GPS component selection process that the selected antenna should provide IT03 with a carrier-to-noise ratio (CNR) of around 45 dB-Hz or more. This value was selected because it was noticed that the receiver does not function reliably with under 40 dB-Hz CNR, and some margin was desired in case other systems of the satellite should cause interference. Reference antennas provided by Fastrax with IT03 provided around 50 dB-Hz of CNR.

Antenna selection proved to be hard, because size and weight budgets were very strict, and Taoglas AP.10F and AP.17E only provided around 40 dB-Hz of peak CNR, which meant that the receiver would work only barely and there was no margin for interference. It was suspected that the low CNR was due to a lower-gain amplifier and smaller antenna element size than in the Fastrax-provided reference antennas. However, a poor cable adapter used in testing could not be ruled out as the cause. Three antennas in total were evaluated, and they and the reference antenna are compared in table 8.

Table 8: Comparison of the three evaluated antennas and the reference antenna provided by Fastrax. The reference antenna had the best performance but didn't fit in the size budget. Peak antenna gain, LNA gain and noise figure are from the antenna datasheets, while the CNR is an approximate value measured with IT03. (Taoglas 2012a) (Taoglas 2012b) (Adactus AB 2010) (Beyondoor 2012)

Name	Peak ant. gain	LNA gain	Noise figure	CNR with IT03
Taoglas AP.10F	-10 dBic	25 dB	2.5 dB	c. 40 dB-Hz
Taoglas AP.17E	-1 dBic	16 dB	2.5 dB	c. 40 dB-Hz
Adactus ADA-15S	0.5 dBic	27 dB	1.5 dB	c. 45 dB-Hz
BY-GPS/Glonass-03	3 dBic	28 dB	1.5 dB	c. 50 dB-Hz

Figure 11: An Adactus ADA-15S active patch antenna. (Adactus AB 2010)

ADA-15S antenna by Adactus AB, depicted in fig. 11, was selected for development, because it was available with MCX, U.FL and SMA connectors and it has an amplifier with a higher gain than AP.17E. MCX connectors would be used in testing with Fastrax IT03 Application Boards, while the IPEX U.FL or SMA connectors could be used in the satellite. ADA-15S also seemed to have better specifications than the tested Taoglas antennas, and ADA-15S was available with custom cable thickness and length and with several connectors. The specifications of the antenna are listed in table 9. Development tests indicated that the ADA-15S antenna provided around 45 dB-Hz of CNR with the tracked satellites. The antenna pattern of the ADA-15S antenna is depicted in fig. 12.

Table 9: Adactus ADA-15S main specifications. (Adactus AB 2010)

Type	Active patch antenna
Frequency	1575.42 ± 3 MHz
Total gain	25 dB
Noise figure	1.5 dB typical
Impedance	50 Ω
VSWR	< 2.0:1
Supply voltage	2.5 V ... 5.5 V
Power consumption	30 mW at 3.3 V
Size	15 mm x 15 mm x 6 mm
Weight	4.0 ± 0.5 g (without cable)

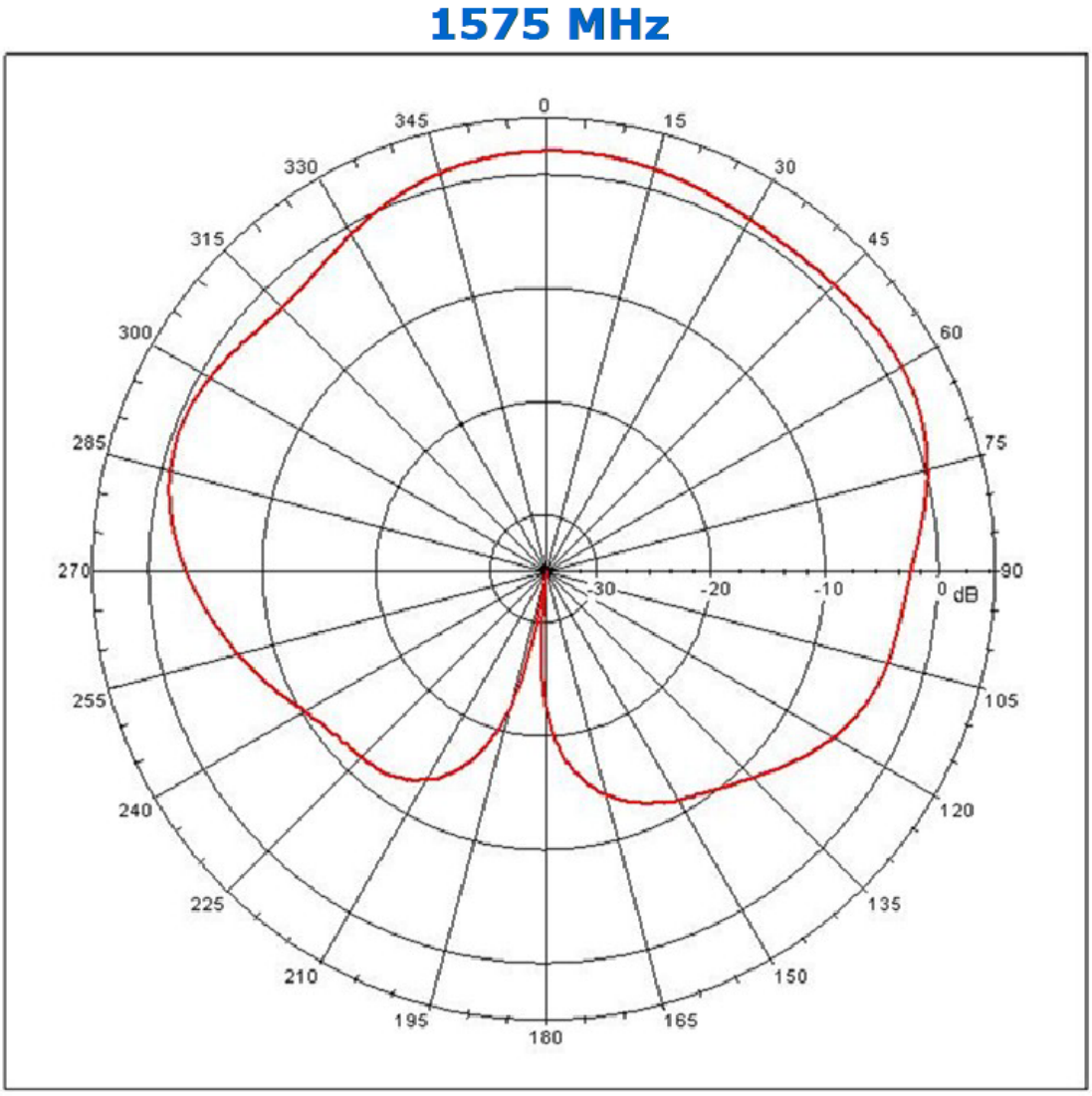

Figure 12: The nearly hemispherical antenna pattern reported in the Adactus ADA-15S datasheet, here "0" direction is up. The direction of the gain is on the perimeter and the gain in dB is shown radially. (Adactus AB 2010)

3.4 System-level description

The GPS subsystem produces accurate position, velocity and time information and communicates this information to the on-board computer via a UART serial line. It consists of two main parts: The GPS subsystem PCB and the active patch antenna. The GPS receiver is powered by a 3.3V bus provided by the electrical power system of the satellite, and the active patch antenna is powered by the receiver. A diagram of GPS subsystem is presented in fig. 13.

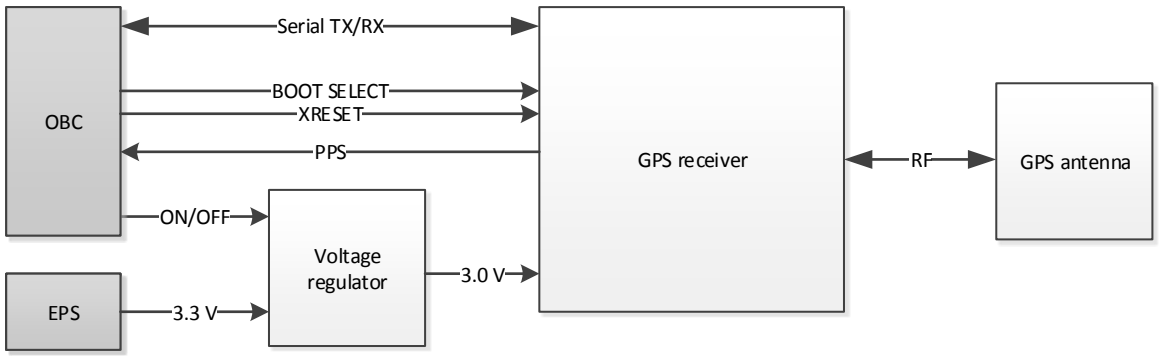

Figure 13: Block diagram of the GPS subsystem. Commands and navigation information are communicated between the on-board computer (OBC) and the GPS subsystem through TX/RX serial lines. BOOT SELECT and XRESET lines enable hardware-based firmware reprogramming in case the firmware on the GPS receiver needs to be updated. The GPS receiver provides the OBC with a pulse-per-second (PPS) signal which allows accurate clock synchronization. The OBC can also control an ON/OFF pin to shut down the GPS subsystem voltage regulator. The electrical power system (EPS) provides the subsystem's voltage regulator with 3.3 volts. The GPS receiver provides the active GPS antenna with a voltage bias and the antenna provides the receiver with GPS signals. All digital signals are at transistor-transistor logic (TTL) levels.

3.5 Mechanical design and integration

The GPS receiver module is situated on the GPS/S-band PCB near center of the satellite. This PCB contains both the S-band radio and GPS circuits. The GPS circuit has a SMA antenna connector for the GPS antenna. Mechanical dimensions of the PCB are adapted from the CubeSat Kit PCB specification, which is derived from the PC/104 specification. (Pumpkin, Inc. 2003) The material of the PCB is the common FR-4 composite. The PCB has four screw holes at its corners, so it can be stacked with other subsystems using screws or rods. A prototype PCB layout is included in Appendix A.

A hole will be made in the -Y side of the satellite frame for the antenna, and the antenna will be attached with an adhesive material to an attachment plate that is mounted to the frame with screws. The antenna cable is then connected to the antenna connector on the PCB, and the cable is fastened along its length to the frame to prevent it damaging itself or other systems due to vibration. The nominal flight mode of the satellite is +X toward nadir and -Y toward flight direction. Placing the antenna on the -Y side of the satellite was a compromise with solar panel placement. The GPS antenna will not point toward zenith in the nominal flight mode, and this is likely to affect positioning accuracy. A sketch of the mechanical design of the satellite is presented in fig. 14.

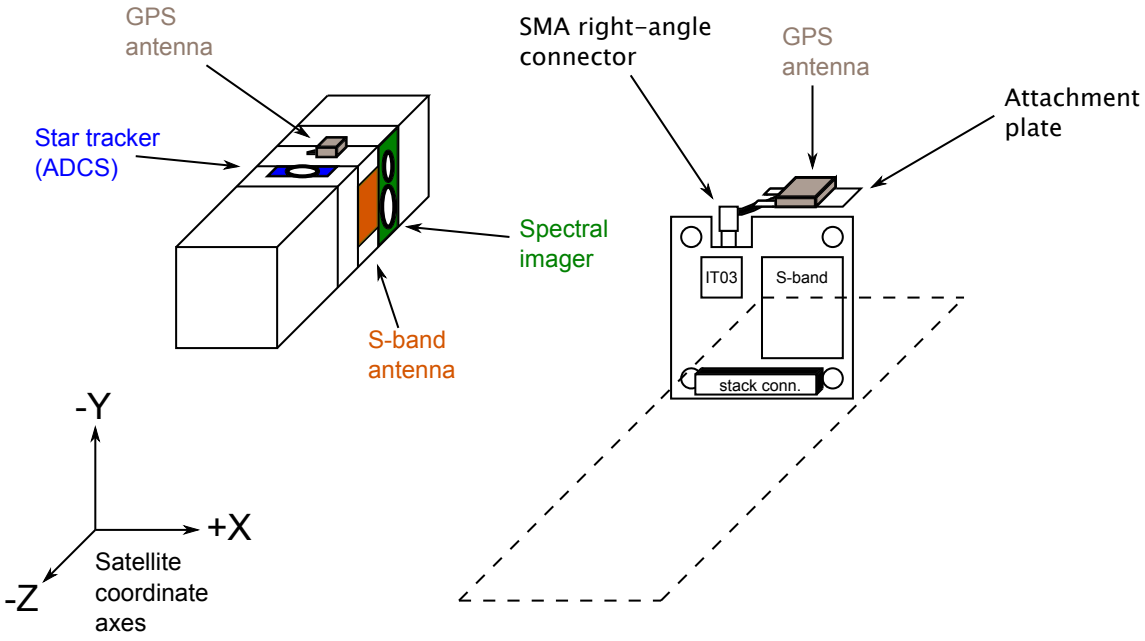

Figure 14: A sketch of the mechanical design of the GPS subsystem.

The antenna connector was initially designed to be IPEX U.FL due to the wide availability of antennas with this connector, and this connector can be seen in the first prototype of the PCB in fig. 16. However, the IPEX U.FL connector is fragile and it was decided that the connector would be switched to a more robust SMA connector. SMA connectors are also used in other RF connections in the satellite. The GPS antennas should be ordered with right-angle SMA connectors and with 5 to 10 cm long cable, the exact length depending on the satellite assembly process.

3.6 Electrical design and integration

The GPS subsystem has been allocated 160 mW of power, of which 130 mW is for the receiver and 30 mW for the active patch antenna. (Näsilä et al. 2012, p. 23)

The subsystem is powered through a 3.3 V bus provided by the EPS of the satellite, and it communicates with the Aalto-1 OBC through a UART serial line and four GPIO pins: ON/OFF, XRESET, BOOT SELECT and PPS. ON/OFF is connected to the enable pin of the voltage regulator supplying power to the receiver. XRESET and BOOT SELECT are used for updating firmware on the receiver. The pulse-per-second (PPS) output of the receiver is used to synchronize the on-board computer clock. The active GPS antenna is powered through the antenna connector.

The TPS73130 voltage regulator by Texas Instruments was selected based on perceived high quality and good environmental specifications. Resistor and bypass capacitor values were selected based on the IT03 and voltage regulator datasheets, and the individual passive components were again selected based on perceived high quality and good environmental specifications. The selected components are listed in table 10.

Table 10: List of electrical components selected for the GPS PCB. The first prototype was built with slightly cheaper components with the same electrical specifications. The prototype also had an IPEX U.FL antenna connector, but the later versions will have a SMA connector. The components were primarily selected for their perceived high quality and wide operating temperature ranges. The AEC-Q200 is a stress test standard used primarily for automotive components. It includes among others the −55° C ... +125° C operating temperature range. (Syfer 2010)

Type	Quantity	Part number	Notes
3.0 V low-dropout voltage regulator	1	TPS73130MDBVREP	Temperature range −55°C ... +125°C
330 Ω resistor	5	CRCW0603330RJNEA	AEC-Q200 qualified
4.7 kΩ resistor	2	CRCW06034K70JNEA	AEC-Q200 qualified
4.7 μF capacitor	2	12105C475K4Z2A	AEC-Q200 qualified
18 pF capacitor	1	06035A180JAT2A	Temperature range −55°C ... +125°C
10 nF capacitor	1	06035C103KAT2A	Temperature range −55°C ... +125°C
SMA connector	1	142-0701-801	Gold plated

Based on the schematic in fig. 15, the PCB prototype depicted in fig. 16 was designed with CadSoft EAGLE.

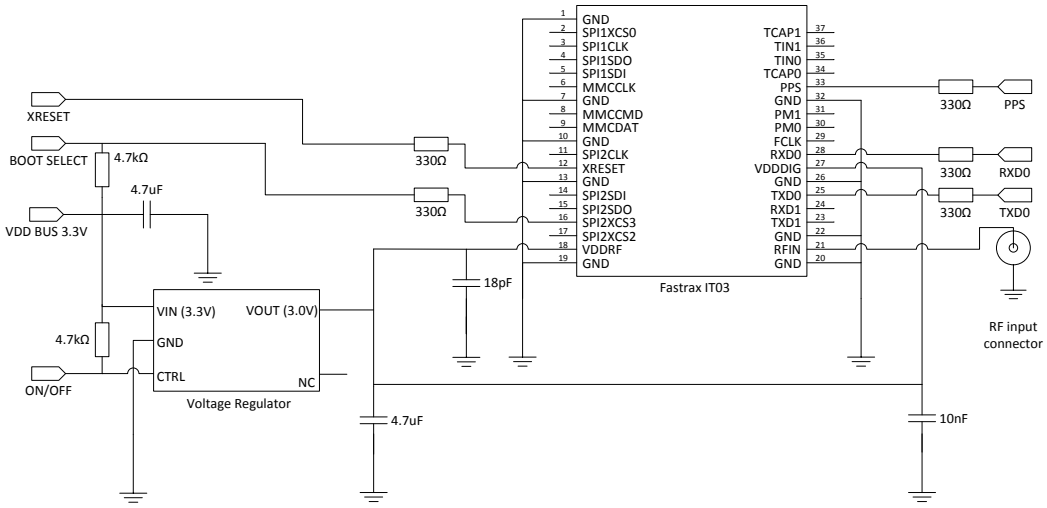

Figure 15: The designed Aalto-1 GPS circuit schematic. 8 pins in total are required from the satellite bus. XRESET and BOOT SELECT are used for firmware reprogramming, ON/OFF for enabling and disabling the voltage regulator, PPS for the timing signal to the OBC, and RXD0 and TXD0 for serial communication with the OBC. Two 4.7 µF decoupling capacitors are placed around the voltage regulator as recommended by the datasheets. Each receiver I/O line has a series 330 Ω resistor as recommended by the IT03 datasheet. BOOT SELECT and ON/OFF signals have 4.7 kΩ pullup resistors from the 3.3V supply.

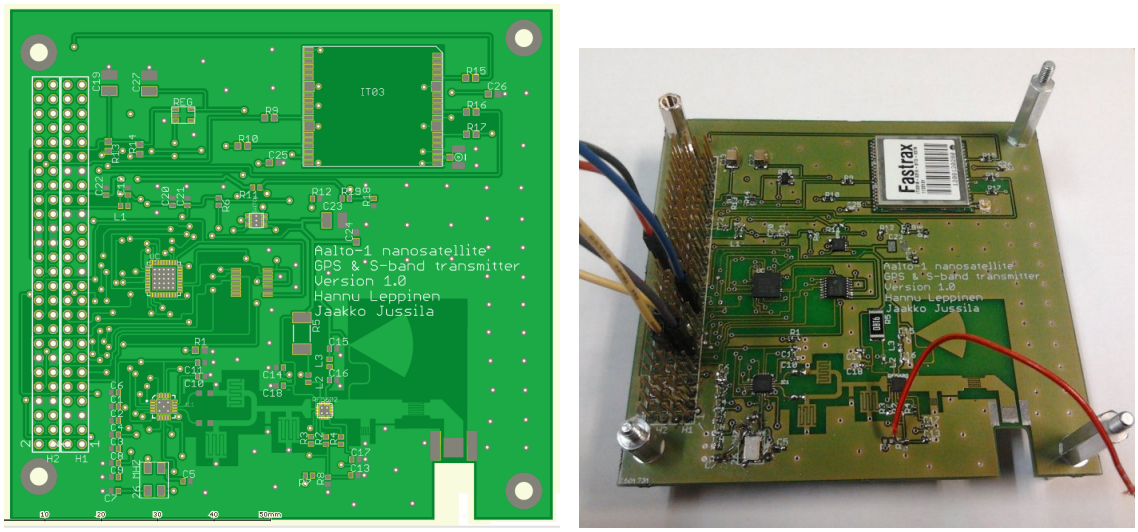

(a) The designed PCB prototype. *(b) The assembled PCB prototype.*

Figure 16: The design for the first prototype of the GPS/S-band PCB. The GPS circuitry occupies approximately one third of the board in the upper part of the picture. The rest of the board is used by the 2.4 GHz S-band radio. The stack connector in the prototype is the wrong way around, the female connector should point up.

3.6.1 Stack connector

Like other subsystems, the GPS/S-band PCB is connected to the satellite bus with a stack connector. The bus has 104 lines with some differences in the signals in the long stack and the short stack. For example, the GPS subsystem only uses pins in the long stack. The stack connector allows connecting the subsystem PCBs to form a stack, and the connector is divided into two 52-pin headers. The connector is the standard CubeSat Kit connector that is derived from the PC/104 stack-through connector. The model of the connector is Samtec ESQ-126-39-G-D, depicted in fig. 17. The pin layout of the long stack can be found in appendix B.

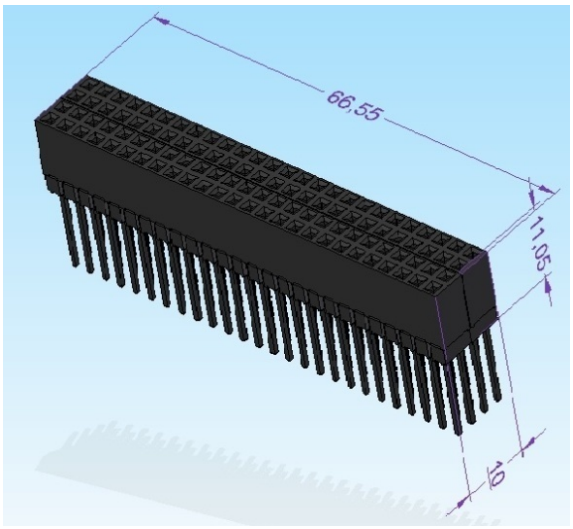

Figure 17: The Aalto-1 stack connector with its two 52-pin headers.

3.6.2 Antenna line

A microstrip line will be used on the PCB to connect the SMA antenna connector to the RFIN pin of the GPS receiver module. Both the connector and the pin have 50 Ω impedance, and the microstrip line should also have 50 Ω impedance to minimize losses due to reflected power. The structure of a microstrip line is depicted in fig. 18.

According to Wheeler (1977), the impedance of a microstrip line can be approximated by

$$Z_m = \frac{Z_0}{2\pi\sqrt{2(1+\epsilon_r)}} \ln\left(1 + \frac{4h}{w_{\text{eff}}}\left(a + \sqrt{a^2 + \pi^2 \frac{1+1/\epsilon_r}{2}}\right)\right), \tag{26}$$

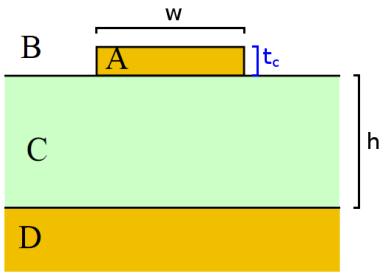

Figure 18: The structure of a microstrip line. A is the conductor, B is the upper dielectric (air or vacuum), C is the PCB substrate and D is the ground plane. The parameters needed for calculating the impedance of the microstrip line are width of the conductor w, thickness of the conductor t_c and height of the substrate h. Adapted from an original by Ulf Seifert.

where

$$a = \frac{14 + 8/\epsilon_r}{11} \frac{4h}{w_{eff}} \tag{27}$$

and

$$w_{eff} = w + t_c \frac{1 + 1/\epsilon_r}{2\pi} \ln\left(4e\left(\sqrt{\frac{t_c^2}{h^2} + \left(\frac{1}{\pi} \frac{1}{w/t_c + 11/10}\right)^2}\right)^{-1}\right). \tag{28}$$

In these equations, Z_0 is the impedance of free space ($\approx 376.73031\ \Omega$), ϵ_r is the relative permittivity of the substrate (≈ 4.1 for FR-4 at around 2 GHz), w is the width of the conductor, h is the height of the substrate (1.55 mm in this PCB) and t_c is the thickness of the conductor (18 μm). The width of the conductor is the parameter that is most easily adjusted in PCB design.

Using the equations above, the correct conductor width for a 50 Ω microstrip line would be around 3.1 mm. This agrees with a Fastrax recommendation (Fastrax Oy 2010, p. 27) of using a conductor width about two times the FR-4 substrate height. However, this is too wide for the receiver module pins which are only 0.7 mm wide with 0.3 mm intervals. The prototype uses an approximately 0.7 mm wide conductor, and with a 1.55 mm substrate the microstrip has an impedance of approximately 100 Ω. If the loss from the unmatched antenna line is considered too high, an additional ground plane could be integrated inside the PCB to reduce the substrate height in the equation. For example, with a 4 layer PCB by Eurocircuits and a ground plane directly below the conductor, the substrate height would be only 0.36 mm. (Eurocircuits 2010) A conductor approximately 0.7 mm wide could then be used, which would match the receiver module pin width.

3.7 Software design and integration

A software running on the Aalto-1 on-board computer controls the operation of the GPS receiver and parses and distributes the position and time information.

The GPS receiver is connected to the on-board computer via a serial line along with four GPIO lines: XRESET, BOOT SELECT and PPS. The onboard computer of Aalto-1 uses a Linux-based operating system, Aalto OS, which allows GPS software running on the operating system to access the required serial port through the device file /dev/ttySx. Using a Linux-based OS in the satellite allows slightly easier software development on Desktop PCs. Most of the satellite software will be written using C.

A program will be written for the OBC that parses the incoming data and sends commands to the GPS receiver. This software will read the navigation data from a serial port connected to the receiver, and send required commands, such as “restart” and “change protocol to iTalk”. The OBC software will make the position and time data available for other subsystems by writing the data to a file.

Receiver firmware reprogramming will be supported. Receiver firmware can be updated before flight with Windows tools. If a firmware already exists in the receiver chip, a basic USB-UART adapter can be used with Fastrax tools with a software boot firmware update. If no firmware exists on the chip, hardware boot needs to be used in firmware update. This is achieved by pulling BOOT SELECT low and toggling XRESET. The receiver then boots up to a mode where it expects the firmware update through the serial line.

The receiver has a pulse-per-second (PPS) pin which provides a PPS signal for timing purposes. The rising edge of this signal is synchronized to start of each GPS second to better than 1 μs accuracy. This allows accurate synchronization of the OBC clock. The receiver PPS pin could be connected to the data carrier detect (DCD) pin of the OBC serial port, because clock synchronization through this pin is supported by available Linux tools. (RJ Systems 2011)

3.7.1 Data protocols

By default, IT03 communicates using the NMEA 0183 protocol. The NMEA 0183 standard is a combined electrical and data standard, defined in 1983 and controlled by the U.S.-based National Marine Electronics Association. In this context, the receiver communicates through the serial line at 4800 baud with standard ASCII character sequences. (Fastrax Oy 2005b)

A NMEA sentence begins with a sentence identifier, followed by data fields separated by commas. A message ends with an asterisk and a checksum. For example, a $GPRMC sentence

```
$GPRMC,105241.16,A,6011.3327,N,02449.8683,E,0.00,117.1, ...
170412,6.1,E,A*0C
```

has the following fields: UTC time (10:52:41.16), fix validity (A=valid), latitude (60° 11.3327'), north (N), longitude (24° 49.8683'), east (E), speed in knots (0.00), heading (117.1°), date (17.4.2012), magnetic variation (6.1), declination (E or W), mode (A = autonomous) and the checksum. A drawback of NMEA sentences is that messages do not contain ECEF position and velocity data, and time data has a limited number of decimals.

Fastrax iTalk™ is a binary format specified by the manufacturer of the GPS receiver. (Fastrax Oy 2005a) The receiver outputs navigation and other data at 115200 baud in bit streams, and relevant information needs to be parsed byte by byte. Unlike NMEA sentences, iTalk messages contain ECEF position and velocity solutions and a time solution with high precision. iTalk messages also contain more information about the internal operation of the receiver, raw pseudorange measurements and more error estimates. Using iTalk is therefore preferable, but NMEA can be used as a backup.

The relevant minimum information that should be parsed from each navigation fix is:

- ECEF position
- ECEF velocity
- UTC time and date
- GDOP

Table 11 lists the exact binary formats in which the receiver communicates the data through the serial line.

Additional data that could be parsed includes number of satellites used for position and velocity solutions, PDOP, TDOP, CNRs of each satellite and possibly raw pseudorange measurements in TRACK and PSEUDO messages. (Fastrax Oy 2005a)

3.7.2 Software operation flow

The planned software operation flow is depicted in fig. 19. When turned on, the receiver will communicate using the NMEA protocol by default. The receiver will be switched from NMEA protocol to iTalk protocol with an NMEA command, and this can only be reversed by restarting the receiver. The receiver has a “ping” command, which can be used to query from the receiver which protocol it is using. The ASCII character string "<?>" is sent to the receiver with 4800 or 115200 baud, to which it will reply with "<?0>" or "<?1>". 0 indicates iTalk and 1 indicates NMEA.

Table 11: Minimum relevant content of an iTalk NAV_FIX message. WORD is a 16-bit unsigned integer, DWORD is a 32-bit unsigned integer and INT32 is a 32-bit signed integer. (Fastrax Oy 2005a)

Name	Data type	Description
NAV_FIX.Dop.wGdop	WORD	GDOP in units of 0.01
NAV_FIX.Utc.Time.wHour	WORD	Hours in 24-hour format
NAV_FIX.Utc.Time.wMinute	WORD	Minutes
NAV_FIX.Utc.Time.wSec	WORD	Whole seconds
NAV_FIX.Utc.Time.dwSubSec	DWORD	Second fraction in nanoseconds
NAV_FIX.Utc.Date.wYear	WORD	Year
NAV_FIX.Utc.Date.wMonth	WORD	Month [1...12]
NAV_FIX.Utc.Date.wDay	WORD	Day of month [1...31]
NAV_FIX.Pos.Xyz.lX	INT32	ECEF X coordinate [cm]
NAV_FIX.Pos.Xyz.lY	INT32	ECEF Y coordinate [cm]
NAV_FIX.Pos.Xyz.lZ	INT32	ECEF Z coordinate [cm]
NAV_FIX.Vel.Xyz.lX	INT32	ECEF VX coordinate [mm/s]
NAV_FIX.Vel.Xyz.lY	INT32	ECEF VY coordinate [mm/s]
NAV_FIX.Vel.Xyz.lZ	INT32	ECEF VZ coordinate [mm/s]

The receiver could be configured by default to use iTalk, but due to the higher baud rate its operation may not be as certain as with NMEA that has a much lower baud rate. In case of serial line problems, fallback to NMEA can be achieved by restarting the receiver.

iTalk protocol will be used to receive ECEF navigation solutions from the receiver. The receiver transmits an iTalk navigation message once a second. These messages are parsed by the OBC, and the navigation information is made available to other subsystems by writing it to a file.

By using the Fastrax iTalk protocol, it is possible to extract position and velocity in the ECEF coordinate frame, which is more useful than the usual latitude, longitude and altitude in the NMEA format.

3.7.3 Example program code

An example program was written that reads iTalk data through the serial port and outputs time and position information to the console. The program code listing can be found in appendix C. References used for writing the code include Fastrax example code written for Windows, and a tutorial on POSIX serial port programming. (Sweet 2005)

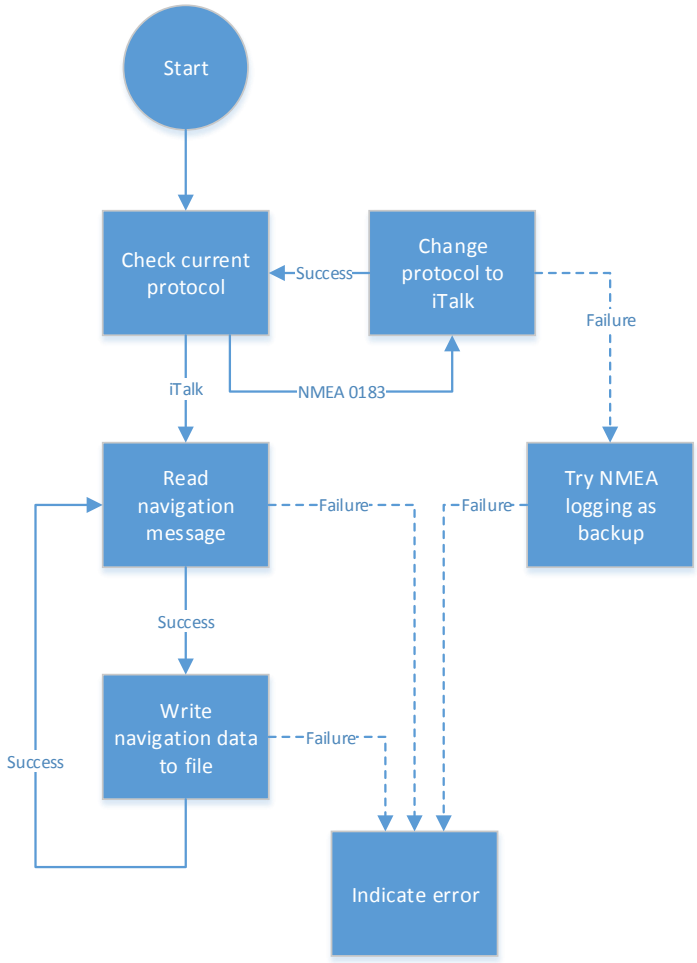

Figure 19: Software operation flow. The nominal operation flow is marked with continuous line, while dotted lines represent response to an error situation. NMEA logging can be used as a backup, but the software should still report that the subsystem does not function correctly. A probable reason is that for some reason OBC commands do not go through to the GPS receiver. It is possible that the GPS to OBC data line works while the OBC to GPS data line does not.

The program first uses the open_serial() function to initialize the serial port to the variable "gps". The software then enters an infinite loop where it keeps reading message headers from "gps" to find type 7 messages, which are navigation fixes. When such a message is found, the program parses relevant content from the message (time, position, velocity, checksum) and outputs them to console. The program also computes a checksum of the received message and for comparison outputs it next to the checksum that was a part of the message. The two should agree if the message has not been corrupted.

A similar test program was written to parse NMEA messages, but it is not included here

due to its similarity to the iTalk parser. One major difference is however that while iTalk messages include a solution in ECEF coordinates, the NMEA messages only include a latitude-longitude-altitude (LLA) solution. A simple geometric conversion from LLA to ECEF can be found in Kaplan and Hegarty (2006, p. 31). The NMEA messages also lack a three-dimensional velocity solution.

Changing the protocol from NMEA to iTalk by using an NMEA command was tested. Sending iTalk commands with C program code was not yet tested, but should not differ much from NMEA. For example, if the serial port is open at 4800 baud NMEA at file descriptor fd, the command that switches the protocol from NMEA to 115200 baud iTalk can be sent as follows:

```
int n = write(fd, "$PFST,ITALK,115200\r", 19);
if (n < 0)
  fputs("write failed\n", stderr);
```

3.8 Operations during the mission

GPS will be used during the Aalto-1 mission to produce position, velocity and time fixes. This fix information can be used to correct the on-board orbit propagator in the satellite, and it can also be downloaded from the satellite and used in more accurate orbit propagators, for example with AGI Satellite Tool Kit. The ADCS of the satellite contains an orbit propagator in order to be able to use active magnetic attitude control.

The GPS subsystem must be accurate enough to position the satellite within 100 meters of the true position near the GPS measurement epoch. Even one good-quality GPS fix provides the satellite with a very accurate knowledge of the translational motion state of the satellite: position and velocity at a certain instant of time.

Orbits could also be obtained from the TLEs published by NORAD, and these would have an accuracy of around 1 kilometer. This accuracy is enough for most nanosatellite missions, and TLEs will be used as a backup source for orbit determination. However, two experiments in Aalto-1 require more accurate position information: the spectral imager and the plasma brake.

During the imaging phase, the spectral imager will be used to image areas of the Earth, and exact positions where the images were taken will be needed in the image processing. In this phase, the GPS antenna will be pointing toward the flight direction, which will effectively cut off half the sky. The accurate positioning provided by the GPS is only required when taking pictures. Therefore, GPS can remain idle for long periods of time. GPS is cold started 15-30 minutes before imaging begins, and a suitable number of fixes is acquired, depending on the power budget. It could also be possible to change the satellite attitude during GPS operation in a way that would point the antenna closer to the zenith, possibly improving navigation performance.

During the spin phase, the plasma brake will be used to decelerate the satellite, making it re-enter the atmosphere. The orbital decay caused by the plasma brake can be determined from GPS measurements. During this phase, the GPS antenna points along the satellite spin axis, which is approximately parallel to the ECEF Z-axis. More precisely, the antenna will point along the positive ECEF Z-axis. Many GPS satellites will therefore be visible when the satellite is in the northern hemisphere and fewer when the satellite is in the southern hemisphere. The best orbit propagators are accurate to within at least a few meters within a few hours. (Vallado 2005) Obtaining a modest set of fixes per orbit should be more than enough to position the satellite with the required accuracy near the measurement epoch. Therefore, during the spin phase, the OBC could operate the GPS as follows:

1. Cold start the GPS receiver.
2. Obtain (for example) 60 good position fixes.
3. Turn off the receiver (cut power).
4. Wait (for example) 60 minutes, return to 1.

Obtaining a few fixes per orbit should be enough for the plasma brake experiment, as the orbit will change very slowly. If more accuracy is desired, the GPS can be used for longer periods of time. The GPS receiver will always be operated with a cold start, because the sleep and idle modes are not of much use. The satellite position changes so rapidly that the internal startup aids that rely on stored position probably will not work well.

In short, the GPS receiver will be cold started when navigation is required. When not needed, power to the receiver is cut off. The GPS subsystem will probably be off most of the time, which may also extend the system lifetime.

4 Verification

4.1 Overview

This chapter describes what kind of verification of the GPS subsystem and its components has been done and will be done in the future. The purpose of verification is to ensure that the subsystem and its components will function in space as required. Much of the testing was performed with Fastrax-provided Mini Evaluation Kits, which offer USB connectivity to IT03 modules soldered on IT03 Application Boards. The exception to this were the tests done with the GPS subsystem prototype PCB. Verification of the GPS software running on the OBC is not discussed, but the principles discussed in this chapter can be applied to it as well.

4.1.1 Testing approaches

According to ECSS (2002, p. 23-26), verification testing in a space project can have the following steps:

- **Development testing.** Development testing is performed during system development to evaluate feasibility of design concepts and to support the design process.
- **Qualification testing.** Qualification testing is performed on the Qualification Model (QM). It aims to formally demonstrate that the implemented system conforms to the specified requirements.
- **Acceptance testing.** Acceptance testing is performed on the Flight Model (FM) and aims to demonstrate that the FM conforms to specifications and acts as quality control screen for manufacturing defects. The tests are usually less severe than in qualification testing to avoid shortening the system lifetime.

The qualification and acceptance steps can be combined to the protoflight testing step:

- **Protoflight testing.** Protoflight tests combine aspects of qualification and acceptance testing. They are executed on items that are to be used in the actual spacecraft. The Protoflight Model (PFM) is a combination of QM and FM, and a combination of qualification and acceptance test are performed on it.

The verification approach usually follows a development-qualification-acceptance or a development-protoflight path, or a combination of them. The first approach has been chosen for the GPS subsystem, while the development-protoflight approach will be used with Aalto-1 as a whole due to the high cost of building the satellite QM and FM separately.

4.1.2 Verification plan

The purpose of verification is to ensure that a system fulfills its requirements; verification procedures are therefore designed to test the compliance of the system to its requirements. Verification requirements for the mission are defined in Näsilä et al. (2012, p. 55-57). The requirements for the GPS subsystem were defined in section 3.2.

Verification methods include testing, analysis and inspection. These methods will be used in GPS qualification and acceptance activities. Verification consists of analyses of the design and performance, component qualification, functional and environmental qualification tests of the qualification model (QM) and final acceptance tests of the flight model (FM). The satellite as a whole will follow a development-protoflight approach, while the GPS subsystem will use the separate QM and FM approach.

Individual components of the subsystem could be qualified separately for the mission, but so far only thermal cycling of the GPS receiver has been done. The chosen approach is to select as high-quality components as possible to minimize the need for individual component qualification. The QM of the whole subsystem will be constructed based on a completed prototype after sufficient development tests have been performed and passed with the prototype and the design is considered mature enough.

After the QM has been verified to comply with the requirements for the GPS subsystem, the FM will be constructed. The flight model will be used in the actual satellite. To screen for manufacturing defects, it can be subjected to a test campaign which should be less severe than with the QM to ensure that the operational life of the FM is not shortened.

The verification approach chosen for the GPS subsystem therefore consists of 3 phases:

1. **Prototype phase.** Prototypes of the subsystem and development testing are used to aid the development process.
2. **Qualification Model phase.** The QM is constructed when the design is considered mature enough. Compliance of the QM to subsystem requirements is tested with qualification tests.
3. **Flight Model phase.** The FM is constructed based on the qualified subsystem and is identical to the QM. The FM is subjected to acceptance testing to screen for manufacturing defects.

As of this thesis, some development tests and one qualification test have been performed and they are described in this chapter. The development tests include GPS signal simulations, PCB prototype testing and antenna performance testing. Thermal qualification of the receiver module has also been performed. Failure modes, effects and criticality analysis (FMECA) of the subsystem has been performed to support the

design process. At the end of the chapter, some untested aspects are discussed and suggestions for QM and FM testing are outlined.

4.2 GPS signal simulations

The capability of the GPS receiver to acquire fixes in orbit was tested at Space Systems Finland Oy in Espoo with a modified Spectracom GSG-55 GPS signal simulator. The simulator simulates the GPS signal environment of a desired scenario, and can therefore be used to input the receiver the kind of signals it would receive in orbit.

4.2.1 Test description

The purpose of GPS signal simulations was to ensure that the receiver can navigate in orbit. The suboptimal GPS antenna placement in Aalto-1 will mean that only around half of the sky will be visible to the GPS antenna, which will reduce the number of visible satellites. Finding out how this affects navigation performance was one of the main motivations for the simulations.

The questions that needed to be answered were:

1. *Can the receiver produce navigation fixes at orbital altitudes and velocities?*
2. *What is the time to first fix (TTFF) with unaided cold starts?*
3. *Does the suboptimal antenna placement affect the navigation performance?*
4. *What is the lowest usable carrier-to-noise ratio for the receiver?*
5. *How accurate are the GPS position and velocity fixes?*

The used test equipment included a laptop for logging the GPS navigation results, a Fastrax IT03 Mini Evaluation Kit with USB and MCX antenna connectivity, a modified Spectracom GSG-55 signal simulator and the required cables and connectors. The signal simulator is shown in fig. 20 and the laptop and evaluation kit in fig. 21.

Two firmware versions were used, which were otherwise essentially similar but one of them had a feature that caused the receiver to perform a cold start after acquiring 60 position fixes. This allowed easy testing of TTFF. Most of the receiver parameters were in their default values, except that search sensitivity was increased, and altitude and velocity limits were increased to orbital levels. Ionospheric and tropospheric corrections and the receiver's Kalman filter were turned on and off for different tests.

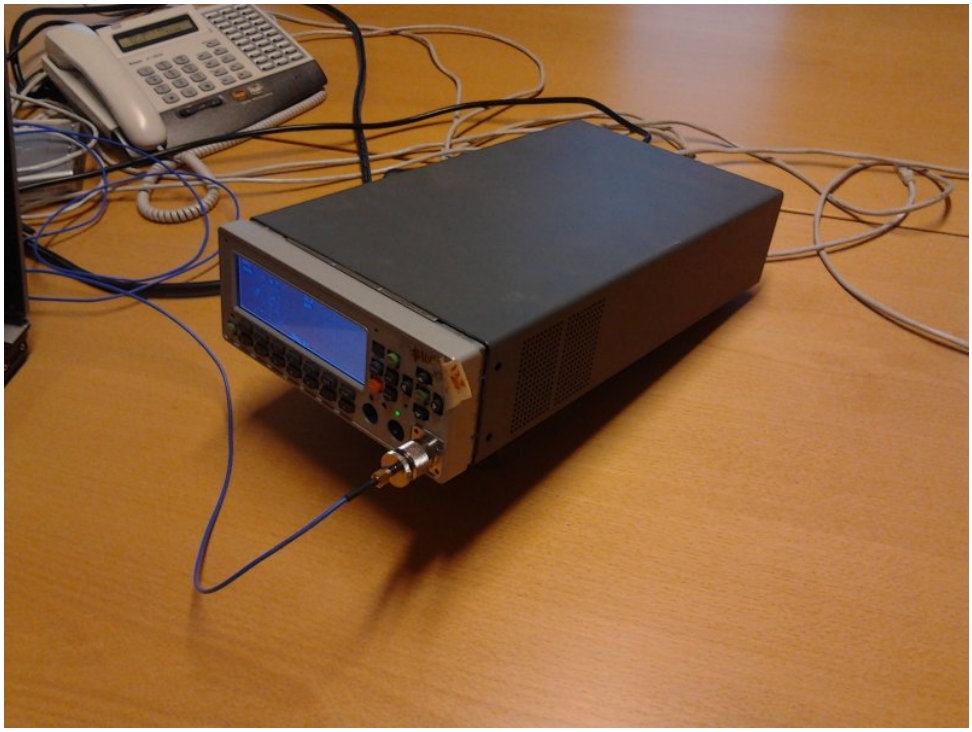

Figure 20: A modified Spectracom GSG-55 GPS signal simulator.

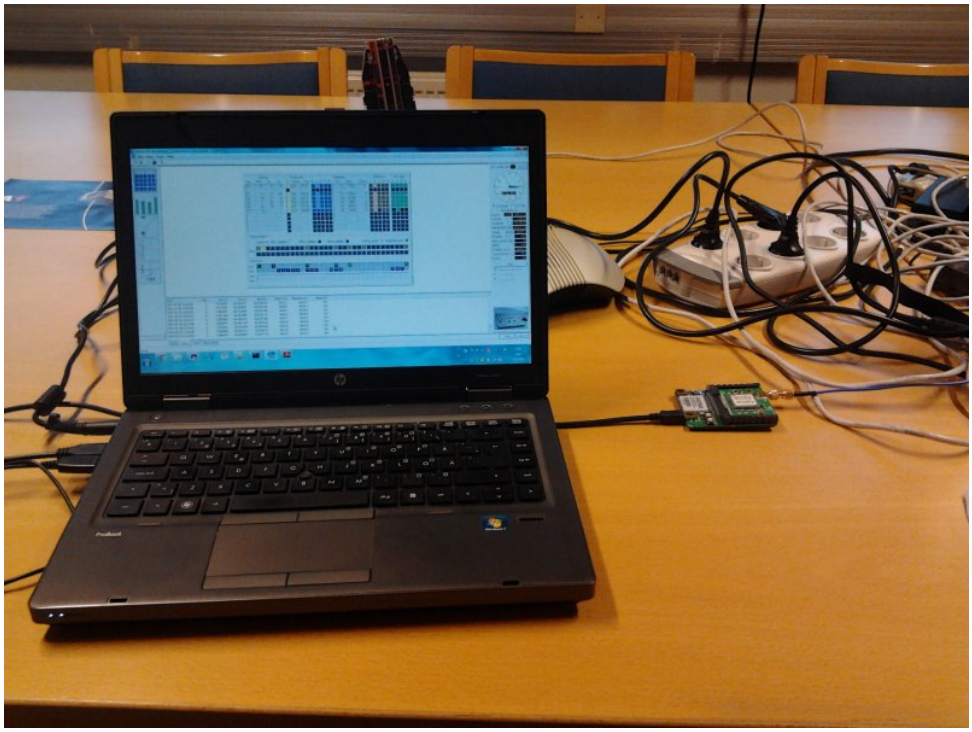

Figure 21: Left: The laptop used for logging the GPS data during the signal simulator tests. Right: Fastrax IT03 Mini Evaluation Kit.

4.2.2 Test procedures

Before the simulations, data on stationary GPS receiver performance was collected. The antenna was positioned near a window of the Department of Radio Science and Engineering in a way that blocked approximately half of the sky. This caused a reduced number of satellites to be visible.

During the GPS simulations, approximately 20 hours of simulation data was collected in five approximately one-hour sessions and in one long 15-hour session. Two circular orbit scenarios were used: first with 630 km altitude and 60° inclination and then with 700 km altitude and 100° inclination.

Stationary reference run (20 hours)

A stationary reference test run was made to determine terrestrial positioning accuracy of the receiver with a limited number of satellites. The antenna was situated near a window in a way which made only around 4 to 6 satellites visible at any time. Average CNR varied from between 37 dB-Hz to 50 dB-Hz, though it was almost always more than 40, with a mean of 47.67 dB-Hz. Around 20 hours of measurements were collected. The obtained reference values for GPS accuracy are presented in table 12.

Table 12: Means and standard deviations of coordinates in the ECEF axes, obtained during the stationary reference run. The upper table summarizes values from the whole test run where GDOP varied from 1.86 to 39.03, and the lower table only includes values from fixes with GDOP < 3. This value was selected because open-sky GDOP should usually be less than 3.

All fixes	**X**	**Y**	**Z**
Mean position	2885018.34 m	1334934.60 m	5510999.26 m
Standard deviation	12.97 m	8.85 m	12.39 m
Mean velocity	0.023 m/s	0.014 m/s	-0.015 m/s
Standard deviation	0.081 m/s	0.122 m/s	0.021 m/s

GDOP < 3	**X**	**Y**	**Z**
Mean position	2885020.09 m	1334932.45 m	5510997.35 m
Standard deviation	9.38 m	6.63 m	5.89 m
Mean velocity	0.027 m/s	0.005 m/s	-0.015 m/s
Standard deviation	0.022 m/s	0.033 m/s	0.005 m/s

It can be seen that the reduced number of visible satellites degrades positioning accuracy from the manufacturer-reported figure of 1.2 m CEP95. Multipath effects from nearby walls may also have degraded positioning accuracy. The velocity error is around

the manufacturer-reported 0.1 m/s. In any case, the accuracy shown in the static test is well within Aalto-1 requirements.

Simulation runs 1 and 2

The first two short simulation runs were done on 5.10.2012 at Space Systems Finland, for a duration of about two hours. The first simulation run tested the receiver performance with a large number of GPS satellites visible and with a good CNR. The second simulation run tested the receiver performance with a relatively large number of satellites visible, but with bad CNR.

The GPS receiver, the GPS simulator and the measurement laptop were set up and connected. The operation of the GPS receiver with the space firmware was observed, and with good carrier-to-noise ratios the receiver could achieve very fast TTFF. When the carrier-to-noise ratios were lowered with a signal simulator setting, TTFF increased accordingly. When the carrier-to-noise ratios fell below approximately 35 dB-Hz, the receiver stopped achieving GPS fixes. As the Taoglas AP.10F antenna initially considered for Aalto-1 could provide 40 dB-Hz at best, these tests initiated a search for a better antenna. A 5 dB-Hz margin would not be much, considering that unexpected EMC or RF issues could decrease the antenna performance.

Simulation run 3

The third simulation run was done on 23.10.2012. The purpose of this simulation run was to study how the receiver would perform with a small number of GPS satellites visible, both with good and bad CNRs.

Simulation runs 4, 5 and 6

Simulation runs 4, 5 and 6 were made during an approximately 24-hour period in 4-5.12.2012. During these test runs, the Kalman filter parameters of the receivers were modified, effectively turning off the Kalman filter and producing least-squares-like solutions. Simulation run 4 was a 30-minute test with modified Kalman filter parameters to see if the receiver still works. Simulation run 5 was an around 15 hour test, which tested if the receiver loses track during long navigation sessions or if something unexpected happens. Simulation run 6 was an around 2-hour test done with further modifications to the Kalman filter. It seemed that modifying the Kalman filter parameters did not noticeably affect the receiver performance.

4.2.3 Results

Unaided time to first fix

Unaided TTFF was tested for operational purposes, as it must be known how long before actual navigation the receiver needs to be turned on. The firmware used in the test kept restarting the receiver with a cold start after achieving 60 position fixes. During a test run of around two hours 36 unaided cold starts were obtained. The test scenario was circular orbit of around 630 km altitude and around 60° inclination with only approximately half of the sky available for the antenna. The TTFF results are visualised in fig. 22. TTFF after cold start varied from around 50 seconds to around 3.5 minutes, which is similar to terrestrial performance and can be considered very good.

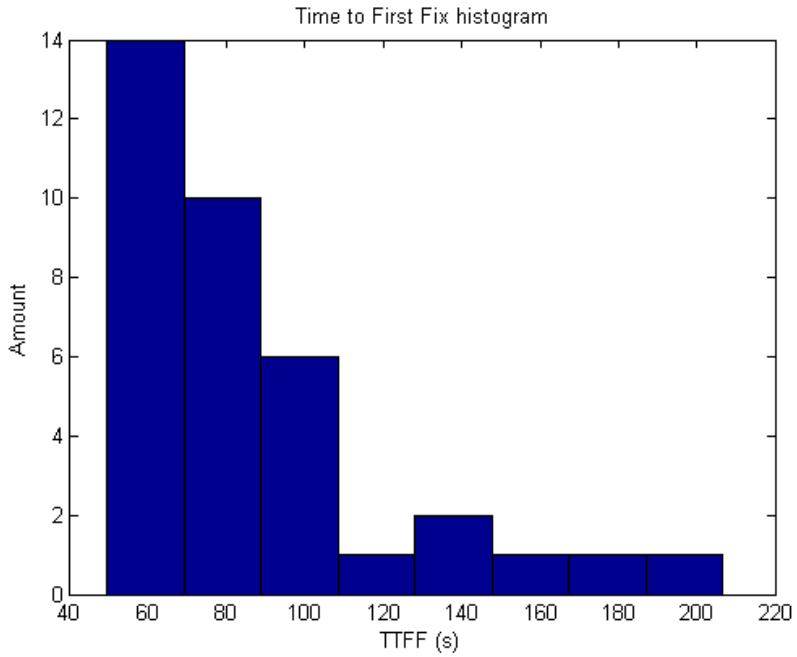

Figure 22: Histogram of the 36 measured TTFF values. The minimum time to TTFF was 49.51 s and maximum was 206.53 s. The minimum time of around 50 s is very close to the manufacturer-given 40 s in terrestrial conditions and can be considered very good. It can be seen that almost all of the 36 first fixes were obtained in under 2 minutes.

Accuracy

Position and velocity accuracy was determined by comparing the position and velocity fixes reported by the receiver to the positions and velocities in the GPS signal simulator scenario at the same instants of time. In the scope of these simulations, the time accuracy of the receiver was considered to be perfect. 1 μs error in time solution would

correspond to around 300 meters of position solution error while even at orbital velocities the satellite would move only around 7 mm during one microsecond. Any time error would have been visible in the position error.

The low number of satellites visible, combined with poor CNRs and poor geometry causes severe degradation of navigation performance. In general it was noted that the receiver performs well when GDOP is below 3. With < 3 GDOP, the spherical position error usually remains well below 100 m, and the velocity error remains below 20 m/s. However, with CNR below 40 dB-Hz, the position solution quality will degrade regardless of the number of satellites visible. The peak position errors were over 1 km, which occurred when only 4 satellites with bad geometry were used in the position fix. The receiver sometimes reported velocity fixes obtained by using only 2 satellites, and peak errors in the velocity fixes were over 100 m/s.

Table 13: Summary of the GPS receiver accuracy and satellite availability, data from the 15-hour test. Only half of the sky was visible, which resulted in degraded performance and availability. However, 96.9 % of good-quality fixes met the 100 m positioning accuracy requirement.

Filtering of position fixes	**Percentage of position fixes**	**Percentage of fixes with < 100 m position error**
None	100.0 %	53.9 %
Only fixes with at least 5 satellites and below 5 GDOP	60.2 %	73.1 %
Only fixes with at least 6 satellites	57.3 %	64.5 %
Only fixes with at least 6 satellites and below 5 GDOP	43.3 %	79.3 %
Only fixes with at least 6 satellites and below 3 GDOP	16.7 %	96.9 %
Only fixes with at least 7 satellites	26.0 %	74.5 %

For some reason, with bad geometry the first position fix after a cold start was usually a very accurate one, but position fixes quickly started to diverge from the right values. It was suspected that this could be related to some non-optimal Kalman filter parameter settings in the receiver, but turning off the Kalman filter did not remove the problem. With velocity error this effect was not so pronounced. Velocity error was closely related to the number of satellites used, with more satellites producing more accurate results.

DOP values are a measure of GPS satellite geometry, which affects the navigation quality. Higher DOP usually means more error in position, velocity and time, and this was

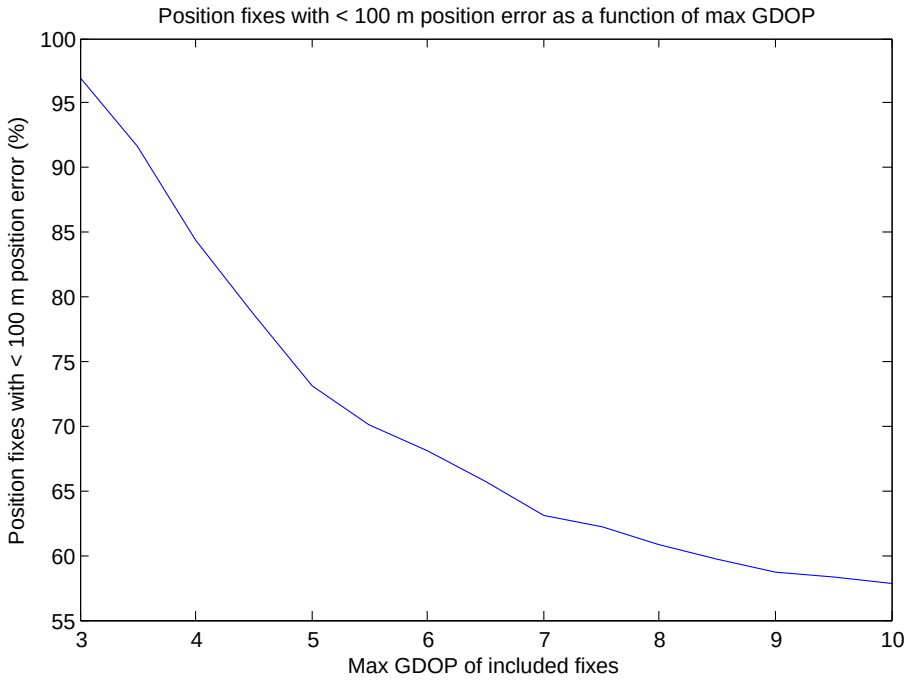

Figure 23: Effect of GDOP on position fix quality. When fixes with GDOP up to 3 are included, more than 95 % of position fixes are accurate to within 100 m. If fixes with higher GDOP are included, the position fix quality decreases.

Table 14: Mean and RMS errors of position and velocity accuracy in radial, flight direction and cross-track directions. Only fixes with < 10 GDOP were included, which amounted to 92.3 % of the fixes. It can be seen that the means are close to zero when compared to the RMS errors, except that cross-track position and velocity have a small unexplained bias. However, it can be concluded that fitting orbits to a large number of such measurements should enable positioning the satellite well within the required 100 m and 20 m/s.

Error type	**Radial**	**Flight direction**	**Cross-track**
Mean position error	-9.35 m	3.13 m	9.87 m
RMS position error	105.08 m	130.37 m	53.41 m
Mean velocity error	0.20 m/s	0.61 m/s	1.49 m/s
RMS velocity error	15.67 m/s	15.13 m/s	7.47 m/s

also evident in the simulation results. It was found that the worst outliers could be removed by removing results with more than 5 or 3 GDOP. Figure 23 shows the effect of GDOP on fix quality. Removing bad fixes reduces the availability of GPS navigation solutions, as can be seen in table 13. Table 14 list accuracy results from simulation run 5, where around 50000 data points were obtained.

Good-quality fixes were studied more to assess the receiver performance with a large number of satellites and good geometry. Tables 15 and 16 show the accuracy of fixes

with GDOP below 3.

Table 15: Mean and RMS errors of position and velocity accuracy in radial, flight direction and cross-track directions with < 3 GDOP fixes. Positioning accuracy is clearly improved, but velocity accuracy is not.

Error type	**Radial**	**Flight direction**	**Cross-track**
Mean position error	0.40 m	3.41 m	-0.95 m
RMS position error	19.84 m	27.48 m	12.33 m
Mean velocity error	0.20 m/s	0.61 m/s	1.49 m/s
RMS velocity error	15.28 m/s	13.51 m/s	5.87 m/s

Table 16: Spherical position and velocity error of position fixes with GDOP < 3. The data is from a simulation with only half of the sky available, and average GDOP was around 2.5. It would likely be lower with the whole sky available, and performance could then probably be even better.

Position error	**% of fixes**
≤ 15 m	54.4 %
≤ 20 m	61.9 %
≤ 25 m	74.4 %
≤ 30 m	82.7 %
≤ 40 m	90.1 %
≤ 50 m	92.4 %
≤ 70 m	95.2 %

Velocity error	**% of fixes**
≤ 20 m/s	61.6 %
≤ 25 m/s	89.4 %
≤ 30 m/s	90.9 %
≤ 40 m/s	95.9 %

Availability

During simulation run 5 the receiver achieved navigation fixes during 95.3 % of the total simulation time. The simulation lasted around 53200 seconds (around 14 hours 47 minutes), and outages lasted a total of 2507 seconds (around 42 minutes). The length of individual outages lasted from a few seconds to a maximum of 5 minutes 5 seconds. These figures were obtained with only half of the sky visible, and with the whole sky the availability would be close to 100 %. Availability is visualized in fig. 24. With poor antenna orientation, the available PDOP was considerably worse than the 2.755 mentioned in FAA (2012). The PDOP distribution is visualized in fig. 25.

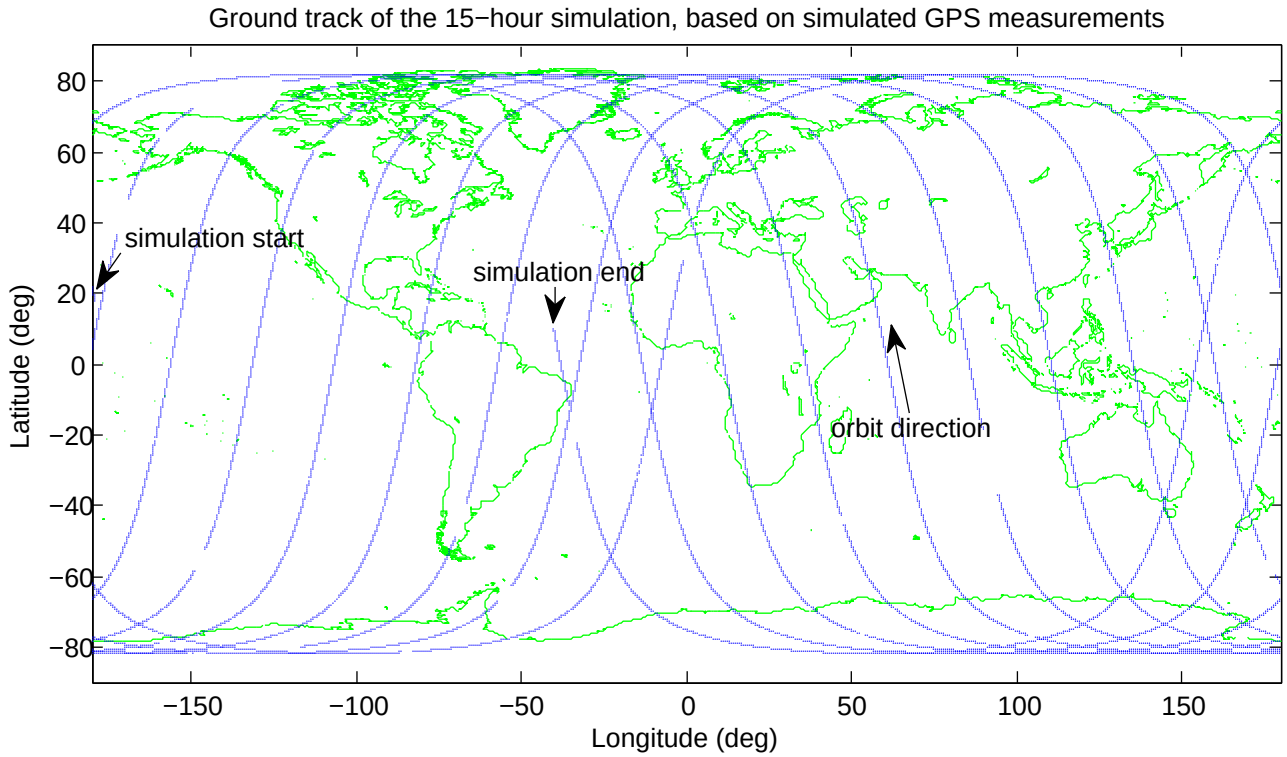

Figure 24: Ground track from the 15-hour simulation, based on simulated GPS measurements. The 700 km orbit has an inclination of around 100 degrees. Gaps in the ground track indicate outages in GPS navigation. The simulation run starts near 20N, 180W, proceeds west (retrograde orbit) and ends at around 10N, 40W. Image created with Matlab functions by Richard Rieber.

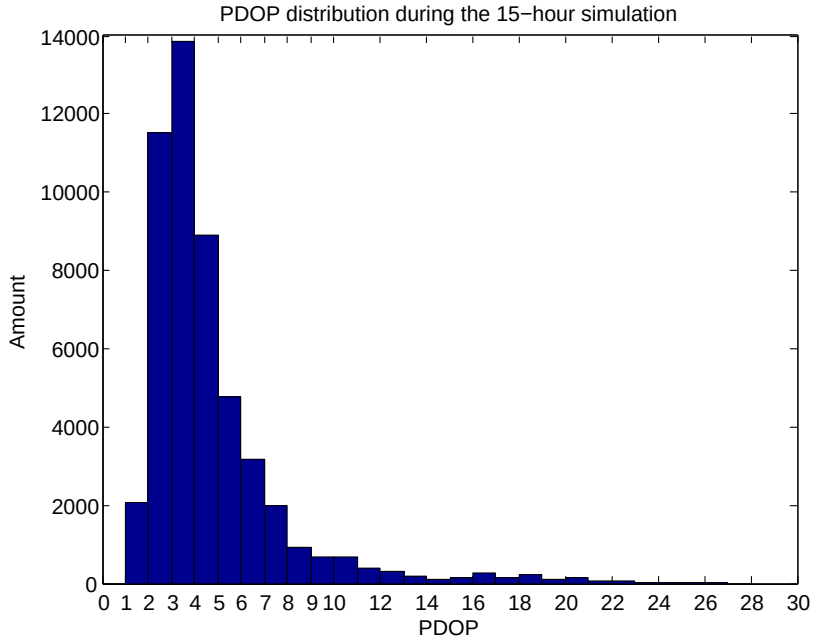

Figure 25: Simulated PDOP distribution during the 15-hour simulation. Poor antenna placement is clearly visible here. For example, measured open-sky PDOP was less than 2.755 for 99.9 % of the time during early summer 2012. (FAA 2012)

4.2.4 Conclusions

The questions that needed to be answered were:

1. *Can the receiver produce navigation fixes at orbital altitudes and velocities?*

   Yes. There were no problems in acquiring navigation fixes in reasonable times. During a 15-hour test, GPS navigation solutions were available more than 95 % of the time.

2. *What is the time to first fix (TTFF) with unaided cold starts?*

   TTFF ranged from a best-case of around 50 seconds to a worst-case of around 3.5 minutes. Fix was usually acquired in less than 2 minutes. This can be considered good performance.

3. *Does the suboptimal antenna placement affect the navigation performance?*

   Yes. The antenna placement effectively cuts off half the sky, which results in only around half of possible satellites being visible. In addition, these satellites are concentrated on a small part of the sky. This results in poor geometry and decreases navigation accuracy.

4. *What is the lowest usable carrier-to-noise ratio for the receiver?*

   It seems that 40 dB-Hz could be used as a safe lower limit for antenna performance.

5. *How accurate are the GPS position and velocity fixes?*

   The accuracy is dependent on the amount of satellites used and their geometry, expressed as a dilution-of-precision (DOP) value. With more than 6 satellites and good geometry (< 3 GDOP), the spherical position error is usually around few tens of meters. With less than 6 satellites and bad geometry, the error can be over a kilometer. Velocity solution is accurate to within few tens of meters per second.

Based on these results, GPS navigation solutions provided by the IT03 should be filtered based on the number of satellites used, CNR of used satellites and DOP values. Fixes made with low number of satellites, low CNRs or high DOP should be used with caution; good-quality fixes can be assigned a large weight. On the other hand, the on-board orbit propagator could be updated even with the poor-quality fixes, because real-time accuracy requirements are not very strict. Measurements can be downloaded from the satellite and post-processed on the ground.

The mean errors of the position fixes are close to zero. The required positioning accuracy of 100 meters can be achieved either by collecting a large number of fixes or by using only good-quality fixes.

Antenna quality and location are extremely important for the overall GPS performance. The satellite could possibly be rotated during GPS operations so that the GPS antenna points toward zenith. A number of good-quality fixes could then be acquired quickly.

4.3 GPS PCB functional testing

The functionality of the GPS PCB depicted in fig. 26 was tested by connecting it to a Desktop PC with a USB-serial adapter. The aim was to see if the designed and assembled circuit works. Tests included sending and receiving serial data, changing the parameters of the receiver, reprogramming the receiver firmware with both software and hardware methods and measuring voltages and currents. Connecting an antenna to the system was not tested because an ADA-15S antenna with an IPEX U.FL connector was not received in time.

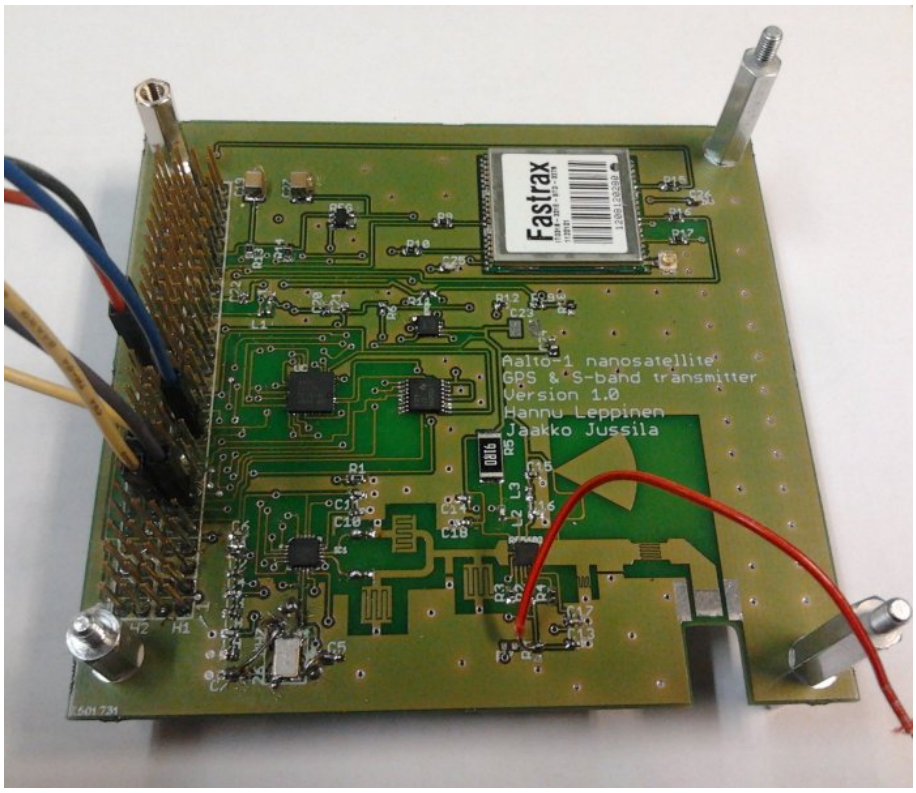

Figure 26: The GPS part of the GPS/S-band PCB prototype undergoing functional testing. The connected signals in the stack connector include 3.3V, GND, TX, RX, XRESET and BOOT SELECT. The red jumper cable in lower right corner is for S-band radio debugging, and is unconnected.

The assembled PCB was tested without an antenna for connectivity to a desktop PC. The purpose was to test if the receiver on the designed PCB can communicate with the desktop PC simulating a satellite OBC. The receiver parameters were readable and writable through the serial line, and the receiver transmitted data to the desktop PC

about its GPS satellite search status. None were found as no antenna was connected. Sending commands, such as "perform cold start", also worked.

Firmware update was tested by both software and hardware methods. In the software method, a dedicated command is sent through the serial line to initiate firmware update and only the serial line and a functioning firmware on the receiver is needed. If the firmware does not exist or is corrupted, the hardware method is used by pulling the BOOT SELECT pin low, toggling the XRESET pin and then uploading the firmware through the serial line. Both firmware update methods were verified to work.

Current consumption and voltage levels of the GPS circuit were also measured. When input voltage to the voltage regulator was 3.3 V, the current consumption was around 40 mA, which translates to a power consumption of around 130 mW. The power consumption of the GPS antenna according to the datasheet is around 30 mW, which would mean that the subsystem could achieve the 160 mW power budget. However, the receiver may use slightly more power when actually computing the navigation solution.

The voltage between the voltage regulator input and ground was measured to be around 3.334 V while between the regulator output and ground it was around 3.032 V. The prototype used a slightly cheaper voltage regulator, but the observed output voltage was at 3.0 V within the accuracy of the voltmeter used in measurement.

4.4 Antenna performance testing

Development tests were performed with three candidate antennas: Taoglas AP.10F, Taoglas AP.17E and Adactus ADA-15S. The first two antennas were abandoned after it was concluded that they barely meet the 40 dB-Hz CNR requirement with the IT03. ADA-15S was then selected for further testing.

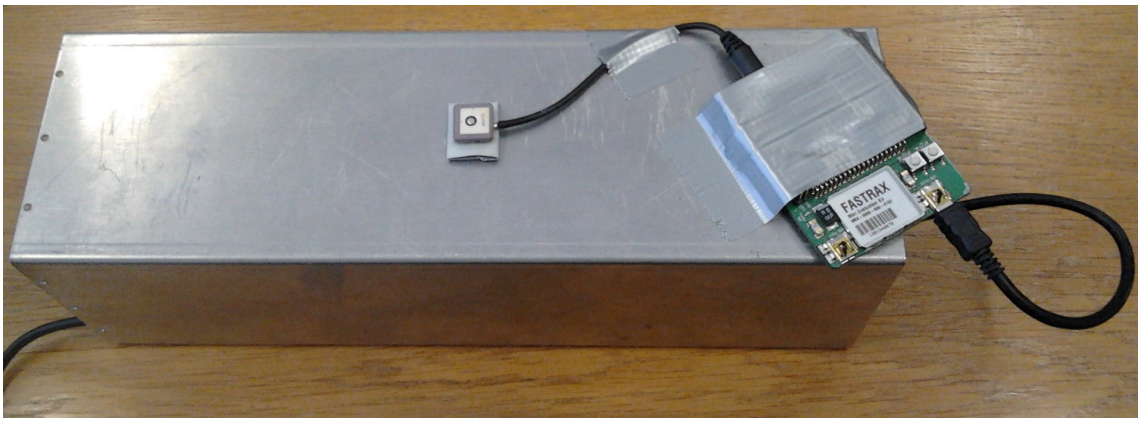

Figure 27: An Adactus ADA-15S antenna attached to an mockup aluminium frame was used in antenna performance testing with a Fastrax Mini Evaluation Kit.

The performance of the selected GPS antenna with a Fastrax Mini Evaluation Kit was

tested on the roof of the Department of Radio Science and Engineering at Aalto University. The setup was positioned to a place with a clear as possible view of the sky. The datasheet of the antenna indicated a nearly hemispherical antenna pattern, as is often required from a GPS antenna. Measurements obtained with less than 10° elevation were treated with skepticism due to some obstacles in the horizon. The antenna provided the receiver with slightly over 40 dB-Hz CNR on average, and peak CNRs were around 45 dB-Hz. While the performance was slightly lower than expected it was deemed sufficient to continue development with the antenna.

The test run was made using a satellite aluminium frame mockup depicted in fig. 27 to test the effect of the frame to the antenna performance. Results from the performance test are presented in table 17. Figure 28 is a sky plot of tracked GPS satellites during the test.

Table 17: A total of 12 satellites were tracked during the first 15-minute ADA-15S antenna test. Mean CNRs were mostly around or slightly above the 40 dB-Hz limit.

Satellite number	**Mean CNR (dB-Hz)**
1	38.89
3	42.53
6	40.27
8	44.20
11	43.21
14	36.14
15	37.46
16	42.27
18	43.82
19	38.66
22	43.82
28	41.50

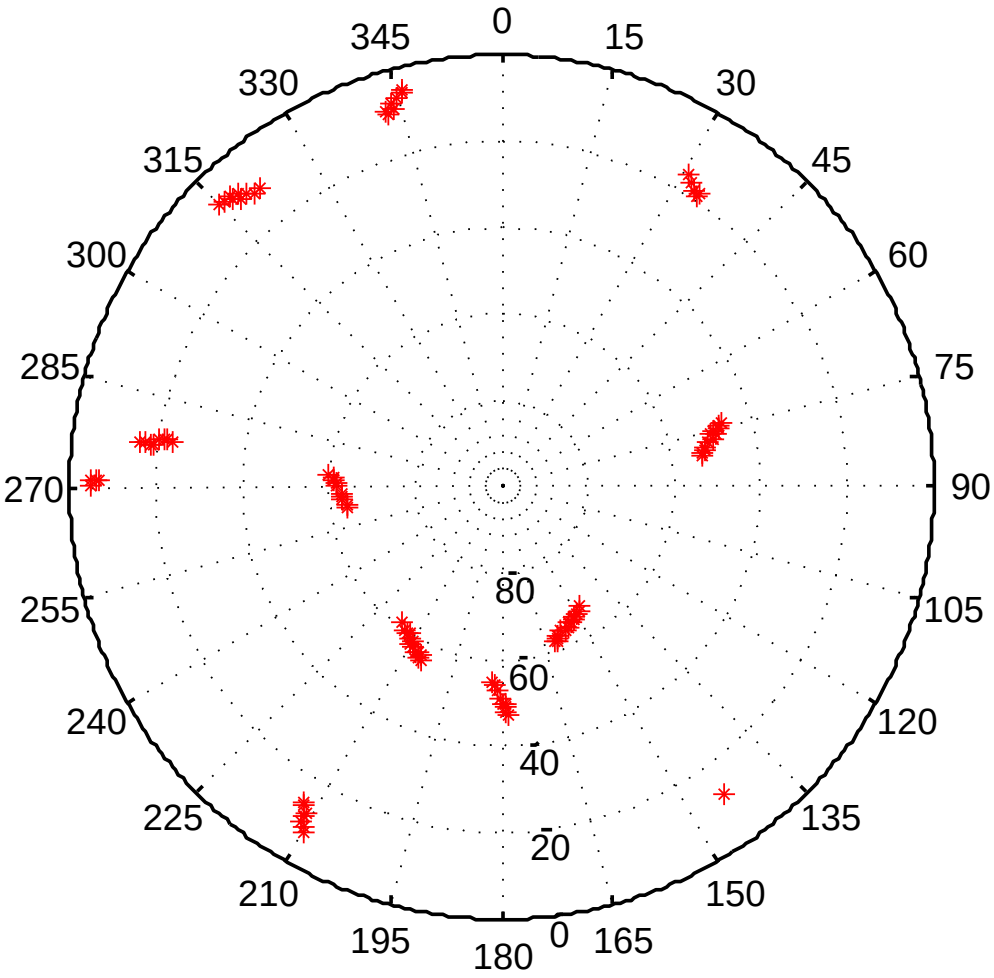

Figure 28: Sky plot of tracked satellites from the 15-minute antenna test, with only > 40 CNR observations included. The antenna seems to provide high enough CNR through almost all elevations and azimuths. Elevation is shown radially and azimuth is shown on the perimeter.

4.5 Receiver thermal qualification

Fastrax IT03 is rated for a temperature range of -40°C to +85°C. It was decided within the Aalto-1 project that important on-board electronic components need to be qualified to a temperature range of -65°C to +90°C. Thermal cycling was performed at the Finnish Meteorological Institute's space instrument calibration laboratory. The aim of the test was to see if temperature variations could break non-powered receivers.

4.5.1 Test description

The GPS receiver performance was measured both before and after thermal cycling, and the aim was to see if thermal variations cause some deterioration in receiver operation. Fastrax IT03 Application Boards, which contain the IT03 module, were used in the tests. Carrier-to-noise ratios from received GPS satellites were used to study the receiver performance. The fact that the receiver can provide the CNRs indicates that the receiver is able to track satellites and communicate through the serial line.

Before taking the receivers to FMI, they were tested at the Aalto University Department of Radio Science and Engineering for 24 hours. The receiver antennas were placed near a window of the laboratory, and the navigation NMEA messages were logged for 24 hours. The GPS antennas used in the tests were Beyondoor BY-GPS/Glonass-03 antennas supplied by Fastrax.

After transportation to FMI, the three receivers were powered up and verified that they still communicate.

The three GPS application boards were placed inside the Weiss DU40-70 test station. They were packed inside an antistatic bag and cushioned with bubble wrap. Vaisala HMT337 temperature and humidity sensors were also set up inside the test chamber. A measurement laptop was set up to log temperature and humidity, but this data was lost due to a hard drive malfunction.

A test program was written for the test station, which performed 50 cycles of first lowering the temperature to -65°C, waiting an hour and then raising the temperature to +90°C, and waiting an hour. The temperature transitions also took time, which resulted in the cycling lasting for 8 days.

After the cycling, the three receivers were removed from the test chamber and visually inspected. They were powered up and connected to a laptop to see if they still communicate.

After transporting the three receivers back to the Aalto University space laboratory, a quick test was made to see if the receivers can still get a position fix.

The three receiver antennas were placed at the same place as in the pre-cycling func-

tional test. Again, 24 hours of NMEA data was logged from the receivers.

4.5.2 Results

The pre- and post-cycling NMEA data from the receivers was compared. Especially the CNRs were of interest, because they indicate the received signal quality from the GPS satellites. Had any one of the receivers degraded or broken, the receiver would have been considered unsuitable for space applications.

No significant degradation of receiver performance was found. Variations in the 24-hour performance can be explained with GPS satellite position geometry. Positioning accuracy was also measured in a static test, and no difference in performance was noted before and after thermal cycling. It should be noted that thermal cycling was performed with non-powered receivers, and therefore the test only serves to indicate that non-powered receivers are not broken by temperature variations alone. It is possible that temperature changes can affect the receiver performance while it is navigating due to clock reference oscillator drift. (Lux and Markgraf 2004)

Figure 29 visualizes the results of the thermal testing. It contains histograms of CNRs from the receivers before and after thermal cycling. Table 18 lists CNR mean values and standard deviations before and after thermal cycling.

Based on these results, the thermal qualification of the GPS receivers was successful.

Table 18: GPS receiver carrier-to-noise ratio means (μ_{C/N_0}) and standard deviations (σ_{C/N_0}) before and after thermal cycling.

Receiver number	Item	Before cycling (dB-Hz)	After cycling (dB-Hz)
0802120661	μ_{C/N_0}	32.6222	32.2867
	σ_{C/N_0}	12.8288	13.7247
0802160656	μ_{C/N_0}	34.0847	34.5350
	σ_{C/N_0}	11.1526	12.8010
0802160651	μ_{C/N_0}	31.8051	31.6888
	σ_{C/N_0}	9.3888	13.6994

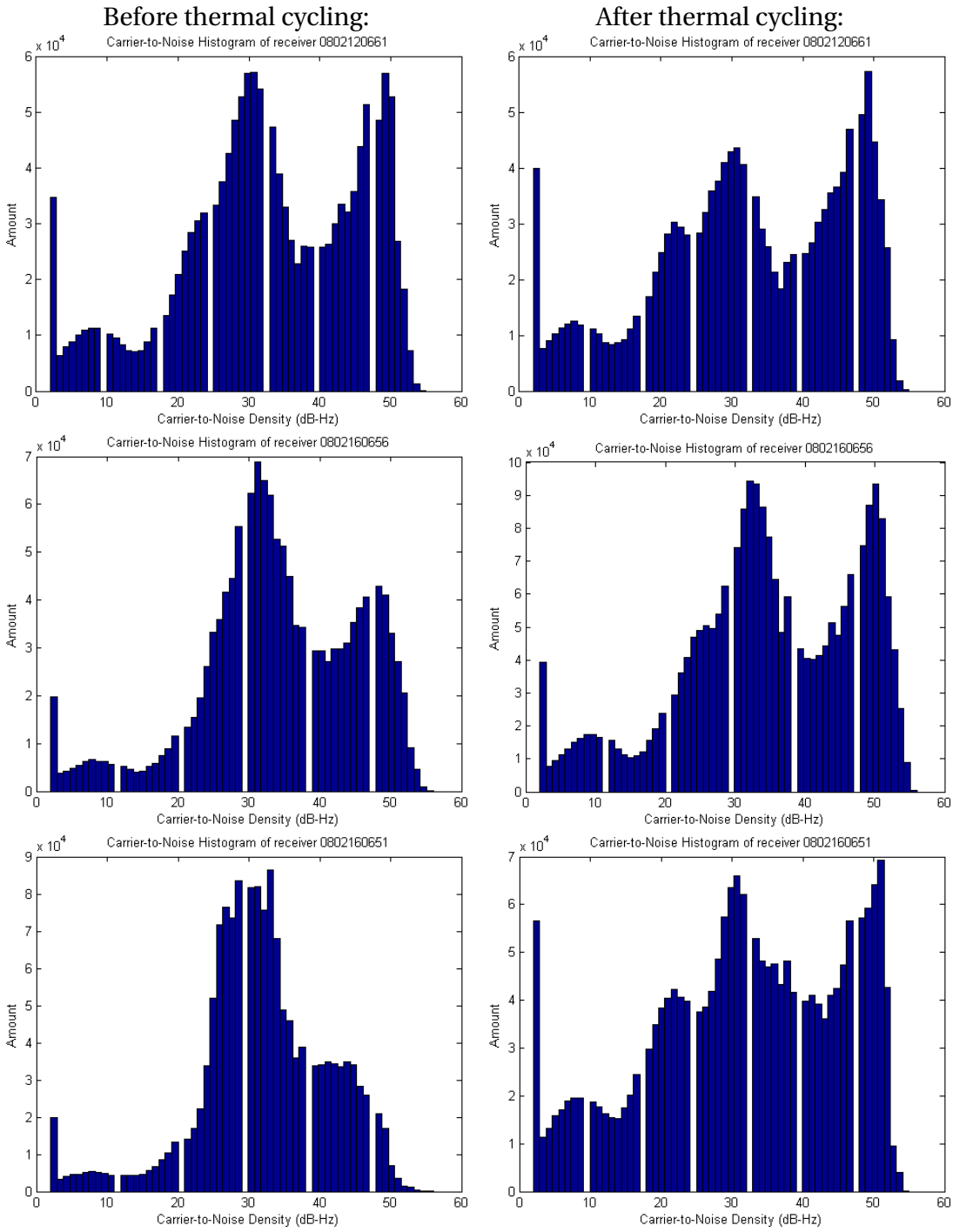

Figure 29: Visualization of the carrier-to-noise ratio measurements of the GPS receivers before and after thermal cycling. Left column has the CNR histograms of the three receivers before thermal cycling, while the right column has the histograms after thermal cycling. The x-axis represents the carrier-to-noise ratios in dB-Hz while the y-axis represents how many occurrences of a ratio were measured. No performance degradation was noted, and variations can be explained with GPS satellite geometry and slight changes in antenna positions.

4.6 Failure modes, effects and criticality analysis (FMECA)

The failure modes, effects and criticality analysis (FMECA) of the GPS subsystem is described in this section. FMECA is a system engineering method originally developed by the U.S. military and applied widely by NASA and ESA in space missions. It can be used to systematically search for potential failures in designed systems. Potential failures are also ranked based on their criticality, and mitigation measures are implemented based on the criticality of failure modes. In FMECA, individual elementary failure modes at component level and their impact on the system as a whole are analysed. FMECA should be used as a tool alongside the development process to continuously improve the design and to remove bad solutions. FMECA documentation can also be useful later during the operational phase of the mission, as reasons and remedies for malfunctions could be found faster. (ECSS 2009)

FMECA of the GPS subsystem was done by analysing the passive components (resistors and capacitors) and pins of the active components (receiver, antenna, voltage regulator). It was found that the GPS subsystem does not have much redundancy, as failure of any active component will lead to failure of the entire subsystem. Passive components are slightly less critical, except those that directly affect the power supply or the serial line from the receiver to the OBC.

Internal failures in the active components were not considered, but their effects would be visible in the input-output signals of the active components. The signal-based approach was chosen for its simplicity compared to analysing internal failure modes of the active components.

Possible failures were assigned severity, probability and criticality numbers (SN, PN, CN respectively). The severity and probability numbers were assigned according to table 19, and CN is the product of SN and PN. Severity numbers were assigned based on the effect to the whole satellite, and therefore only values 1 and 2 were used as the GPS subsystem is not absolutely critical to the operation of the satellite. There was no data available for accurate failure probability analysis, so the same PN value 2 was used for all failures.

Table 19: Explanations for the severity numbers (SN) and probability numbers. (ECSS 2009) The severity numbers were assigned based on the effect to the whole satellite, therefore the GPS subsystem was only assigned severity numbers 1 and 2. A total failure of the GPS subsystem wouldn't threaten the satellite as a whole, but would negatively affect the mission. Due to lack of failure probability data, PN value 2 was used for each failure.

SN	Description
1	Negligible
2	Major
3	Critical
4	Catastrophic

PN	Description	Probability
1	Extremely remote	P < 0.001 %
2	Remote	0.001 % < P < 0.1 %
3	Occasional	0.1 % < P < 10 %
4	Probable	P > 10 %

The sheet used in the FMECA is included in appendix D. Based on the FMECA, it was concluded that choosing reliable active and passive components and carefully soldering them to the PCB is the best way to reduce the risk of failure. The PCB should also be designed to be as easy as possible for manual soldering. A current limit could be implemented in the 3.3 V bus to limit damage from a short circuit in the GPS subsystem. The voltage regulator in the GPS subsystem has overcurrent protection.

4.7 Untested aspects

This section mentions aspects that are relevant to the development of the system but were not tested in course of the thesis. They could be tested later if considered necessary.

4.7.1 Radiation

As explained in Section 2.3.6, the effects of radiation on electronics can be divided into total dose and single-event effects.

Based on the planned Aalto-1 mission length and expected orbits, it was decided that ionizing radiation total dose tests are unnecessary. Simulations (Vainio 2011) had been done for sun-synchronous orbits at 500 km and 1000 km altitudes to study the accumulated total dose within an 1.5 mm thick aluminium frame. The simulations indicate that the accumulated dose during 2 years at planned orbits for Aalto-1 is around 2 krad, while untested COTS parts can reasonably be expected to survive total doses of at least 5 krad (Fortescue, Stark, and Swinerd 2003, p. 590-591). It is therefore expected that the system will not fail due to accumulated total dose. Single-event effects can be more dangerous, as energetic particles can corrupt data or cause short circuits.

Data corruption can occur either in run-time or in long-term memory. The effects are unpredictable, but they can include noise in the data and errors in software execution. Long-term data, such as the firmware of the GPS receiver, is subject to randomization due to radiation-induced bit flips. (Fortescue, Stark, and Swinerd 2003, pp. 474-475) Run-time memory problems can be corrected by restarting the receiver, and the receiver has a watchdog that restarts the receiver if a timer is not reset within a default time of 5 seconds. The receiver will be restarted frequently in any case as a part of planned operations. The GPS subsystem has support for hardware reprogramming of the receiver in case the GPS firmware becomes corrupted. OBC can reflash the firmware with a copy either stored in the OBC memory or uploaded from the ground. The integrity of the firmware copy in the OBC memory can be verified with a checksum, and some error correction scheme could be used to correct any possible errors in the copy.

The effects of latchup-caused short circuits could be mitigated by limiting currents

to safe levels. The probability of short circuits is also decreased by the receiver being turned off most of the time.

The simulated 2 krad total dose applies to the part of the GPS subsystem shielded by the aluminium frame of the satellite. The GPS antenna, situated on the surface of the satellite, lacks this protection and will therefore be subjected to more radiation than the components internal to the satellite.

4.7.2 Thermal vacuum, vibration and shocks

Radiation, thermal variations and vacuum are encountered in orbit while vibration and shocks are mostly limited to the launch.

The main effect vacuum can have on materials is outgassing, which is also dependent on temperature. Outgassing can be problematic if the outgassed material affects the lenses on optical instruments, or if outgassing causes components to malfunction or their performance to degrade. Outgassing can be mitigated by avoiding materials that easily outgas. Another issue could arise if components have pockets of air inside them, which could then damage components by escaping because of the pressure differential. The components and materials used in the GPS subsystem were deemed not to be excessively sensitive to vacuum.

Temperature variations can affect the electrical characteristics of the subsystem components. Most notably the clock reference oscillator in the GPS receiver could be affected by temperature variations, which could decrease positioning accuracy. (Lux and Markgraf 2004)

Thermal vacuum issues are considered unlikely to be critical in the case of the GPS subsystem, but performance degradation could occur. Testing could be performed in a vacuum chamber with adjustable temperatures, if such facilities can be found. Live GPS navigation testing would also require an antenna connection to be available.

Vibration and shocks are also unlikely to be major issues specifically with the GPS subsystem, and they will be tested in the later stages of the satellite project, possibly in the protoflight testing of the whole satellite.

4.7.3 Operation during the spin phase

It is somewhat unclear what effect the spin mode will have on the GPS navigation performance. The antenna will point approximately along the positive Z-axis of the ECEF frame, parallel to the satellite spin axis. The Aalto-1 spin rate will initially be up to 200 $^{\circ}$/s, and as the tether is extended the spin rate will slow down due to preservation of angular momentum. If track of some GPS satellites is lost during a revolution, they will be unavailable in the navigation solution. In the acquisition phase, data frames from

satellites need to be received in their entirety and their transmission takes 5 seconds per frame.

GPS operation in the spin phase could be tested with the Space Systems Finland GPS simulator equipment, but this was not done as part of this thesis. If there are no unexpected discontinuities in the GPS antenna pattern that could cause loss of signal, GPS navigation should work during the spin phase as well.

4.8 Summary of verification

A verification plan was outlined in the beginning of this chapter that will be used with the GPS subsystem to ensure that the subsystem conforms to its requirements. As a part of this thesis, it was possible to complete only the initial steps of the verification plan. GPS signal simulations were performed as a part of the development tests, and indicated that the subsystem is capable of navigating in orbit. A prototype of the GPS PCB was built and development tests were performed with it. Other functional tests were performed with the selected antenna. Both the prototype PCB and the antenna worked functionally as required. Thermal qualification of the receiver module was performed successfully.

The qualification model of the subsystem can be built based on the design presented in the thesis. The QM must then be subjected to a test campaign that tests its conformance to the requirements for the subsystem. Operational and functional requirements can be tested with functional tests. Environmental requirements should be tested with environmental tests. According to Kestilä et al. (2013), planned environmental tests for Aalto-1 as a whole will include:

- thermal cycling on systems with identified critical temperature variations
- vacuum degassing and testing on materials with risk of outgassing
- radiation testing on radiation sensitive systems
- thermal vacuum qualification tests on the satellite system as a whole

Of these, thermal and radiation testing are probably the most important for the GPS subsystem.

After the QM test campaign has been performed successfully, the FM of the subsystem can be constructed. To screen for possible manufacturing defects, a less severe testing campaign can be performed on it.

5 Conclusions

The purpose of this thesis was to develop the design for a GPS subsystem that would provide the Aalto-1 nanosatellite mission with the positioning accuracy required by its scientific payloads. The required accuracy was defined as better than 100 m near the GPS measurement epoch. The GPS subsystem will also provide accurate velocity and time information. The navigation data provided by the GPS subsystem can be used either on-board the satellite in real-time, or downloaded from the satellite for post-processing on the ground. Solving the position at any instant of time near the measurement epoch can be achieved by determining the orbit of the satellite based on the GPS measurements.

The design and a plan for the integration and verification of a GPS subsystem into the Aalto-1 nanosatellite were presented in this thesis. The Aalto-1 nanosatellite, fundamentals of GPS navigation, and satellite tracking with GPS were presented as background information. It was found that GPS is a common tool for LEO satellite navigation, as the GPS signal environment is similar from sea level to an altitude of around 3000 km. Small and low-power GPS receivers have made it possible to use GPS navigation also in nanosatellites.

Requirements were defined for the GPS subsystem, and suitable components were then selected. The designed GPS subsystem is based on the Fastrax IT03 receiver module, which is very small and low-power. The GPS antenna, Adactus ADA-15S, was selected after performing development tests with several candidates. A high-quality Texas Instruments voltage regulator with a wide operating temperature range was selected to supply the power to the subsystem, and resistors and capacitors were selected based on wide operating temperature ranges. Mechanical, electrical and software design and integration was also presented. Based on the design, a prototype PCB was constructed.

A verification plan for the subsystem was also outlined. The verification of the GPS subsystem will consist of the prototype phase, the qualification model phase and the flight model phase.

The prototype PCB and Fastrax Mini Evaluation Kits were used to perform several development tests, including GPS signal simulations, PCB functional testing and antenna performance testing. The GPS signal simulations indicated that the receiver is able to provide fixes that fulfill the 100 m requirement, but the poor antenna placement on the flight direction side of the satellite reduces the number of available GPS satellites and degrades positioning accuracy. The PCB functional tests and antenna performance tests indicated that both items work as required. Thermal qualification of the GPS receiver was also performed successfully.

In the course of this thesis, the subsystem design was nearly completed and a prototype was produced. The design should still be finalized, and suggestions in Section 5.1 can be used as a starting point. The most important modification to be done is

replacing the U.FL antenna connector with a SMA connector.

The qualification model of the subsystem can be built after the design described in this thesis has been finalized. The compliance of the QM to subsystem requirements should be tested. The exact tests need to be defined but will probably include both functional and environmental tests. For example, functional tests could include GPS signal simulations and antenna performance tests, while environmental tests could include thermal vacuum, radiation, vibration and shock tests. The exact tests were not specified in the thesis, and should be decided within the project.

After the QM has passed the qualification tests, the flight model of the subsystem can be built based on the QM. The FM should then be subjected to acceptance testing to screen for manufacturing defects. All possible functional tests should be performed, and possibly environmental tests that do not shorten the system lifetime.

5.1 Suggestions for further work

Suggestions for continued development and operations during the mission are included here.

- A SMA antenna connector should be incorporated into the PCB. The microstrip antenna line could be matched to 50 Ω if the mismatch loss is considered too great.
- Software for controlling the GPS subsystem should be developed for the OBC. This software should also be verified.
- Antenna tests with the PCB prototype were not performed due to lack of time and delays in obtaining suitable antennas. The antenna line mismatch effect on CNR was not tested. Antenna tests should also be performed with as realistic model of the satellite as possible to reveal any problems with antenna coverage or CNRs.
- No interfacing tests with an on-board computer prototype have yet been performed.
- The exact power, voltage and current levels of the subsystem should be measured with the final prototype when it is actually navigating.
- The PPS signal provided by the GPS receiver was only measured with an oscilloscope. Reference material about clock synchronization using the serial port DCD pin was found, but this was not actually tested.
- The IT03 showed much worse velocity accuracy in GPS signal simulations than other receivers used in space applications. The reason could be investigated.

- If firmware corruption by radiation is considered a high enough risk, software should be developed for the OBC that could update the firmware on the receiver in case it becomes corrupted. Support from Fastrax Oy will be required to produce such software.
- The QM and FM need to be constructed, and the qualification and acceptance tests of the subsystem need to be performed.
- During the imaging phase of the mission, the ADCS could be used to rotate the satellite in such a way that the GPS antenna points toward local zenith. This could be done when the spectral imager is not operated. This should increase the number of available satellites and therefore the fix quality. The feasibility of this option could be studied.

5.2 Final thoughts

The designed subsystem conforms to the operational, mechanical, electrical and software requirements, but the environmental requirements are the greatest concern. If discovered either before or during the mission, a serious flaw in environmental durability of the subsystem could still render the design nearly useless.

During the research done for the background chapter of this thesis, no academic publications about using such a low-power GPS receiver for nanosatellite navigation were found. While IT03 does not perform as well as other, more power-hungry C/A receivers, such a low-power receiver could be used in a satellite if the power budget is strict but accuracy requirements are moderate. A paper about the subsystem design, *"Design of a Low-power GPS Subsystem for a Nanosatellite Science Mission"*, was submitted to and presented in the 2nd IAA Conference on University Satellite Missions and Cubesat Winter Workshop in Rome, Italy in February 2013.

If the GPS subsystem can successfully perform its task in orbit during the Aalto-1 mission, it could encourage other nanosatellite teams to consider using similar low-power GPS components to provide moderately accurate navigation information for nanosatellites with tight power budgets. The low-power IT03 receiver seems to provide an intermediate option between accurate, power-hungry high-end GPS receivers and inaccurate TLEs.

References

Adactus AB (2010). *ADA-15S GPS Patch Antenna*. Datasheet.

Arlas, Jessica and Sara Spangelo (2012). "GPS Results for the Radio Aurora Explorer II CubeSat Mission". In: *American Institute of Aeronautics and Astronautics 2012 AIAA Region III Student Conference*.

Balan, Mugurel et al. (2008). "Goliat space mission: Earth observation and near Earth environment monitoring using nanosatellites". In: *International Astronautical Congress 2008, IAC-08, p. B4.6.A13*.

Beyondoor (2012). *BY-GPS/Glonass-03 Specification*. Datasheet.

Bouwmeester, J. and J. Guo (2010). "Survey of worldwide pico- and nanosatellite missions, distributions and subsystem technology". In: *Acta Astronautica 67, p. 854-862*.

Bridges, C. et al. (2011). "STRaND-1: The world's first smartphone nanosatellite". In: *2nd International Conference on Space Technology (ICST), 15-17 Sept. 2011*.

Bureau International des Poids et Mesures (2006). *The International System of Units (SI), 8th edition*. Standard. Bureau International des Poids et Mesures.

Clark, Craig and Ritchie Logan (2011). *Power budgets for mission success*. Presentation. Clyde Space Ltd.

Cluster, Jordan (2007). *AggieSat 2: Command and Data Handling*. Technical report. Embry-Riddle Aeronautical University.

Cote, Keith et al. (2011). "Mechanical, Power, and Propulsion Subsystem Design for a CubeSat". Bachelor's thesis. Worcester Polytechnic Institute.

Dwyer, Mark (2009). "Embedded Software Design for the Canadian Advanced Nanospace eXperiment Generic Nanosatellite Bus". Master's thesis. University of Toronto.

ECSS (2002). *ECSS-E-10-03A: Space engineering: Testing*. Standard. European Cooperation for Space Standardization.

— (2009). *ECSS-Q-ST-30-02C: Space product assurance - Failure modes, effects (and criticality) analysis (FMEA/FMECA)*. Standard. European Cooperation for Space Standardization.

Eurocircuits (2010). *Eurocircuits - Standard board build up 0-8 layers*. Technical specification. Eurocircuits.

Fastrax Oy (2010). *Fastrax IT03 OEM GPS Receiver: Technical Description*. Technical description.

Fastrax Oy (2005a). *iSuite^{TM} 3 SDK Protocols - iTalk*. URL: http://isuite.fastrax.fi/sdk/341/protocols/pro_italk.html (visited on Feb. 12, 2013).

— (2005b). *iSuite^{TM} MP SDK Protocols - NMEA*. URL: http://isuite.fastrax.fi/sdk/341/protocols/pro_nmea.html (visited on Feb. 12, 2013).

— (2007). *iTrax03 OEM GPS Receiver Module*. Datasheet.

Federal Aviation Administration William J. Hughes Technical Center (2012). *Global Positioning System (GPS) Standard Positioning Service (SPS) Performance Analysis Report. Reporting Period: 1 April – 30 June 2012*. Technical report. FAA William J. Hughes Technical Center.

Fortescue, Peter, John Stark, and Graham Swinerd (2003). *Spacecraft Systems Engineering. Third Edition*. Wiley.

Gao, S. et al. (2009). "Antennas for Modern Small Satellites". In: *IEEE Antennas and Propagation Magazine, Vol 51, No. 4*.

Greene, Michael R. and Robert E. Zee (2009). "Increasing the Accuracy of Orbital Position Information from NORAD SGP4 Using Intermittent GPS Readings". In: *23rd Annual AIAA/USU Conference on Small Satellites*.

Indian Institute of Technology Kanpur (2011). *Technical details of Jugnu*. URL: http://www.iitk.ac.in/infocell/jugnu_news/Brief%20write%20up%20on%20Jugnu.pdf (visited on July 12, 2012).

Ingvarson, Per et al. (2007). *A GPS antenna for precise orbit determination of the SWARM satellites*. Technical note. Saab Space, SE-405 15 Gothenburg, Sweden, 2007.

Kahr, E. et al. (2011). "GPS tracking on a nanosatellite - the CanX-2 flight experience". In: *8th International ESA Conference on Guidance, Navigation and Control Systems, Karlovy Vary, Czech Republic, 5-10 June 2011*.

Kaplan, Elliott D. and Christopher J. Hegarty (2006). *Understanding GPS: Principles and Applications. Second Edition*. Artech House.

Kestilä, A. et al. (2013). "Aalto-1 nanosatellite – technical description and mission objectives". In: *Geoscientific Instrumentation Methods and Data Systems, 2, 121–130, 2013*.

Langley, R.B. et al. (2004). "Qualification of a Commercial Dual-Frequency GPS Receiver for the e-POP Platform onboard the Canadian CASSIOPE Spacecraft". In: *2nd ESA Workshop on Satellite Navigation User Equipment Technologies, NAVITEC'2004, 8-10 Dec. 2004, Noordwijk, The Netherlands*.

Lux, H. and M. Markgraf (2004). *Thermal-Vacuum Testing of the Phoenix GPS Receiver*. Technical note. Space Flight Technology, German Space Operations Center (GSOC).

Markgraf, M. et al. (2010). “Phoenix-GPS navigation system onboard the Proba-2 spacecraft - first flight results”. In: *Small Satellites Systems and Services - The 4S Symposium, 31 May - 4 June 2010, Madeira, Portugal*.

Montenbruck, O. and C. Renaudie (2007). *Phoenix-S/-XNS Performance Validation*. Technical note. Space Flight Technology, German Space Operations Center (GSOC).

Montenbruck, Oliver and Eberhard Gill (2003). *Satellite Orbits: Models, Methods, Applications*. Springer.

Montenbruck, Oliver et al. (2007). “GPS for microsatellites - status and perspectives”. In: *6th IAA Symposium on Small Satellites for Earth Observation, Berlin*.

National Imagery and Mapping Agency (2000). *Department of Defense World Geodetic System 1984: Its Definition and Relationships with Local Geodetic Systems*. Technical Report.

Näsilä, Antti et al. (2012). *Aalto-1 Experiment Interface Document*. Technical report. Aalto University School of Electrical Engineering.

Paolillo, Fabrizio (2008). “Technologies and methods employed to design a university-class microsatellite, according to ESA standards”. PhD thesis. Sapienza University of Rome.

Petit, Gerard and Brian Luzum (2010). *IERS Conventions*. Technical note. International Earth Rotation and Reference Systems Service.

Praks, Jaan et al. (2011). “Aalto-1 - an experimental nanosatellite for hyperspectral remote sensing”. In: *Geoscience and Remote Sensing Symposium (IGARSS), 2011 IEEE International, pages 4367 – 4370*.

Pumpkin, Inc. (2003). *CubeSat Kit PCB Specification Rev. A5*. Technical specification. Pumpkin Incorporated.

RJ Systems (2011). *Synchronizing ntpd to a Garmin GPS 18 LVC via gpsd*. URL: `http://www.rjsystems.nl/en/2100-ntpd-garmin-gps-18-lvc-gpsd.php` (visited on Feb. 25, 2013).

Rush, John (2000). “Current issues in the use of the Global Positioning System aboard satellites”. In: *Acta Astronautica Vol. 47, Nos. 2-9, p. 377-387*.

Saarnimo, Timo (2010). *GPS Module Application Design*. Technical note. Fastrax Oy.

Schmidt, Marco et al. (2008). “Attitude Determination for the Pico-Satellite UWE-2”. In: *Proceedings of the 17th World Congress, The International Federation of Automatic Control, Seoul, Korea, July 8-11, 2008*.

Scholz, A. et al. (2010). “Flight results of the COMPASS-1 picosatellite mission”. In: *Acta Astronautica 67, p. 1289-1298*.

Sweet, Michael R. (2005). *Serial Programming Guide for POSIX Operating Systems*. URL: `http://www.easysw.com/~mike/serial/serial.html` (visited on Jan. 31, 2013).

Syfer (2010). *Automotive Electronics Council-Q200 Stress Test Qualification for Passive Components, Syfer AEC-Q200-Rev C Qualification*. Technical note. Syfer Technology Limited.

Taoglas (2012a). *AP.10F.07.0039B Specification*. Datasheet.

— (2012b). *AP17E.07.0064A Specification*. Datasheet.

USDOD (2008). *Global Positioning System Standard Positioning Service Performance Standard, 4th Edition*. Standard. United States Department of Defense.

Vainio, Rami (2011). *A short summary of how different orbit heights affects the radiation enviroment of the spacecraft*. Technical note. Aalto University Department of Radio Science and Engineering.

Vallado, David A. (2005). "An Analysis of State Vector Propagation Using Differing Flight Dynamics Programs". In: *15th AAS/AIAA Space Flight Mechanics Meeting January 23-27, 2005, Copper Mountain, Colorado*.

Wheeler, Harold A. (1977). "Transmission-Line Properties of a Strip on a Dielectric Sheet on a Plane". In: *IEEE Transactions on Microwave Theory and Techniques, Vol. MTT-25, No.8, August 1977*.

A Circuit schematic and board layout

This appendix contains the circuit schematic and board layout of the first GPS subsystem prototype.

A.1 Layout

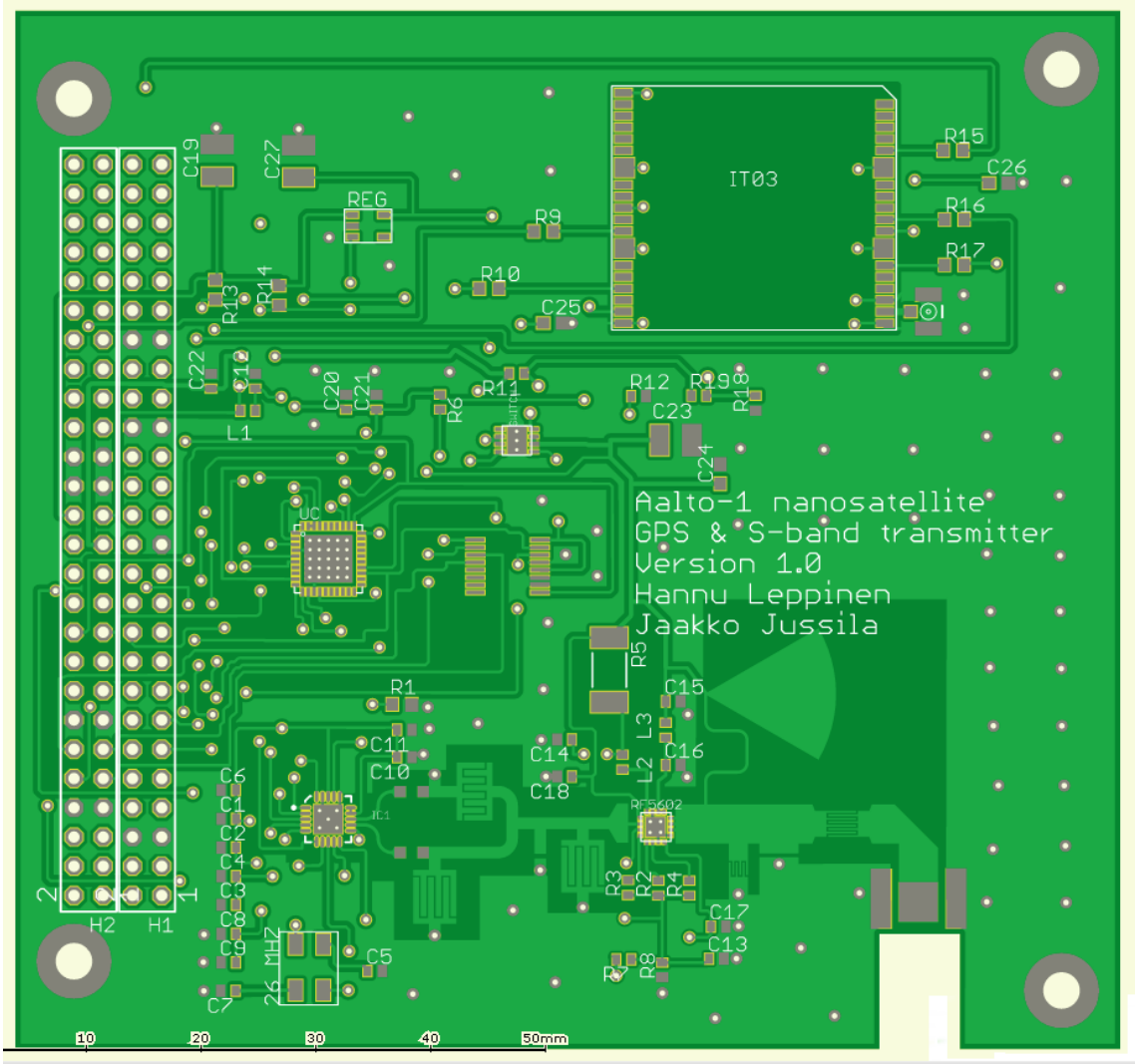

A.2 Schematic

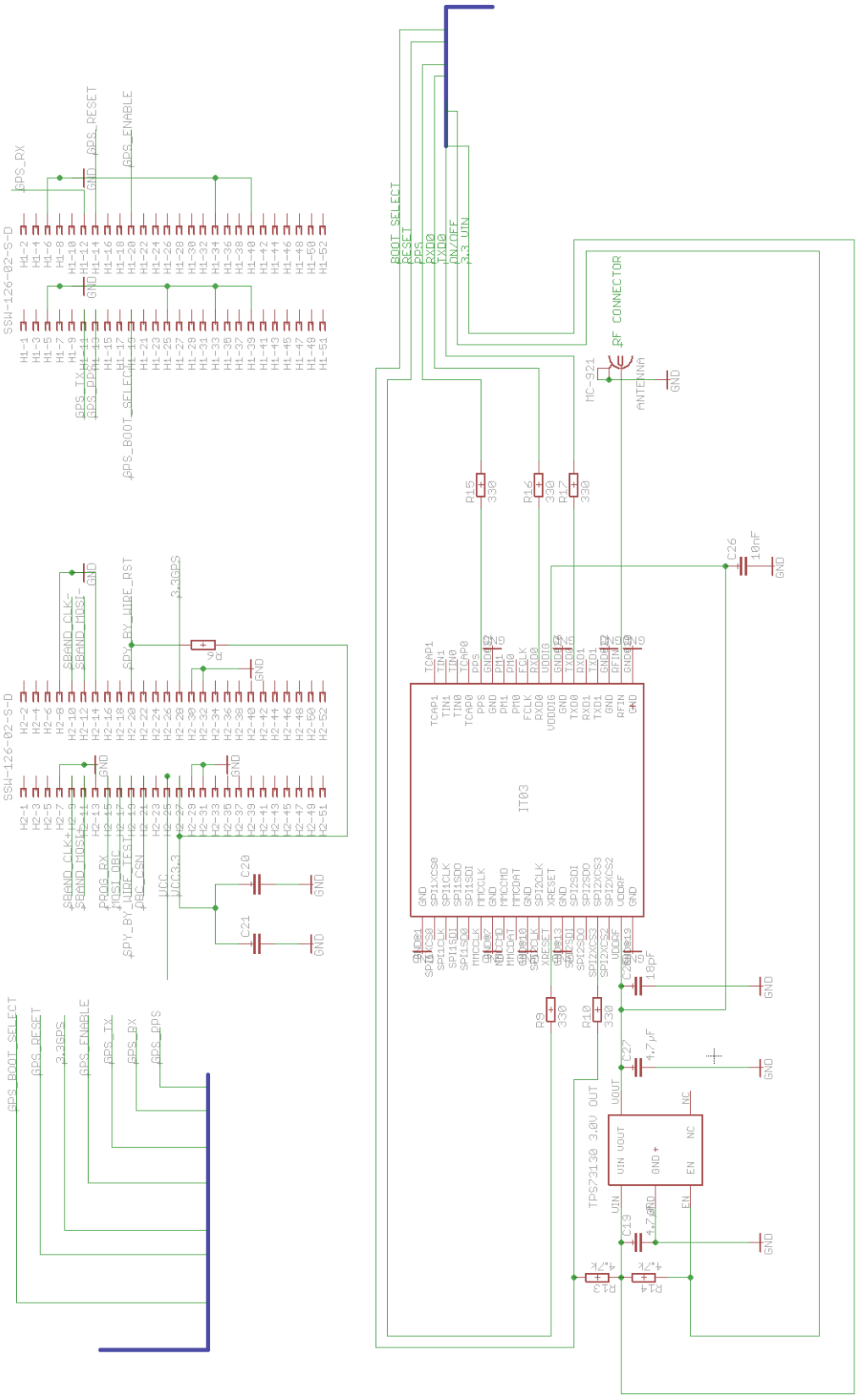

B Satellite bus pin layout

This appendix contains the pin layout for the long stack part of the Aalto-1 satellite bus.

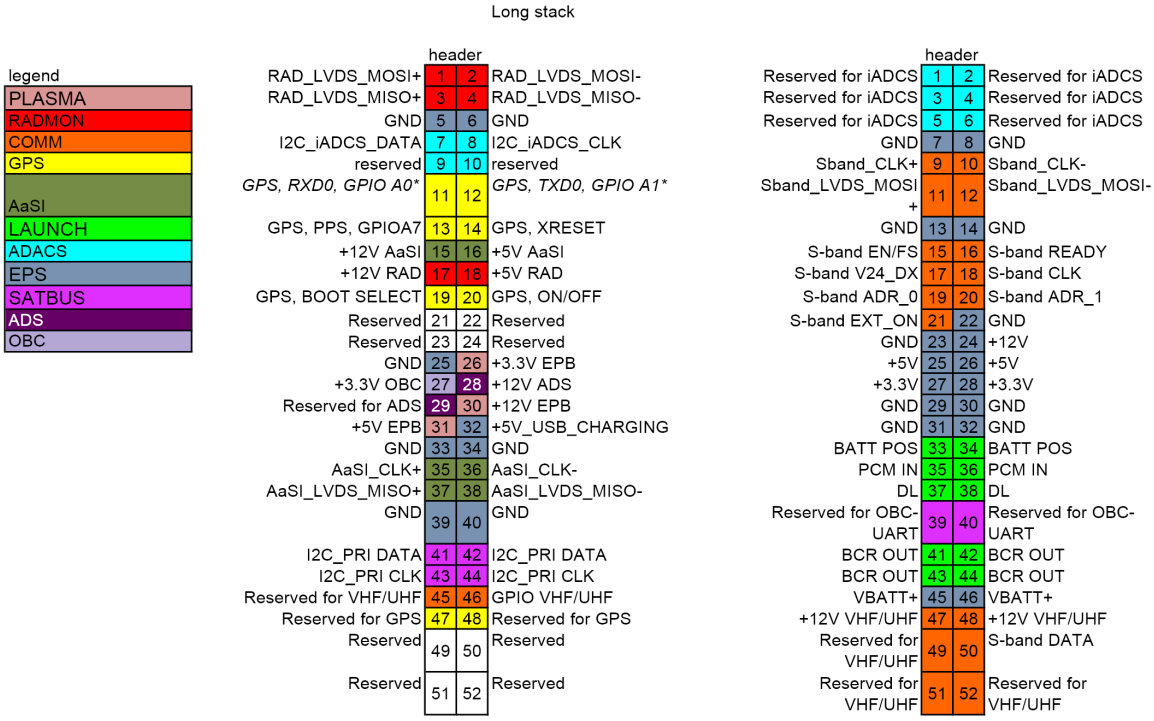

** crossed in GPS PCB (GPS TX --> OBC RX, OBC TX --> GPS RX)*

C Program code example

This appendix contains an example program that can be used to parse incoming navigation data from the serial line. An example output of the program is also provided. The program assumes that the serial port protocol of the receiver at startup is iTalk at 115200 baud.

C.1 main.c

```
#include <stdio.h>
#include <stdlib.h>
#include <errno.h>
#include <string.h>
#include <fcntl.h>
#include <termios.h>
#include <time.h>
#include <sys/types.h>
#include <sys/stat.h>
#include <sys/select.h>
#include <unistd.h>
#include <stdint.h>
#include "italk.h"

#define BAUDRATE B115200
#define PORT_NAME "/dev/ttyUSB0"

/* Serial port variables */
static struct termios oldtio, newtio;
static int fd = 1; /* output initially goes to standard output */

/*
 * 'open_port()' - Open serial port 1.
 *
 * Returns the file descriptor on success or -1 on error.
 */

int open_serial(char *device)
/* open the serial port and set it up */
{
    /*
     * Open modem device for reading and writing and not as controlling
     * tty.
     */
    if ((fd = open(device, O_RDWR | O_NOCTTY)) == -1) {
fprintf(stderr, "aalto1gps: error opening serial port\n");
exit(1);
    }

    /* Save current serial port settings for later */
    if (tcgetattr(fd, &oldtio) != 0) {
fprintf(stderr, "aalto1gps: error reading serial port settings\n");
exit(1);
    }

    /* Clear struct for new port settings. */
    /*@i@*/ bzero(&newtio, sizeof(newtio));

    /* make it raw */
    (void)cfmakeraw(&newtio);
    /* set speed */
```

```
    /*@i@*/ (void)cfsetospeed(&newtio, BAUDRATE);

    /* Clear the modem line and activate the settings for the port. */
    (void)tcflush(fd, TCIFLUSH);
    if (tcsetattr(fd, TCSANOW, &newtio) != 0) {
(void)fprintf(stderr, "aalto1gps: error configuring serial port\n");
exit(1);
    }

return fd;
}

int main(void){

int gps = open_serial(PORT_NAME);

printf("%d\n", gps);
int r;

while(1){

int error = -2;
int length = 0;
int type = 0;
do
   {
error = ITK_ReadMsgHeader(gps, &length, &type);
     } while ((error == -2));

if(type == 7){
printf("data size: %d\n", length);
printf("type: %d\n", type);
char message[1000] = {0};
uint16_t cs = 0;

NavFix navfix;

ITK_ReadMsgData(gps, message, &cs, length);
ParseNavFix(message, &navfix);

printf("UTC: %d.%d.%d %d:%d:%d.%d\n", navfix.day, navfix.month, navfix.year, ...
navfix.hour,navfix.minute, navfix.second, navfix.nano);
printf("ECEF X: %8.3f m Y: %8.3f m Z: %8.3f m\n", navfix.x*0.01, navfix.y*0.01, navfix.z*0.01);
printf("ECEF V_X: %5.3f m/s V_Y: %5.3f m/s V_Z: %5.3f m/s\n", navfix.vx*0.001, ...
navfix.vy*0.001, navfix.vz*0.001);

uint16_t cscalc = ITK_CalcChecksum(message, length);
printf("checksum in message: %x\n", cs);
printf("calculated checksum: %x\n", cscalc);

}

}

close(gps);


return 0;
}
```

C.2 italk.h

```
#ifndef ITALK_H
```

```
#define ITALK_H

#include <stdint.h>

typedef struct
{
uint16_t year, month, day, hour, minute, second; // UTC time
uint32_t nano; // UTC time, nanosecond part
int32_t x, y, z, vx, vy, vz; // position and velocity
} NavFix;

int PORT_ReadByte(int pPort, unsigned char *pBuffer);

int ITK_ReadMsgHeader(int hPort, int* dataSize, int* messageType);

int ITK_ReadMsgData(int hPort, unsigned char* message, uint16_t* cs, int length);

unsigned short ITK_CalcChecksum(const unsigned char* message, int length);

int ParseNavFix(const unsigned char* message, NavFix* navfix);

#endif
```

C.3 italk.c

```
#include <stdio.h>
#include <time.h>
#include <stdint.h>
#include "italk.h"

// Read a byte from serial port
int PORT_ReadByte(int pPort, unsigned char *pBuffer)
{
    unsigned char x;

if (pPort){

int r = (int)read(pPort, pBuffer, sizeof(char));
return 1; // should be 0 on success

}

    return 0;
}


/// Read the header of an iTalk message from the given port.
int ITK_ReadMsgHeader(int hPort, int* dataSize, int* messageType)
{
    unsigned char wData;

    // Read the SYNC1 character.
    if (PORT_ReadByte(hPort, &wData) == 0)
    {
        return -1; // other failure
    }
    if (wData != '<')
    {
        return -2; // sync failed
    }
```

```
    // Read the SYNC2 character.
    if (PORT_ReadByte(hPort, &wData) == 0)
    {
        return -1;
    }
    if (wData != '!')
    {
        return -2; // sync failed
    }

PORT_ReadByte(hPort, &wData);
PORT_ReadByte(hPort, &wData);
PORT_ReadByte(hPort, &wData);
*messageType = (int)wData;

PORT_ReadByte(hPort, &wData);
PORT_ReadByte(hPort, &wData);
*dataSize = (int)wData;

    return 0;
}


/// Read the message data of an iTalk message from the given
/// port. This function assumes that the message header has already
/// been read using the ITK_ReadFrameHeader function.
int ITK_ReadMsgData(int hPort, unsigned char* message, uint16_t* checksum, int length)
{

    unsigned char wData;


// first read the data
int i = 0;
for(i; i < 2*length; i++){
PORT_ReadByte(hPort, message+i);

}

// then read the checksum
    PORT_ReadByte(hPort, &wData);
*checksum = ((unsigned short)wData);
PORT_ReadByte(hPort, &wData);
*checksum = *checksum + ((unsigned short)wData << 8);


PORT_ReadByte(hPort, &wData); // read the ending ">" character


    // The message was successfully read.

if (wData == '>'){
     return 0;
}

return -1;
}

/// Compute the checksum for an iTalk message.
uint16_t ITK_CalcChecksum(const unsigned char* message, int length)
{
    uint16_t i;
    uint16_t wCheckSum = 0;

    // Exclude system header from checksum
    uint16_t* pW = (uint16_t*)(&(message[0]));

    for (i = 0; i < length; i++)
```

```
    {
        uint32_t dwTmp;

        dwTmp = ((uint32_t)wCheckSum + 1) * ((uint32_t)(*pW) + i);
        wCheckSum ^= (dwTmp ^ (dwTmp >> 16));
        pW ++;
    }

    return wCheckSum;
}

int ParseNavFix(const unsigned char* message, NavFix* navfix){

uint8_t a, b, c, d; // Use these for parsing

// Get hour from NAV_FIX message
a = message[66];
b = message[67];
navfix->hour = (b << 8) + a;

// Get minute from NAV_FIX message
a = message[68];
b = message[69];
navfix->minute = (b << 8) + a;

// Get second from NAV_FIX message
a = message[70];
b = message[71];
navfix->second = (b << 8) + a;

// Get nanos from NAV_FIX message
a = message[72];
b = message[73];
c = message[74];
d = message[75];
navfix->nano = (d << 24) + (c << 16) + (b << 8) + a;

// Get year from NAV_FIX message
a = message[76];
b = message[77];
navfix->year = (b << 8) + a;

// Get month from NAV_FIX message
a = message[78];
b = message[79];
navfix->month = (b << 8) + a;

// Get day from NAV_FIX message
a = message[80];
b = message[81];
navfix->day = (b << 8) + a;

// Get ECEF XYZ from NAV_FIX message

a = message[96];
b = message[97];
c = message[98];
d = message[99];
navfix->x = (d << 24) + (c << 16) + (b << 8) + a;

a = message[100];
b = message[101];
c = message[102];
d = message[103];
navfix->y = (d << 24) + (c << 16) + (b << 8) + a;

a = message[104];
b = message[105];
```

```
c = message[106];
d = message[107];
navfix->z = (d << 24) + (c << 16) + (b << 8) + a;

// Get ECEF V_XYZ from NAV_FIX message

a = message[186];
b = message[187];
c = message[188];
d = message[189];
navfix->vx = (d << 24) + (c << 16) + (b << 8) + a;

a = message[190];
b = message[191];
c = message[192];
d = message[193];
navfix->vy = (d << 24) + (c << 16) + (b << 8) + a;

a = message[194];
b = message[195];
c = message[196];
d = message[197];
navfix->vz = (d << 24) + (c << 16) + (b << 8) + a;

return 0;
}
```

C.4 Example output

The example output does not represent accurately what data would be output to a file, as that would likely be more compressed. Note that the single-digit minutes in the UTC time don't have a preceding 0 due to a bug in output formatting. In addition to the position and time, the number of satellites and DOP values would be of interest to assess fix quality. "Data size" refers to the size of the data in the read iTalk message in 16-bit words. Type 7 message is a navigation fix. Checksums are compared to ensure message integrity.

```
data size: 143
type: 7
UTC: 31.1.2013 8:4:43.501101163
ECEF X: 2885010.330 m Y: 1334934.190 m Z: 5510997.140 m
ECEF V_X: 0.036 m/s V_Y: -0.002 m/s V_Z: -0.018 m/s
checksum in message: e53
calculated checksum: e53
data size: 143
type: 7
UTC: 31.1.2013 8:4:44.501748904
ECEF X: 2885012.130 m Y: 1334934.520 m Z: 5510995.800 m
ECEF V_X: 0.032 m/s V_Y: 0.001 m/s V_Z: -0.017 m/s
checksum in message: 307d
calculated checksum: 307d
data size: 143
```

```
type: 7
UTC: 31.1.2013 8:4:45.502396646
ECEF X: 2885011.740 m Y: 1334931.290 m Z: 5510995.930 m
ECEF V_X: 0.036 m/s V_Y: 0.000 m/s V_Z: -0.019 m/s
checksum in message: f4cf
calculated checksum: f4cf
data size: 143
type: 7
UTC: 31.1.2013 8:4:46.503044390
ECEF X: 2885010.060 m Y: 1334932.370 m Z: 5510996.440 m
ECEF V_X: 0.038 m/s V_Y: -0.004 m/s V_Z: -0.019 m/s
checksum in message: 1db3
calculated checksum: 1db3
data size: 143
type: 7
UTC: 31.1.2013 8:4:47.499689546
ECEF X: 2885007.920 m Y: 1334931.410 m Z: 5510997.220 m
ECEF V_X: 0.038 m/s V_Y: -0.005 m/s V_Z: -0.018 m/s
checksum in message: e100
calculated checksum: e100
```

D FMECA sheet

This appendix contains as an example the failure modes, effects and criticality analysis (FMECA) done on February 1, 2013.

FAILURE MODES, EFFECTS AND CRITICALITY ANALYSIS (FMECA)												
Mission: Aalto-1			Subsystem: GPS (see schematic on sheet 2)								Date: 1.2.2013	
No.	Item	Function	Failure mode	Failure cause	Failure effects	Detection	Prevention	Mitigation	SN	PN	CN	Notes
1	IT03 receiver module	DIG/RF supply voltage	Receiver supply voltage failure	SC/OC (short circuit/open circuit)	Loss of subsystem	Higher or lower current to the subsystem than normal	High-quality solders	-	2	2	4	
2	IT03 receiver module	UART TX/RX	Receiver serial line failure	SC/OC	Loss of subsystem	No data to OBC from GPS	High-quality solders	-	2	2	4	
3	IT03 receiver module	RF IN	Antenna input failure	SC/OC	Loss of subsystem	No GPS satellites detected	High-quality solders and antenna connector	-	2	2	4	
4	IT03 receiver module	Other I/O	Other I/O failure	SC/OC	Degradation of subsystem: loss of firmware update, PPS	No PPS signal or unsuccessful firmware update	High-quality solders	-	1	2	2	
5	Antenna connector	Antenna signal	No antenna signal	SC/OC	Loss of subsystem	No GPS satellites detected	High-quality solders and antenna connector	-	2	2	4	
6	Active patch antenna	Antenna signal	No antenna signal	SC/OC	Loss of subsystem	No GPS satellites detected	High-quality antenna, solders and antenna connector	-	2	2	4	
7	330 ohm OBC to GPS resistor	OBC-GPS data line	GPS receiver does not receive commands from OBC	OC	Degradation of subsystem: loss of command capability	GPS receiver does not accept commands	High quality solders and resistors	Fallback to NMEA communication	1	2	2	
8	330 ohm GPS to OBC resistor	OBC-GPS data line	OBC does not receive navigation data from GPS	OC	Loss of subsystem	No data to OBC from GPS	High quality solders and resistors	-	2	2	4	
9	330 ohm PPS line resistor	Time sychronization line	OBC does not receive time synchronization pulse	OC	Degradation of subsystem: loss of time sync pulse	No time sync pulse	High quality solders and resistors	-	1	2	2	
10	330 ohm XRESET line resistor	Receiver reset for firmware update	Reset does not work, firmware update mode cannot be entered	OC	Degradation of subsystem: loss of HW firmware update capability	Unsuccessful HW firmware update	High quality solders and resistors	-	1	2	2	
11	330 ohm BOOT SELECT line resistor	Boot select for firmware update	Boot select does not work, firmware update mode cannot be entered	OC	Degradation of subsystem: loss of HW firmware update capability	Unsuccessful HW firmware update	High quality solders and resistors	-	1	2	2	
12	4.7 kohm BOOT SELECT pullup resistor	Pulls BOOT SELECT up for normal operation	Boot select needs to be actively pulled up by OBC to operate GPS	OC	Degradation of subsystem: OBC needs to actively pull BOOT SELECT up	Possibly no effects depending on how OBC operates the pin	High quality solders and resistors	-	1	2	2	Pull-up resistor is needed to operate the subsystem without BOOT SELECT separately connected and pulled up.
13	4.7 kohm VREG ENABLE pullup resistor	Pulls VREG ENABLE up for normal operation	Voltage regulator enable needs to be actively pulled up by OBC to operate GPS	OC	Degradation of subsystem: OBC needs to actively pull VREG ENABLE up	Possibly no effects depending on how OBC operates the pin	High quality solders and resistors	-	1	2	2	Pull-up resistor is needed to operate the subsystem without VREG ENABLE separately connected and pulled up.
14	3.0 V regulator	Input voltage	Voltage regulator input voltage is short circuited	SC	Loss of subsystem, possible damage to 3.3 V bus	High current, no navigation data	High quality solders	Current limit in the 3.3 V bus	2	2	4	Probably worst-case scenario
15	3.0 V regulator	Input voltage	Voltage regulator input voltage is open circuited	OC	Loss of subsystem	No current to GPS subsystem, no navigation data	High quality solders	-	2	2	4	
16	3.0 V regulator	Other pins	Other voltage regulator signals are open circuited or short circuited	SC/OC	Loss of subsystem	High or low current to GPS subsystem, no navigation data	High quality solders	-	2	2	4	
17	4.7 µF VIN bypass capacitor	Noise reduction, voltage regulator	Short circuit of a bypass capacitor	SC	Loss of subsystem, possible damage to 3.3V bus	High current, no navigation data	High quality solders and capacitors	Current limit in the 3.3 V bus	2	2	4	Equally bad as #14
18	4.7 µF VIN bypass capacitor	Noise reduction, voltage regulator	Open circuit of a bypass capacitor	OC	Degradation of subsystem: possibly more voltage noise	Possibly no effects	High quality solders and capacitors	-	1	2	2	
19	4.7 µF VOUT bypass capacitor	Noise reduction, voltage regulator	Short circuit of a bypass capacitor	SC	Loss of subsystem	High current, no navigation data	High quality solders and capacitors	-	2	2	4	
20	4.7 µF VOUT bypass capacitor	Noise reduction, voltage regulator	Open circuit of a bypass capacitor	OC	Degradation of subsystem: possibly more voltage noise	Possibly no effects	High quality solders and capacitors	-	1	2	2	
21	18 pF VDDRF bypass capacitor	Noise reduction, voltage regulator	Short circuit of a bypass capacitor	SC	Loss of subsystem	High current, no navigation data	High quality solders and capacitors	-	2	2	4	
22	18 pF VDDRF bypass capacitor	Noise reduction, voltage regulator	Open circuit of a bypass capacitor	OC	Degradation of subsystem: possibly more voltage noise	Possibly no effects	High quality solders and capacitors	-	1	2	2	
23	10 nF VDDDIG bypass capacitor	Noise reduction, voltage regulator	Short circuit of a bypass capacitor	SC	Loss of subsystem	High current, no navigation data	High quality solders and capacitors	-	2	2	4	
24	10 nF VDDDIG bypass capacitor	Noise reduction, voltage regulator	Open circuit of a bypass capacitor	OC	Degradation of subsystem: possibly more voltage noise	Possibly no effects	High quality solders and capacitors	-	1	2	2	